UNIVERSITY OF CALIFORNIA
RIVERSIDE

AND

SAN DIEGO STATE UNIVERSITY

Introgression and the Evolution of the *Habronattus americanus* Subgroup (F. Salticidae), With Particular Consideration of Multiple Patterns of Discordance

A Dissertation submitted in partial satisfaction
of the requirements for the degree of

Doctor of Philosophy

in

Evolutionary Biology

by

Tierney Bougie

June 2022

Dissertation Committee:
Dr. Marshal Hedin, Co-Chairperson
Dr. Alan Brelsford, Co-Chairperson
Dr. Lluvia Flores-Renteria
Dr. Mark Springer

The Dissertation of Tierney Bougie is approved:

Committee Co-Chairperson

Committee Co-Chairperson

University of California, Riverside
San Diego State University

ACKNOWLEDGEMENTS

I thank my advisor, Marshal Hedin, for supporting my research and development as an evolutionary biologist. Thank you for helping me navigate graduate school and showing me countless beautiful places during field collections. I have learned so much from you. Thank you to my co-advisor, Alan Brelsford, for teaching me ddRADseq methods and many useful skills. I also thank my other dissertation committee members: Lluvia Flores-Renteria and Mark Springer. Thank you Lluvia for reminding me that women belong in science and that we do not need to apologize for our accomplishments. Thank you to my program coordinator, Liz Waters, for helping me navigate my program and listening to me when I needed support.

I did not anticipate the difficulties of moving across the country alone and away from family and friends. I found family here that gave me unconditional love and support every step of the way. I thank Bri and Admon Dallo (and Nellee) for welcoming me into their lives, introducing me to their friends (all of which are great people), and always making me feel comfortable and safe in San Diego. Bri, thank you for answering all my random grad affairs questions lol. Thank you, Julie Eiter for considering me a part of your family and inviting me to any holiday or social gatherings. I thank Reema Poles for her unending love and support and many, many puzzle nights. I thank Kathy O'Neill and Eric Wetzel for their friendship and very delicious meals cooked in the old apartment. Kathy, thank you for all your love and understanding when I needed it most in Riverside, the books you gave me kept me sane. I am grateful to have found a group of supportive

members of the LGBTQ+ community: Racquel Freed, Jessah Goldner, Miranda Hildreth, Emma Lennon, Casey Parrington, and Reema Poles. Thank you all for welcoming me and always supporting me as I finished up my Ph.D. C. Parrington, thank you for encouraging me to be myself, I am always learning from you. M. Hildreth, thank you for always making me laugh and listening with all the kindness when I needed to vent. Rocky, your heart is so big for the ones you love, thank you for showing me some of that. Thank you, Rick and Rebecca Arevalo for welcoming me into your home and allowing me to care for your animals. You have become family to me and have given me so much support. Thank you to all the dogs and cats I have cared for over my Ph.D.

I entered my program with an amazing cohort of MS students: Alex Sumarli, Sam Fellows, Rosalyn Price-Waldman, and Erik Ciaccio you were all an important piece of my development into an evolutionary biologist. Thank you for countless discussions of evolutionary theory and methods, but also for many moments of friendship and experiencing San Diego together. I thank many past and present graduate students at San Diego State University and UC Riverside, thank you for your camaraderie. Abdul Ada, thank you for your friendship and helping me understand methods and stats. I thank many educators, the courses I took and conversations I had with them have greatly contributed to my understanding of evolutionary biology. Thank you to current and former lab mates Guilherme Azevedo, Ben Brenner-Gibson, Brendan Boyer, Mercedes Burns, Erik Ciaccio, Leslie Johnson, Sean Kelly, Rodrigo Monjaraz Ruedas, Victoria Rayno, and Casey Richart. Many graduate and undergraduate students helped field collection efforts and I thank them for that: Danielle Asfour, E. Ciaccio, Gabe Greenberg-Pines, Catherine

Isip, V. Rayno, Eli Selvidge, and Karina Silvestre. Thank you to Daniel Pierce, Madison Sankovitz, Elisa Henderson, and K. Silvestre for help collecting molecular data. Thank you G. Azevedo for many discussions about ddRADseq methods. Thank you to the Flores-Rentería and Reeder Labs for access to laboratory equipment. Thank you to Damian Elias and Elias Lab members for help during field collection and data collection used in Chapter 3. Thank you to the staff at both San Diego State University and UC Riverside for help navigating between two universities. I have met many lifelong friends and colleagues in the arachnology community, thank you for sharing your research and support. Thank you to Physalia workshops, I learned many methods I used in my dissertation research from the speciation genomics course. Thank you to several funding sources for enabling me to conduct my research: American Arachnology Society, National Science Foundation (to M. Hedin), U.C. Riverside department of Ecology, Evolution and Organismal Biology, San Diego State University, Society for Systematic Biologists.

Lastly, thank you to my family and friends in Wisconsin for supporting me any way possible. Thank you, mom (Stacey Bougie) and dad (Bob Bougie) for your unending support and love. I have learned so much from you both and am in awe of your dedication to raise Tybias. As a twin, it is unimaginable to think what life would have been like without my literal other half, Tiffany Bougie. Thank you for being my best friend and support system for my entire life and during this Ph.D. Thank you, Andy Richard for countless talks about life and your support throughout my Ph.D. And of course, thank you Cedar, you are one special pup.

The text of this dissertation, in part, is a reprint of the material as it appears in Bougie, T., Brelsford, A., Hedin, M., 2021. The co-authors M. Hedin and A. Brelsford listed in that publication directed and supervised the research which forms the basis for this dissertation.

DEDICATION

For the spiders and the dogs.

ABSTRACT OF THE DISSERTATION

Introgression and the Evolution of the *Habronattus americanus* Subgroup (F. Salticidae), With Particular Consideration of Multiple Patterns of Discordance

by

Tierney Bougie

Doctor of Philosophy, Graduate Program in Evolutionary Biology
University of California, Riverside and San Diego State University, June 2022
Dr. Marshal Hedin and Dr. Alan Brelsford, Co-Chairpersons

My dissertation focuses on the evolutionary effects of introgression on a complex group of paradise spiders that experience strong sexual selection. I use an integrative approach to evaluate morphological, genetic, and behavioral consequences of gene flow across species boundaries in the *Habronattus americanus* subgroup. In Chapter 1, I uncover extensive genomic homogenization between members of the *americanus* subgroup, such that evolutionary lineages reflect geography rather than species or morph type. Despite the genomic homogenization, selective forces maintain the very diverse male courtship ornamentation of different species and morphs. In Chapter 2, behavioral analyses of courtship display traits indicate a geographical pattern with a southeastern display group and a western+northern display group. Courtship displays in the southeastern distribution include more fling repetitions and longer introductory motif times compared to courtship displays from other geographical areas. Patterns of courtship display diversity are discordant with patterns of morphological diversity and seem to align more with geographical location than morph or species identity. In Chapter 3,

population genetic and morphological analyses from a *H. americanus* x *H. kubai* hybrid zone near Mt. Shasta, CA uncover very little genomic diversity but substantial morphological diversity of male courtship ornamentation traits, which seem easily introgressed across species boundaries. Hybrid zone dynamics at Mt. Shasta appear to act as a microcosm for periodic processes of divergence and reticulation in the entire *americanus* subgroup. In its entirety, my dissertation offers an integrative analysis of the effects introgression may have on diverging lineages and highlights the importance of new perspectives on how we think about speciation and lineage diversification.

TABLE OF CONTENTS

LIST OF TABLES

LIST OF FIGURES

LIST OF SUPPLEMENTARY FIGURES

Chapter 1

INTRODUCTION OF THE DISSERTATION

Hybridization and introgression – defined here as gene flow across species boundaries – can have important evolutionary consequences, including extinction and speciation. Numerous recent studies have used naturally occurring hybrid zones to investigate links between genes and morphological traits to further understand the evolutionary history of a group and how introgression of certain traits may have sparked rapid speciation events. The growing interest in hybridization in the evolutionary biology community has enabled new perspectives on traditional viewpoints, such as the bifurcating nature of speciation. It is now accepted in the scientific community that hybridization is much more common in nature than previously believed and exploring how this phenomenon impacts evolutionary dynamics and relationships can provide us with new insights into how species boundaries are (or are not) maintained.

Hybridization in animals ultimately requires behavioral interactions between mating pairs, making the study of courtship displays and sexually selected traits, in addition to genetic data, a key component to truly understanding how hybridization and introgression may influence evolutionary trajectories. In my dissertation, I used a variety of data sources to explore the impacts of introgression on a rapidly evolving group that exhibits substantial amounts of sexual selection and was affected by repeated climatic changes during the Pleistocene. Discordance in the patterns of evolution between these datasets is a common theme identified throughout my research, with evidence of discordance at some level identified in all three chapters. My dissertation research

evaluates the evolutionary consequences of hybridization and introgression with a particular focus on multiple types of discordance in a group of paradise spiders (*Habronattus*).

Habronattus are a species rich group of jumping spiders with over 100 described species. Adult males have brightly colored sexual ornamentation and elaborate courtship behavior, and many of these traits are affected by hybridization. Previous work has documented genetic evidence of hybridization in several different *Habronattus* species groups, including the *H. americanus* group. My dissertation focuses on many of the described species and lineages belonging to the *americanus* subgroup – a subset of the *H. americanus* group – which includes five described species (*H. americanus*, *H. kubai*, *H. bulbipes*, *H. sansoni*, and *H. waughi*). Currently described species within the *americanus* subgroup were originally delimited along morphology lines, with male courtship ornamentation weighing heavily on species identity. My research provides a new perspective with respect to the diversification of the *americanus* subgroup and similar systems, stressing the role of frequent introgression in leading to a group of closely related species essentially evolving as one complex unit throughout their divergence history.

In Chapter I, I focused on exploring the evolutionary history of the entire *americanus* subgroup and document how introgression might have impacted both the genomes and the morphology of lineages in the group. This broadscale study identified the degree to which introgression has homogenized the genomes of *americanus* subgroup members while selective forces maintain a striking amount of morphological diversity in

the males. I hypothesized two different possible divergence scenarios for the group that are both dependent on climatic changes as the lineages evolved. Since introgression ultimately relies on behavioral interactions between mates, I described male courtship behaviors of different *americanus* subgroup members and place these courtship routines in the context of the evolutionary history of the group for my Chapter II research. My Chapter III research takes a closer look at the population dynamics occurring within a contemporary hybrid zone near Mt. Shasta, California. I characterized morphological diversity and spatial structure and assessed genomic ancestry in this hybrid zone between *H. americanus* and *H. kubai*. Dynamics within the Mt. Shasta hybrid zone might act as a microcosm for divergence processes in the *americanus* subgroup, and possibly even the entire genus *Habronattus*.

My three dissertation chapters together comprise an integrated analysis of the evolutionary consequences of introgression in a group of charismatic jumping spiders at multiple spatial scales and considering behavioral, morphological, and genomic data. I explore the impact frequent introgression coupled with rapid lineage divergence had in the diversification of the *americanus* subgroup. While my research is focused on a single taxonomic group, my findings can be applied to similar systems experiencing extensive amounts of introgression. As such my dissertation research provides valuable results to a growing field within evolutionary biology.

CHAPTER 1

Evolutionary impacts of introgressive hybridization in a rapidly evolving group of jumping spiders (F. Salticidae, *Habronattus americanus group*)

Abstract

Introgressive hybridization can be a powerful force impacting patterns of evolution at multiple taxonomic levels. I aimed to understand how introgression has affected speciation and diversification within a species complex of jumping spiders. The *Habronattus americanus* subgroup is a recently radiating group of jumping spiders, with species now in contact after hypothesized periods of isolation during glaciation cycles of the Pleistocene. Effects of introgression on genomic data (RADseq, ultraconserved elements (UCEs)) and morphology were investigated using phylogenomic and clustering methods. I characterized 14 unique species/morphs using non-metric multidimensional scaling of morphological data, a majority of which were not recovered as monophyletic in phylogenomic analyses. Morphological clusters and genetic lineages are highly incongruent, such that geographic region was a greater predictor of phylogenetic relatedness and genomic similarity than species or morph identity. STRUCTURE analyses support this pattern, revealing clusters corresponding to geographic regions. A history of rapid radiation in combination with frequent introgression seems to have mostly homogenized the genomes of species in this system, while selective forces are

hypothesized to maintain distinct male morphologies. GEMMA analyses (which test for associations between SNPs and designated groups of individuals) support this idea by identifying SNPs correlated with distinct male morphologies. Overall, I have uncovered a system at odds with a typical bifurcating evolutionary model, instead supporting one where closely related species evolve together connected through multiple introgression events, creating a reticulate evolutionary history.

VI. INTRODUCTION

Introgressive hybridization (IH, or introgression), a process by which genetic material is exchanged across species boundaries (Gompert et al. 2008), can be a powerful evolutionary force at several taxonomic levels (Abbott et al. 2016). For example, IH may lead to divergent lineages sharing morphological features (Nadeau et al. 2013; Martin et al. 2013; Poelstra et al. 2014; Martin et al. 2019). While the cross-species transfer of phenotypic traits has been documented to result in prezygotic or postzygotic reproductive isolation (Jiggins et al. 2001, 2008), some lineages may not develop barriers to gene flow and will continue to hybridize. Ongoing hybridization has the potential to degrade classical species boundaries by enabling the exchange of genetic material across most of the genome, effectively homogenizing genomes of divergent lineages. In these cases, only small fractions of the genome are divergent, often coding for differences in phenotypes and species identity (Toews et al. 2016; Stryjewski and Sorenson 2017; Campagna et al. 2017; Brelsford et al. 2017; Martin et al. 2019). Complete disintegration of species boundaries is also possible, where there are no divergent areas between genomes, leading to species collapse (e.g., Grant and Grant 2002; Taylor et al. 2006; Kleindorfer et al. 2013).

Because closely related species experiencing rapid diversification are highly prone to IH (Seehausen 2004; Abbott et al. 2013), it is not surprising that many studies identifying homogenized genomes have worked with systems experiencing a rapid radiation (Campagna et al. 2017; Stryjewski and Sorenson 2017; Toews et al. 2016;

Brelsford et al. 2017). Recent research has suggested that hybridization can generate substantial variation through recombination, which has been documented to play an important role in the generation of new phenotypes involved in sexual selection and species identity (Malinsky et al. 2015; Stryjewski and Sorenson 2017; Meier et al. 2017). Such phenotypic diversification may fuel rapid radiations, which can lead to more introgression and subsequently more novel phenotypes, resulting in a positive feedback loop increasing the propensity for introgression (e.g., Stryjewski and Sorenson 2017; Meier et al. 2017).

IH can obviously complicate reconstruction of evolutionary history, especially in rapidly radiating species complexes. Contemporary and historical introgression has the potential to produce conflicting tree topologies and poor resolution on short branches (Alexander et al. 2017). Shared genetic material resulting from IH will cause discordance between morphological and genetic datasets and between different genetic datasets (Cui et al. 2013; MacGuigan and Near 2018). Historically, it has been difficult with limited genetic data to detect signals of discordance or distinguish between causes of discordant patterns (Maddison 1997; Degnan and Rosenberg 2009). However, genomic-scale data enables us to ask and answer questions surrounding the evolutionary impacts of introgression, even in historically challenging groups (Fontaine *et al.* 2014; Mallet *et al.* 2016).

A well-suited group to explore how introgression impacts species relationships in recent and rapidly diverging taxa is the jumping spider genus *Habronattus*, commonly known as paradise spiders. *Habronattus* is a species rich taxon (>100 described species)

that diverged relatively recently – possibly less than 5 million years ago (Bodner and Maddison 2012). *Habronattus* have keen vision (Zurek et al. 2015) and adult males are famous for elaborate colored ornaments and courtship behavior (Masta and Maddison 2002; Elias 2003; Elias et al. 2006). Many of these important courtship characters are influenced by hybridization, making them useful for identifying hybrids (Griswold 1987; Maddison and Hedin 2003). Additionally, since these characters are presented to females during courtship displays, IH may affect patterns of mate selection. In addition to morphological evidence of hybridization, several groups within *Habronattus* also show genetic/genomic evidence of hybridization (Masta 2000; Maddison and Hedin 2003; Hedin and Lowder 2009; Blackburn and Maddison 2014; Leduc-Robert and Maddison 2018; Hedin et al. 2020). *Habronattus* appears to have generally weak pre-mating isolation, which may allow and/or promote hybridization. Males court willingly with heterospecifics, and females sometimes show xenophilic mating preferences (Hebets and Maddison 2005; Elias et al. 2006; Blackburn and Maddison 2013; Taylor et al. 2017).

The *H. americanus* species group is a monophyletic group within *Habronattus* (Griswold 1987; Leduc-Robert and Maddison 2018). It is comprised of 10 described species found primarily in western North America (Griswold 1987), including a clade of five closely related described species, herein called the "*americanus* subgroup" – *H. americanus, H. bulbipes, H. kubai, H. waughi,* and *H. sansoni*. The time to the most recent common ancestor (tMRCA) between *H. americanus* and *H. sansoni* was estimated to be around 200,000 years ago using secondary calibration (see figure 4, Hedin et al. 2020). However, documented cases of introgression between *americanus* subgroup

members and members of its sister clade, the *tarsalis* subgroup may pull estimated divergence times closer to the present (Leduc-Robert and Maddison 2018). Members of the *americanus* subgroup are mostly distributed across mountainous regions of western North America, but can be found at lower elevations at higher latitudes (e.g., beaches on the coast of OR, WA, and British Columbia; **Figure 1.1**). Because of montane habitat preferences, distributions of the group have almost certainly been impacted by Pleistocene glaciation.

Described species within the *americanus* subgroup show extensive geographic variation, where geographically separated populations differ in patterns of male ornamentation (Griswold 1987; Blackburn and Maddison 2014; see **Figures 1.1** and **1.2**). In addition to geographic variation within species, there are known interspecific hybrid zones at high elevations in the Sierra Nevada and Cascade Mountains, where parental species and intermediate morphologies are found at a single geographic location. This contrasts with the more general pattern found in the subgroup, where spiders at any single geographic location share a single morphology, with variation across geography (**Figure 1.1)**. Previous genetic studies have documented hybridization and introgression within the *americanus* subgroup, both between phenotypically divergent populations of the same species (Blackburn and Maddison 2014) and between two or more different species (Leduc-Robert and Maddison 2018).

Using genomic and morphological datasets, I aim to (1) characterize the extreme morphological diversity within the *americanus* subgroup in the context of introgression, (2) explore the effects of introgression on genomic relationships of the *americanus*

subgroup, (3) explore the role IH may play in the disintegration of species boundaries, and (4) discuss alternative models of divergence that could produce patterns recovered in my results. My disintegration model refers to the breakdown of genetic divergence between different species, such that heterospecifics may contain only few divergent areas in the genome. Under this model, I expect frequent hybridization and introgression events between divergently evolving lineages throughout their evolution. I also predict that populations- regardless of species identity- in close geographic proximity will be more genetically similar to each other than to geographically-distant populations. As such, currently described species may not form monophyletic groups or exclusive genetic clusters, but rather geography may be a better predictor of phylogenetic relatedness and genomic similarity.

II. MATERIALS AND METHODS

(1) Specimen collection

Sample sites included locations throughout the montane western United States and southwestern Canada, including the Rocky Mountains, Sierra Nevada Mountains and Cascade Mountains (**Appendix 1.1)**. Griswold (1987) formally described species in the *americanus* subgroup using morphological characters primarily of the male face, palps, and leg I; I collected specimens that matched each of these described species, except for *H. waughi,* geographically-isolated in eastern Canada. Because *americanus* subgroup members are highly morphologically variable, some included populations do not match

previously described species diagnoses and are given new informal names based on their morphologies.

(2) Morphological Data Collection and Analysis

Twenty-three discrete morphological characters were scored for specimens that also have genomic data available (**Table 1.1, Appendix 1.2**). My morphology sample includes 84 males representing 4 described species and 16 morphological variants (3 *H. americanus* morphs described in Blackburn and Maddison 2017 and 13 newly defined morphs- see Results). Following Blackburn and Maddison's (2017) scheme for defining *H. americanus* morphs, I defined (*a priori*) variants primarily by palp color, chelicerae hair bundle color, leg I color and length of leg I ventral hairs. I used additional characters of some described species (*H. kubai* and *H. sansoni*) to further define morph types for these groups. Griswold (1987) scored 164 male characters, of which I chose those most feasible for accurate scoring and those variable within the *americanus* subgroup, with the addition of the expanded tarsus character not present in Griswold's revision. Characters were scored by examining individuals preserved in 100% ethanol under a dissecting microscope. To summarize morphological variation and visualize morphological clusters, I performed a non-metric multidimensional scaling (NMDS) analysis using the metaMDS function in the R package Vegan v2.5-6.

(3) Samples, RAD Data Collection & Analysis

The molecular sample included all specimens used for the morphological analysis (except for *H. kubai* Great Basin, *H. americanus* Manti La Sal, and *H. americanus* Sevier Lake, which were collected after molecular data was gathered) with the addition of 9 individuals – 95 specimens total. These samples include most described species and morphological variants recovered in my morphological analysis (see **Appendix 1.2**). DNA extraction was performed using the Qiagen Dneasy Blood & Tissue protocol (Qiagen, Valencia, CA). Two to three legs were used for extraction, unless legs were unavailable, then the dorsal half of the cephalothorax was used. All genomic DNA extractions were quantified using a Qubit Fluorometer and quality of extractions was assessed using gel electrophoresis. I used both target capture of ultraconserved elements (UCEs) and double digest restriction-site associated DNA sequencing (ddRADseq) to gather genomic-scale data.

The ddRADseq dataset includes 95 specimens (see **Appendix 1.2**). I used the protocol described in Brelsford et al. (2016), using SbfI and MseI enzymes – a combination that increases sequencing depth while accounting for large *Habronattus* genome sizes (~5.586 Gb, Gregory and Shorthouse 2003). Sequencing was completed using 150PE reads on an Illumina Hiseq4000 platform at the University of California Berkeley's QB3 Vincent J. Coates Genomics Sequencing Laboratory.

Raw ddRADseq data were demultiplexed using STACKS v2.3.0 with default settings. The remaining data assembly was completed using iPYRAD v.0.7.30 (Eaton and Overcast 2020). All iPYRAD settings were left as default, with the exception of the

clustering threshold for de novo assembly, set to 90% and the maximum number of indels allowed in a locus, which was set to 5. I created several alignments requiring data for different numbers of individuals in order to retain that locus in the alignment. These include alignments requiring loci to be shared by at least 48 (minsamp48), 24 (minsamp24), 10 (minsamp10), and 4 (minsamp4) individuals (similar to MacGuigan and Near 2018). I also created two smaller alignments that contained fewer samples. The "trimmed" alignment included 67 samples, with a subsampling of individuals from three heavily collected sites (Sonora Pass, Mt. Ashland, and Mt. Hood), in attempt to reduce any sampling bias. The "core" alignment included the minimum number of individuals needed to account for morphological and geographic diversity (n = 40 samples) and required loci to be shared by at least half the samples (24).

I estimated phylogenomic relationships with ddRADseq data using concatenated and coalescent approaches. I concatenated each of the four complete alignments (minsamp 48, minsamp 24, minsamp 10, and minsamp 4) and conducted maximum likelihood tree reconstructions for each minsamp dataset using IQ-Tree v1.2.1 (Nguyen et al. 2015). Branch support was estimated using the ultrafast bootstrap method (Hoang et al. 2018). I ran IQ-Tree with ModelFinder to estimate the correct substitution model (Kalyaanamoorthy et al. 2017). I performed constrained analyses in IQ-Tree v2.0.0 to identify whether my molecular data included any phylogenetic signal (similar to Willis et al. 2013) and to test different topology hypotheses. Two different constrained phylogenetic analyses were completed using each minsamp concatenated alignment and best fit substitution model estimated by ModelFinder. Constraint 1 required currently

described species to form individual clades, without any constraints on internal nodes. Constraint 2 required currently described species to form individual clades, with the addition that morphological variants within each described species were also constrained as clades nested within the species clade. I performed the Shimodaira-Hasegawa (SH test; Shimodaira and Hasegawa 1999) and Kishino-Hasegawa (KH test; Kishino and Hasegawa 1989) tree topology tests implemented in IQ-Tree v2.0 to identify the topology with the highest likelihood score. Species trees for the minsamp datasets were also inferred using unlinked SNPs under the multi-species coalescent using *tetrad* implemented in IQ-Tree v1.2.1 (Nguyen et al. 2015). For each *tetrad* analysis, I sampled all quartets and ran 100 bootstrap replicates. Resulting trees were plotted using a custom R script.

I conducted two STRUCTURE 2.3.4 (Pritchard et al. 2000) analyses under non-admixture and admixture models using the trimmed data matrix of 67 individuals and 810 unlinked SNPs. STRUCTURE was run for clusters K=2 to K=10, each replicated 10 times. Each run included 100,000 generations with the first 10,000 removed as burnin. I used CLUMPAK (Kopelman et al. 2015) to summarize results. Optimal K values were chosen based on the prob(k) method (Pritchard et al. 2000), and I used a custom R script to plot pie charts of admixture proportions onto a map corresponding to sample locations.

To identify possible SNPs associated with each of the 14 morphs, I performed a GEMMA analysis (Zhou and Stephens 2012) on both the minsamp48 unlinked SNPs and all SNPs datasets. Within GEMMA, I used univariate linear mixed models (LMM) to perform the Wald association test, which can identify significant associations between

SNPs and a predefined phenotype. I adjusted p-values for each dataset using the more conservative Bonferroni correction to correct for multiple comparisons; corrected p-values for the unlinked SNPs dataset was 0.0000768 and 0.00000421 for the all SNPs dataset. Results were graphed using a custom R script.

(4) UCE Data Collection & Analysis

The UCE dataset includes 16 ingroup samples from the four *americanus* group species used in morphological analysis and two outgroup individuals (*H. tuberculatus* and *H. aestus*; see **Appendix 1.2**). UCE ingroup specimens were chosen to cover the geographic range of the subgroup, but do not include all morphological variants defined in the morphological analysis. I used the UCE probe set designed for Arachnida (Faircloth et al. 2016), with data collected and sequenced as in Hedin et al. (2020).

Raw UCE data were processed using the Phyluce pipeline (Faircloth et al. 2016). Assemblies were created using Trinity (Haas et al. 2013) within the Phyluce pipeline. Minimum coverage and maximum identity values for probe matching were set to 90. UCE loci were aligned with MAFFT and trimmed using Gblocks at settings: b1 = 0.5, b2 = 0.5, b3 = 8, b4 = 10. Alignments with less than 85% identical sites were flagged for manual examination and edited if necessary, using the program Geneious 11.0.4 (Biomatters). All loci were examined and corrected for large internal gaps in the conserved UCE region and obvious alignment errors.

IQ-Tree v2.0 was used to create a maximum likelihood concatenated UCE phylogeny with branch support estimated with the ultrafast bootstrap method (Nguyen et

al. 2015; Hoang et al. 2018). I used ModelFinder implemented in IQ-Tree to estimate the best substitution model (Kalyaanamoorthy et al. 2017), presuming a single data partition. I measured genealogical concordance using the Concordance Factor function in IQ-Tree v2.0 (Minh et al. 2020). To estimate concordance factors, I used IQ-Tree to infer a maximum likelihood concatenated reference tree with 1000 bootstrap replicates on which concordance factors were annotated. In addition to calculating the gene concordance factor (gCF), this method can also calculate the site concordance factor (sCF), which is useful when gene alignments are relatively uninformative, creating uncertain gene trees (Minh et al. 2020). I suspect my individual UCE locus alignments may be relatively uninformative due to the recent divergence time and extensive gene flow between populations in the *americanus* subgroup.

To test alternative topology hypotheses, I completed constrained analyses for the concatenated UCE dataset using IQ-Tree v2.0.0 using the best fit nuclear substitution model estimated by ModelFinder. I completed two constraint analyses as for the ddRAD data above and performed the KH and SH tree topology tests to identify the most likely topology of each minsamp dataset.

III. RESULTS

(1) Morphological Analyses

Character scorings for all specimens are provided in **Appendix 1.2**. The NMDS plot supports several distinct clusters corresponding loosely to assigned species identity

or morph type (**Figure 1.2)**. There are two distinct *H. kubai* clusters, a southern cluster – comprised of individuals collected in the central Sierra Nevada (*kub* south) and a northern cluster – comprised of samples collected mostly from northern California and Southern Oregon (*kub* north), plus individuals collected from the central Sierra Nevada (HA0939 and HA1469) and near Great Basin National Park (*kub* Great Basin). The *H. americanus* cluster occupies a large area of the NMDS plot, indicating substantial morphological diversity within this species. Previously defined morphs of *H. americanus* (P, PL, PLC; Blackburn and Maddison 2014) and newly defined *H. americanus* morphs fail to cluster together when all characters are analyzed, emphasizing high character variability in *H. americanus*. Based on my NMDS results in conjunction with previously defined morphological types, I identified 17 morphological forms (including one described species with just one morph: *H. bulbipes*): *kub* south, *kub* north, *kub* Great Basin, *sans* white, *sans* red, *sans* SCC, BSK, *bulb*, Gunnison, *amer* PLC, *amer* PL, *amer* P, *amer* PC, *amer* PLE, *amer* Pahvant, *amer* Sevier Lake, and *amer* Manti La Sal (**Appendix 1.1**). The Gunnison and BSK forms are newly identified morphs within the *americanus* subgroup that are not assigned a described species identity. Three newly recognized *H. americanus* morphs were also discovered (*amer* PLE, *amer* Sevier Lake, *amer* Manti La Sal).

(2) ddRAD Data & Analysis

ddRADseq data was recovered for 95 out of 96 samples sequenced. Raw reads are available at the Short Read Archive (BioProject ID: PRJNA716323) and data matrices

are available at Dryad (https://doi.org/10.6086/D16D6B). My trimmed dataset (minsamp = 33) included 810 retained loci with an average of 608 loci per sample. The complete sample datasets included 37687, 8406, 2374, and 655 retained loci after filtering for the minsamp4, minsamp10, minsamp24, and minsamp48 datasets, respectively.

ModelFinder estimated the best fit substitution model for the minsamp4 and minsamp10 datasets as TVM+F+R2 and TPM+F+R3 for the minsamp24 and minsamp48 datasets. IQTREE recovered similar topologies for each concatenated maximum likelihood phylogeny of the complete sample datasets despite different levels of missing data (**Figure 1.3**; **Supplemental Figures 1.1- 1.3**). All four phylogenies identify four major lineages that loosely correspond with geography. The minsamp4, minsamp10, and minsamp24 phylogenies identify similar lineages: Rockies (RO), southern Oregon + northern California (SONC), and Sierra Nevada + southern California (SNSC), and a northern lineage composed of individuals from Oregon + Canada (NO). Lacking an outgroup, the minsamp4, 10, and 24 concatenated phylogenies were rooted between the NO and RO lineages. I chose to root at this branch because it establishes the monophyly of the NO lineage, placing northern *H. sansoni* individuals into a single clade. The minsamp48 phylogeny instead only fully supports the SNSC and NO lineages. The remaining two lineages (RO, SONC) are still present but became paraphyletic (**Supplemental Figure 1.3**). Three specimens move between clades depending on the dataset (HA1123, HA1649, and HA1652). Support for deeper nodes increases with a lower minsamp value, likely due to number of sites used to construct the tree (more sites supporting a specific split = higher bootstrap support). The addition of more sequence

data from RADseq methods has been documented to increase bootstrap support in a system that underwent a rapid radiation event (Wagner et al. 2013); the same could be occurring with my ddRADseq data. I refer to the four geographic groupings present in the minsamp4, 10, and 24 phylogenies moving forward.

The KH and SH topology tests supported topologies for the unconstrained minsamp phylogenies over both constraint topologies for each minsamp dataset (**Table 2;** constraint phylogenies for each minsamp dataset can be found in **Supplemental Figures 1.4 – 1.11**).

Tetrad trees for each minsamp dataset yielded similar topologies to the concatenated IQ-Tree phylogenies (**Supplemental Figures 1.12 – 1.15**). Tetrad phylogenies were rooted similarly to concatenated phylogenies. All minsamp species trees recover four geographical lineages similar to the four geographic groupings (NO, RO, SONC, and SNSC) identified by the concatenated phylogenies. The same individuals that moved between clades in the IQ-Tree phylogenies (HA1123, HA1649, and HA1652) behave similarly in my Tetrad analyses, sometimes forming small clades of their own.

The optimal K value for the admixture STRUCTURE run was chosen as K=3 (**Figure 1.4c**). The three clusters align with geographic location and major phylogenetic lineages, with the exception of the disappearance of the NO lineage in which all NO individuals were included in the SONC cluster (purple). The optimal K value for the non-admixture STRUCTURE run was chosen as K=4 (**Supplemental Figure 1.16**) The four genetic clusters generally follow geography and correspond with major lineages

identified in the phylogenetic analyses. However, individuals collected in southern California are included in three different genetic clusters (NO, RO, SNSC).

GEMMA analyses identified between 0 and 10 significant SNPs in the unlinked SNPs dataset and between 0 and 159 significant SNPs in the all SNPs dataset. The *amer* PL morph had 0 significant SNPs in both datasets (**Supplemental Figures 1.17** [all SNPs] and **1.18** [unlinked SNPs]). Without a reference genome, I cannot identify the genomic location of each significant SNP and am therefore unable to correlate these loci to any known candidate loci (e.g., color genes, etc.).

(3) UCE Data & Analysis

I recovered 260 UCE loci with a mean length of 369bp (**Appendix 1.1)**. The mean number of parsimonious informative sites per locus was only 2.29, indicating that my UCE loci may be too conserved to successfully resolve phylogenetic relationships between populations and species. Raw reads are available at the Short Read Archive (BioProject ID: PRJNA719119) and data matrices are available at Dryad (doi: https://doi.org/10.6086/D16D6B).

ModelFinder estimated the best-fit substitution model for the concatenated UCE alignment as TPM2u+F+R2. The concatenated UCE phylogeny is summarized in **Figure 1.4**. Similar to the ddRADseq phylogenetic analyses, the tree topology appears to reflect geography more than species or morph identity. Each of the four ingroup lineages – here referred to as SONC, Sierra Nevada, west Rockies, and 'A' lineage – includes at least two different species or morphs and most of the lineages contain individuals collected

from specific geographic regions. The UCE lineages only loosely reflect those recovered in ddRADseq analyses. The largest difference being the absence of the NO clade, with individuals from that clade now included in the SONC clade (similar to STRUCTURE K=3 results). Two individuals (HA0333 and HA0449) form the unlikely 'A' lineage, composed of samples collected in southern California and Colorado. The Sierra Nevada lineage includes samples from the central Sierra Nevada mountains, one sample from Wyoming and two British Columba samples; the latter three samples being discordant with the SNSC ddRAD lineage.

The gCF at many nodes appears to be low, ranging from 0% to 32.2% of loci supporting a node split, with all but two nodes below 10% of loci supporting a particular split. The sCF at each node ranges from 28.1% to 94% of sites supporting a particular split. KH and SH tree topology tests supported topologies for the unconstrained UCE phylogeny over both constraint topologies (**Table 1.2;** constraint UCE phylogenies can be found in **Supplemental Figures 1.19** [const 1] and **1.20** [const2]).

IV. DISCUSSION

(1) Morphological-genomic discordance

There is considerable morphological variation both within and between *americanus* subgroup species. While species/morph specific clusters can be identified in my NMDS analysis, most clusters occupy large areas within the plot, highlighting within-species diversity (**Figures 1.1 & 1.2**). *Habronattus kubai* morphs (*kub* south, *kub* north,

kub Great Basin) and *H. sansoni* morphs (*sans* white, *sans* red, and *sans* SCC) both form two distinctly separated clusters, implying morphological diversity within a described species. The NMDS also implies considerable morphological variation within *H. americanus,* however, it is more difficult to identify distinct morphological clusters than within *H. kubai* and *H. sansoni*. Although my morphological character matrix is smaller than that originally used by Griswold (1984), this matrix includes all variable characters within the *americanus* subgroup that could be reliably scored, with the exception of genitalia. Griswold (1984) found that genitalic diversity in the *americanus* subgroup is highly conserved; I doubt that inclusion of such data would identify more clearly separated clusters defined by described species.

Phylogenetic and clustering analysis of genomic data fails to mirror patterns reflected by morphology in *americanus* subgroup individuals. For example, on the ddRAD phylogeny the *kub* north morph is spread between both the SONC and SNSC lineages and the *amer* PL morph is included in all 4 genomic lineages (**Figure 1.3**). Multiple *H. amer* PL morphs are spread throughout the UCE phylogeny and are intermixed with *sans* white and *kub* north morphs in some clades (**Figure 1.4**). STRUCTURE analyses identify genetic clusters that include between three (SNSC) to five (RO and SONC) different species/morphs. All genomic clusters form somewhat geographically cohesive groups despite the number of distinct morphs included within each cluster (**Figure 1.4c**). Most morphological types are not monophyletic in the ddRAD and UCE phylogenies and several morphological types appear in multiple places across the phylogeny (**Figures 1.2** – **1.4**). Constraint topologies that restrict clades to

morphologically described species/morphs were never recovered as the most likely topology for any dataset (**Table 1.2**), supporting both signal in the genomic data, and discordance between morphology and genomic data.

(2) Prior *Habronattus* Studies Supporting Introgression

A genus-wide transcriptome study identified evidence of introgression affecting phylogenetic relationships at several levels within *Habronattus*, including within and between species groups (Leduc-Robert and Maddison 2018). In particular, evidence supported admixture between members of the *americanus* group (see figure 4, Leduc-Robert and Maddison 2018). Evidence for intraspecific introgression within *H. americanus* in the Sierra Nevada has also been documented, where different *H. americanus* morphs remained distinct despite genome wide IH (Blackburn and Maddison 2014). Since previous studies did not include all *americanus* subgroup species and/or divergent morph types, effects of IH on specific phylogenetic relationships between members of the *americanus* subgroup were not examined.

Here, I identified patterns of geographically defined phylogenetic lineages within the *americanus* subgroup across different tree reconstruction methods, including a multispecies coalescent method (MSC; **Supplemental Figures 1.12 – 1. 15**). Traditionally, MSC approaches can be used to identify underlying patterns of divergence that might go undetected in concatenated datasets, because of the increased variance with the addition of many loci, or failure of concatenated approaches to identify signal from less variable loci (Maddison 1997; Willis et al. 2013). However, my tetrad species trees

mostly coincided with concatenation results, supporting geographically defined genetic lineages.

UCE lineages also remain primarily defined by geographic location (**Figure 1.4**). Small shifts in lineage composition from ddRADseq data is expected because of differences in number of samples, individuals included (species/morph and population identity), and lower resolution of the UCE data. The utility of UCEs to estimate phylogenetic relationships has been documented at multiple taxonomic levels, including recently diverged taxa (Smith et al. 2014; Starrett et al. 2017). However, my UCE data, like my ddRAD data, remained unable to detect the complete *americanus* subgroup speciation signal. My phylogenomic analyses of both ddRADseq data and UCE data suggest that a homogenizing force is acting on the genomes of *americanus* subgroup members. Below I discuss alternative scenarios that may have led to genomic homogenization.

(3) Competing models of divergence

I define my null hypothesis as one in close agreement with the taxonomy proposed by Griswold (1987) with four named species – *H. americanus* (all forms), *H. sansoni* (red, white, SCC forms), *H. kubai* (north, south, Great Basin forms), *H. bulbipes* – and two unnamed forms – BSK, Gunnison. I discuss below two alternative hypotheses that could explain the evolutionary patterns I recovered in the *americanus* subgroup (*although more might apply*): (A) species as defined above (i.e., the null hypothesis),

with introgression within geographic centers, and (B) the *americanus* subgroup is instead comprised of several geographically localized, highly polymorphic species.

Null Hypothesis. Introgression within geographic centers

Introgression within geographic centers could explain the patterns I recovered in genomic and morphological datasets under my null hypothesis. The *americanus* subgroup is estimated at only 200,000 years old (Hedin et al. 2020), subjecting evolving populations to climatic shifts during the Pleistocene epoch (2,580,000 – 11,700 years ago). Previous studies in other systems suggest that climatic events during the Pleistocene likely isolated populations to smaller refugia, affecting population genetic structure, genetic diversity and lineage divergence (e.g., Hewitt 1996; Shafer 2010; Hewitt 2011). As glacial ice retreated, population ranges likely expanded, possibly enabling contact with other previously isolated populations (Davis 2001). It is possible to imagine this scenario for *americanus* subgroup species, as they inhabit regions throughout western North America (Griswold 1987) that were impacted by glaciation events. Additionally, several current hybrid zones are found at elevations that were likely covered in glacial ice as recently as the last glacial maximum (LGM), including Sonora Pass (~2700 m), Mt. Shasta (~2350 m), Mt. Ashland (~2000 m), and Mt. Hood (~960 m).

Climatic changes may have enabled divergent *americanus* subgroup populations to come into secondary contact following range expansions (e.g., Maddison and McMahon 2000); current hybrid zones may be testament to this. A lack of complete reproductive isolation between diverging *americanus* subgroup species/morphs could

have allowed for IH, enabling gene exchange across species boundaries. In conjunction with a recent and rapid divergence, hybridization between species/morphs in close geographic proximity could explain genomic results where I recovered lineages and admixture proportions defined by geographic location rather than morphological identity (**Figure 1.3, 1.4**). I used the MSC in effort to identify underlying patterns of divergence that concatenation may have failed to identify. However, species trees also failed to recover groups defined by morphology (**Supplemental Figures 1.12 – 1.15**). Rapid radiation events, like those that occurred within *Habronattus* (Leduc-Robert and Maddison 2018) encourage the retention of ancestral variation, causing conflicts between the most probable gene tree and the species branching pattern; this discordance is further exacerbated when hybridization is present (Maddison 1997).

Because sexual selection is believed to be strong in *Habronattus* (Peckham and Peckham 1889; Peckham and Peckham 1890; Masta and Maddison 2002; Elias et al. 2003; Hebets and Maddison 2005; Elias et al. 2006; Elias et al. 2012), it may be expected that genomic regions underlying male phenotypes are under strong selection relative to other areas of the genome (e.g., male *Lycaeides* characters, Nice and Shapiro 1999; Nice et al. 2005; Gompert et al. 2008). If this is the case in the *americanus* subgroup, then selection has maintained male morphologies despite widespread genome homogenization. GEMMA results appear to support this scenario by identifying at least one significant SNP associated with each morph, aside from *amer* PL (**Supplemental Figures 1.17** and **1.18**). Although I cannot identify where in the genome these SNPs are located or what specific trait they are correlated with, these results are consistent with

small genomic regions differentiating morphs in some way. Of course, ddRAD loci are likely not dense enough to capture all SNPs associated with the morphs. I might also expect sexual selection to reinforce membership in species/morph clades. Instead, my results suggest that while sexual selection may be preserving divergent male phenotypes, widespread introgression in remaining parts of the genome could be swamping any speciation signal, resulting in a pattern of little correlation between species boundaries and genetic markers (similar to *Lycaeides*, Nice and Shapiro 1999; Nice 2005; Gompert et al. 2008). To summarize, if I accept the null hypothesis, *americanus* subgroup individuals likely speciated along color lines (male morphologies) followed by introgression within geographic regions, leading to rejection of a typical bifurcating evolutionary model (Gompert et al. 2014).

Alternative Hypothesis. americanus subgroup taxa are composed of four polymorphic species

This hypothesis rejects the current taxonomy, instead favoring the presence of several highly polymorphic species; these four species include SONC, SNSC, RO, and NO, unless noted otherwise. This scenario intuitively fits with my phylogenomic data where species lineages correlate with geography. High levels of morphological diversity in these species and shared morphs across species could have occurred via maintained ancestral polymorphism at color loci, in a manner similar to that described by Jamie and Meier (2020). These authors describe three non-exclusive processes that could lead to identical polymorphisms across species: inheritance via ancestral variation, mutation, and

introgression. Guerrero and Hahn (2017) describe how ancestral polymorphisms may remain present in descending species via a speciation sieve-like process, where balancing selection in an ancestral species eventually leads to fixation of different allelic classes in diverging lineages (see figure 1, Guerrero and Hahn 2017). If balancing selection is no longer acting on these alleles in descendent species, the result is blocks of highly diverged and selectively neutral haplotypes between species that can persist through several speciation events, resulting in species pairs sharing sieved regions (Campagna et al. 2017; Guerrero and Han 2017).

Under the sieve hypothesis, each geographically defined *americanus* subgroup species may share neutral, fixed polymorphic alleles (and additional linked genes) near ancestral loci that were once under strong selection, which may include color traits. However, the likelihood that identical polymorphisms across species could be the only cause for such variation within and among species in the group seems unlikely. Differences in male morphs are determined by more than one trait and almost certainly more than one genetic locus. While reports of selection maintaining polymorphisms at a single locus and recurring in multiple members of a species radiation are well documented (see Table 1, Jamie and Meier 2020), few cases demonstrate this occurrence in a multilocus setting (Llaurens et al. 2017), although still theoretically possible (Turelli and Barton 2004). I view it as unlikely that the loci responsible for morph variation in *americanus* subgroup species were both maintained from ancestral polymorphism and sieved in populations of each species in such a way that leads to a clear, congruent morphological pattern. However, if I accept that color polymorphisms could account for

at least some of the morphological variation, such polymorphisms would need to be maintained. If polymorphisms were a result of a speciation sieve, they may be selectively neutral and easily remain in each species. Alternatively, some form of negative frequency dependent selection that is not dependent on a population's ecology (e.g., NFDS on alternative mating types) – ecologies shared across geographic regions (here species) are similar in many cases– could be responsible for maintaining polymorphisms across species (Jamie and Meier 2020). However, there is currently no evidence that any morph type has a selective benefit over others, likely ruling out convergence as a means responsible for identical morph types occurring in different genetic lineages.

Introgression, the third process that Jamie and Meier (2020) describe for shared polymorphisms across species, is present throughout the history of *Habronattus* (Masta 2000; Maddison and Hedin 2003; Hedin and Lowder 2009; Blackburn and Maddison 2014; Leduc-Robert and Maddison 2018; Hedin et al. 2020). Such IH could have introduced additional variation in the ancestor of the *americanus* subgroup. It is also possible that throughout the recent divergence of the four geographic species, some populations came into contact with others, enabling hybridization and subsequent introgression. Similar to my null hypothesis, biogeographic conditions could have brought diverging species together as the climate shifted, resulting in introgression of male color morphs to each of the four geographically defined species. Therefore, the regional species may exhibit identical male morphological traits across species and highly variable traits within species due to both retention of ancestral polymorphism and introgression.

My genomic data could support a scenario similar to the alternative hypothesis, although my STRUCTURE results would support only three "species" (**Figure 1.4**) instead of the four recovered in my phylogenomic analyses (**Figure 1.3**). This hypothesis assumes only four species that have extreme morphological diversity through retention of polymorphisms and/or gene flow via introgression. While this is a possibility, it seems unlikely considering that in most populations, there is only a single male morph represented. If these lineages did correspond to four highly polymorphic and morphologically diverse species, with little evidence for any selective benefit of different male morphs, it might be expected that several morph types would be present at a single collection locality. This occurrence is relatively rare, only observed at a few locations where different morph types hybridize (**Figure 1.1)**.

V. CONCLUSIONS

Additional research is needed to identify whether the *americanus* subgroup speciated along color lines followed by introgression within geographic centers (null hypothesis) or along geographic lines with retention of polymorphism at a few color genes and/or introgression between diverging lineages (alternative hypothesis). Evidence presented here suggests that the former hypothesis is more likely, but I cannot confidently reject the latter. Identification of divergent genomic loci responsible for different male phenotypes could provide insight into speciation modes and how different morphs developed (Campagna et al. 2017). Mating experiments and additional population genetic

analyses at hybrid zone sites could aid in identifying the directionality of gene flow – e.g., are *H. americanus* females promoting hybridization by choosing males of different species or are all *H. americanus* subgroup females choosing heterospecific mates? It is clear that many questions remain to be answered in this system. However, opportunities for future research could lead to new discoveries in speciation and evolutionary dynamics of rapidly radiating and highly diverse systems.

Regardless of the mode of divergence, it appears the *americanus* subgroup is evolving as a complex unit of closely related taxa. Currently described species and newly identified morphs might be categorized as "nascent" species – defined as recently-diverged lineages not yet having developed intrinsic reproductive isolation (Cutter and Gray 2016). Complete reproductive isolation has not yet been established in the *americanus* subgroup, as species readily hybridize in rare areas of sympatry, and the group appears to be very young. As such, *americanus* subgroup members share both characteristics of nascent species.

Frequent introgression between nascent species might make them susceptible to population fusion – an avenue leading to extinction (Rhymer and Simberloff 1996). It is possible that throughout the evolution of this group, some lineages succumbed to lineage fusion as gene flow from frequent introgression overwhelmed any divergent selection. Alternatively, frequent IH between evolving *americanus* subgroup members might have led to speciation through combinatorial mechanisms (Marques et al. 2019). As such, the same force that might have been creating nascent species also possibly reabsorbed nascent species in the *americanus* subgroup. This cycle of ephemeral speciation

throughout the evolutionary history of this group could lead to the extreme genomic homogenization identified today, where only small divergent areas of the genome responsible for species identity remain differentiated.

Systems experiencing rapid radiations and substantial hybridization challenge the current understanding of speciation and evolution. As introgression acts as a powerful force promoting radiation, it can be beneficial to think about each radiating cluster as a single community. The community is composed of closely related species that actively share genetic material and may compete for resources, but essentially evolve as a single lineage (Zhang et al. 2019; Buck and Flores-Rentería 2022). An increasing number of studies are calling into question the traditional bifurcating model of evolution/speciation, supporting instead a reticulate pattern with multifurcating branches (Abbott et al. 2013; Mallet et al. 2016; Wen et al. 2016). It appears as though the *americanus* subgroup falls into the category of a complex of closely related, nascent species evolving together through multiple introgression events creating a reticulate evolutionary history.

VI. REFERENCES

Abbott, R., Albach, D., Ansell, S., Arntzen, J. W., Baird, S. J. E., Bierne, N., Boughman, J., Brelsford, A., Buerkle, C.A., Buggs, R., Butlin, R.K., Dieckmann, U., Eroukhmanoff, F., Grill, A., Cahan, S.H., Hermansen, J.S., Hewitt, G., Hudson, A.G., Jiggins, C., Jones, J., Keller, B., Marczewski, T., Mallet, J., Martinez-Rodriguez, P., Möst, M., Mullen, S., Nichols, R., Nolte, A.W., Parisod, C., Pfennig, K., Rice, A.M., Ritchie, M.G., Seifert, B., Smadja, C.M., Stelkens, R., Szymura, J.M., Väinölä, R., Wolf, J.B.W., Zinner, D., 2013. Hybridization and speciation. J. Evol. Biol. 26 (2), 229–246. Doi: 10.1111/j.1420-9101.2012.02599.x

Abbott, R.J., Barton, N.H., Good, J.M., 2016. Genomics of hybridization and its evolutionary consequences. Mol. Ecol. 25 (11), 2325–2332. Doi: 10.1111/mec.13685

Alexander, A.M., Su, Y.-C., Oliveros, C.H., Olson, K.V., Travers, S.L., Brown, R.M., 2017. Genomic data reveals potential for hybridization, introgression, and incomplete lineage sorting to confound phylogenetic relationships in an adaptive radiation of narrow-mouth frogs: Brief Communication. Evol. 71 (2), 475–488. Doi: 10.1111/evo.13133

Blackburn, G.S., & Maddison, W.P., 2014. Stark sexual display divergence among jumping spider populations in the face of gene flow. Mol. Ecol. 23 (21), 5208–5223. Doi: 10.1111/mec.12942

Brelsford, A., Toews, D.P.L., Irwin, D.E., 2017. Admixture mapping in a hybrid zone reveals loci associated with avian feather coloration. P. Royal Soc. B: Biol. Sci. 284 (1866), 20171106. Doi: 10.1098/rspb.2017.1106

Buck R, Flores-Rentería L., 2022. The syngameon enigma. Plants (Basel). 11 (7), 895. Doi: 10.3390/plants11070895.

Campagna, L., Repenning, M., Silveira, L.F., Fontana, C.S., Tubaro, P.L., Lovette, I.J., 2017. Repeated divergent selection on pigmentation genes in a rapid finch radiation. Sci. Adv. 3 (5), e1602404. Doi: 10.1126/sciadv.1602404

Cote, C.L., Gagnaire, P.A., Bourret, V., 2013. Population genetics of the American eel (*Anguilla rostrata*): FST=0 and North Atlantic Oscillation effects on demographic fluctuations of a panmictic species. Mol. Ecol. 22 (7), 1763-1776. Doi: https://doi.org/10.1111/mec.12142

Cui, R., Schumer, M., Kruesi, K., Walter, R., Andolfatto, P., Rosenthal, G.G., 2013. Phylogenomics reveals extensive reticulate evolution in *Xiphophorus* fishes: phylogenomics of *Xiphophorus* fishes. Evolution. 67 (8), 2166–2179. Doi: 10.1111/evo.12099

Cutter, A.D., Gray, J.C., 2016. Ephemeral ecological speciation and the latitudinal biodiversity gradient: perspective. Evolution. 70 (10), 2171–2185. Doi: 10.1111/evo.13030

Davis, M.B., 2001. Range Shifts and Adaptive Responses to Quaternary Climate Change. Science. 292 (5517), 673–679. Doi: 10.1126/science.292.5517.673

Degnan, J.H., Rosenberg, N.A., 2009. Gene tree discordance, phylogenetic inference and the multispecies coalescent. Trends. Evol. 24 (6), 332–340. Doi: 10.1016/j.tree.2009.01.009

Eaton D.A.R, Overcast I., 2020. Ipyrad: Interactive assembly and analysis of RADseq datasets. http://ipyrad.readthedocs.io

Elias, D.O., 2003. Seismic signals in a courting male jumping spider (Araneae: Salticidae). J. Exp. Biol. 206 (22), 4029–4039. Doi: 10.1242/jeb.00634

Elias, Damian O., Hebets, E.A., Hoy, R.R., 2006. Female preference for complex/novel signals in a spider. Behav. Ecol. 17 (5), 765–771. Doi: 10.1093/beheco/arl005

Elias, D.O., Maddison, W.P., Peckmezian, C., Girard, M.B., Mason, A.C., 2012. Orchestrating the score: complex multimodal courtship in the *Habronattus coecatus* group of *Habronattus* jumping spiders (Araneae: Salticidae): multimodal courtship in *Habronattus*. Biol. J. Linn. Soc. 105 (3), 522–547. Doi: 10.1111/j.1095-8312.2011.01817.x

Faircloth, B.C., 2016. PHYLUCE is a software package for the analysis of conserved genomic loci. Bioinformatics. 32, 786-788.

Fontaine, M.C., Pease, J.B., Steele,A., Waterhouse, R.M., Neafsey, D.E., Sharakhov, I.V., Jiang, X., Hall, A.B., Catteruccia, F., Kakani, E., Mitchell, S.N., Wu, Y.-C., Smith, H.A., Love, R.R., Lawniczak, M.K., Slotman, M.A, Emrich, S.J., Hahn, M.H., Besansky, N.J., 2015. Extensive introgression in a malaria vector species complex revealed by phylogenomics. Science. 347 (6217), 1258524. Doi : 10.1126/science.1258524

Gompert, Z., Forister, M.L., Fordyce, J.A., Nice, C.C., 2008. Widespread mito-nuclear discordance with evidence for introgressive hybridization and selective sweeps in *Lycaeides*. Mol. Ecol. 17 (24), 5231–5244. Doi: 10.1111/j.1365-294X.2008.03988.x

Gompert, Z., Lucas, L.K., Buerkle, C.A., Forister, M.L., Fordyce, J. A., Nice, C.C., 2014. Admixture and the organization of genetic diversity in a butterfly species complex revealed through common and rare genetic variants. Mol. Ecol. 23 (18), 4555–4573. Doi: 10.1111/mec.12811

Grant, P. R., 2002. Unpredictable Evolution in a 30-Year Study of Darwin's Finches. Science. 296 (5568), 707–711. Doi: 10.1126/science.1070315

Gregory, T. R., 2003. Genome Sizes of Spiders. J. Hered. 94 (4), 285–290. Doi: 10.1093/jhered/esg070

Griswold, C.E., 1987. A revision of the jumping spider genus Habronattus F.O.P. Cambridge (Araneae; Salticidae), with phenetic and cladistic analyses. Univ. California Pub. Ent. 107, 1-344.

Guerrero, R.F., Hahn, M.W., 2017. Speciation as a sieve for ancestral polymorphism. Mol. Ecol. 26 (20), 5362–5368. Doi: 10.1111/mec.14290

Haas, B. J., Papanicolaou, A., Yassour, M., Grabherr, M., Blood, P.D., Bowden, J., Couger, M.B., Eccles, D., Li, B., Lieber, M., MacManes, M.D., Ott, M., Orvis, J., Pochet, N., Strozzi, F., Weeks, N., Westerman, R., William, Thomas., Dewey, C.N., Henschel, R., LeDuc, R.D., Friedman, N., Regev, A. (2013). De novo transcript sequence reconstruction from RNA-seq using the Trinity platform for reference generation and analysis. Nat. Protoc. 8(8), 1494–1512. Doi: 10.1038/nprot.2013.084

Han, F., Lamichhaney, S., Grant, B.R., Grant, P.R., Andersson, L., Webster, M.T., 2017. Gene flow, ancient polymorphism, and ecological adaptation shape the genomic landscape of divergence among Darwin's finches. Genome Res. 27 (6), 1004–1015. Doi: 10.1101/gr.212522.116

Hebets, E.A., Maddison, W.P., 2005. Xenophilic mating preferences among populations of the jumping spider *Habronattus pugillis* Griswold. Behav. Ecol. 16 (6), 981–988. Doi: 10.1093/beheco/ari079

Hedin, M., Foldi, S., Rajah-Boyer, B., 2020. Evolutionary divergences mirror Pleistocene paleodrainages in a rapidly-evolving complex of oasis-dwelling jumping spiders (Salticidae, *Habronattus tarsalis*). Mol. Phylogenet. Evol. 144, 106696. Doi: 10.1016/j.ympev.2019.106696

Hedin, M., Lowder, M.C., 2009. Phylogeography of the *Habronattus* amicus species complex (Araneae: Salticidae) of western North America, with evidence for localized asymmetrical mitochondrial introgression. Zootaxa. 2307 (1), 39–60. Doi: 10.11646/zootaxa.2307.1.2

The Heliconius Genome Consortium, 2012. Butterfly genome reveals promiscuous exchange of mimicry adaptations among species. Nature. 487 (7405), 94-98. Doi: 10.1038/nature11041. Doi: 10.1038/nature11041

Hewitt, G., 1996. Some genetic consequences of ice ages, and their role in divergence and speciation. Biol. J. Linn. Soc. 58 (3), 247–276. Doi: 10.1006/bijl.1996.0035

Hewitt, G.M., 2011. Quaternary phylogeography: the roots of hybrid zones. Genetica. 139 (5), 617–638. Doi: 10.1007/s10709-011-9547-3

Hoang, D.T., Chernomor, O., von Haeseler, A., Minh, B.Q., Vinh, L.S., 2018. UFBoot2: Improving the ultrafast bootstrap approximation. Mol. Biol. Evol. 35 (2), 518–522. Doi: 10.1093/molbev/msx281

Jamie, G.A., Meier, J.I., 2020. The Persistence of Polymorphisms across Species Radiations. Trends Ecol. Evol. S0169534720301117. Doi: 10.1016/j.tree.2020.04.007

Jiggins, C.D., Naisbit, R.E., Coe, R.L., Mallet, J., 2001. Reproductive isolation caused by colour pattern mimicry. Nature. 411 (6835), 302–305. Doi: 10.1038/35077075

Jiggins, C.D., Salazar, C., Linares, M., Mavarez, J., 2008. Hybrid trait speciation and *Heliconius* butterflies. Philos. T. R. Soc. B: Biol. Sci. 363 (1506), 3047–3054. Doi: 10.1098/rstb.2008.0065

Kearns, A.M., Restani, M., Szabo, I., Schrøder-Nielsen, A., Kim, J.A., Richardson, H.M., Marzluff, J.M., Fleicher, R.C., Johnson, A., Omland, K.E., 2018. Genomic evidence of speciation reversal in ravens. Nat. Commun. 9 (1), 906. Doi: 10.1038/s41467-018-03294-w

Kishino, H., Hasegawa, M., 1989. Evaluation of the maximum likelihood estimate of the evolutionary tree topologies from DNA sequence data, and the branching order in *Hominoidea*. J. Mol. Evol. 29 (2), 170–179. Doi: 10.1007/BF02100115

Kleindorfer, S., O'Connor, J.A., Dudaniec, R.Y., Myers, S.A., Robertson, J., Sulloway, F.J., 2014. Species collapse via hybridization in Darwin's tree finches. Am. Nat. 183 (3), 325–341. Doi: 10.1086/674899

Kopelman, N.M., Mayzel, J., Jakobsson, M., Rosenberg, N.A., Mayrose, I., 2015. CLUMPAK : a program for identifying clustering modes and packaging population structure inferences across K. Mol. Ecol. Resour. 15 (5), 1179–1191. Doi: 10.1111/1755-0998.12387

Leduc-Robert, G., Maddison, W.P., 2018. Phylogeny with introgression in *Habronattus* jumping spiders (Araneae: Salticidae). BMC Evol. Biol. 18 (1), 24. Doi: 10.1186/s12862-018-1137-x

Llaurens, V., Whibley, A., Joron, M., 2017. Genetic architecture and balancing selection: the life and death of differentiated variants. Mol. Ecol. 26 (9), 2430–2448. Doi: https://doi.org/10.1111/mec.14051

MacGuigan, D.J., Near, T.J., 2019. Phylogenomic signatures of ancient introgression in a rogue lineage of darters (Teleostei: Percidae). Syst. Biol. 68 (2), 329–346. Doi: 10.1093/sysbio/syy074

Maddison, W., Hedin, M., 2003. Phylogeny of *Habronattus* jumping spiders (Araneae: Salticidae), with consideration of genital and courtship evolution: *Habronattus* spider phylogeny. Syst. Entomol. 28 (1), 1–22. Doi: 10.1046/j.1365-3113.2003.00195.x

Maddison, W.P., 1997. Gene trees in species trees. Syst. Biol., 14 (3), 523-536.

Malinsky, M., Challis, R.J., Tyers, A.M., Schiffels, S., Terai, Y., Ngatunga, B.P., Miska, E.A., Durbin, R., Genner, M.J., Turner, G.F., 2015. Genomic islands of speciation separate cichlid 37ctomorphs in an East African crater lake. Science, 350 (6267), 1493–1498. Doi : 10.1126/science.aac9927

Mallet, J., Besansky, N., Hahn, M.W., 2016. How reticulated are species? BioEssays. 38 (2), 140–149. Doi: 10.1002/bies.201500149

Marques, D.A., Meier, J.I., Seehausen, O., 2019. A combinatorial view on speciation and adaptive radiation. Trends Ecol. Evol. 34 (6), 531–544. Doi: 10.1016/j.tree.2019.02.008

Martin, S.H., Dasmahapatra, K.K., Nadeau, N.J., Salazar, C., Walters, J.R., Simpson, F., Blaxter, M., Manica, A., Mallet, J., Jiggins, C.D., 2013. Genome-wide evidence for speciation with gene flow in *Heliconius* butterflies. Genome Res. 23 (11), 1817–1828. Doi: 10.1101/gr.159426.113

Martin, S.H., Davey, J.W., Salazar, C., Jiggins, C.D., 2019. Recombination rate variation shapes barriers to introgression across butterfly genomes. PLOS Biol. 17 (2), e2006288. Doi: 10.1371/journal.pbio.2006288

Masta, S.E., Maddison, W.P., 2002. Sexual selection driving diversification in jumping spiders. Proc. Natl. Acad. Sci. 99 (7), 4442–4447. Doi: 10.1073/pnas.072493099

Meier, J.I., Marques, D.A., Mwaiko, S., Wagner, C.E., Excoffier, L., Seehausen, O., 2017. Ancient hybridization fuels rapid cichlid fish adaptive radiations. Nat. Commun. 8 (1), 14363. Doi: 10.1038/ncomms14363

Minh, B.Q., Hahn M.W., Lanfear, R., 2020. New methods to calculate concordance factors for phylogenomic datasets. Mol. Biol. Evol. In press. https://doi.org/10.1093/molbev/msaa106

Nadeau, N.J., Martin, S.H., Kozak, K.M., Salazar, C., Dasmahapatra, K.K., Davey, J. W., Baxter, S.W., Blaxter, M.L., Mallet, J., Jiggins, C.D., 2013. Genome-wide patterns of divergence and gene flow across a butterfly radiation. Mol. Ecol. 22 (3), 814–826. Doi: 10.1111/j.1365-294X.2012.05730.x

Nguyen, L.-T., Schmidt, H.A., von Haeseler, A., Minh, B.Q., 2015. IQ-TREE: A fast and effective stochastic algorithm for estimating maximum-likelihood phylogenies. Mol. Biol. Evol. 32 (1), 268–274. Doi: 10.1093/molbev/msu300

Nice, C.C., Shapiro, A.M., 1999. Molecular and morphological divergence in the butterfly genus *Lycaeides* (Lepidoptera: Lycaenidae) in North America: evidence of recent speciation. J. Evol. Biol. 12 (5), 936–950. Doi: 10.1046/j.1420-9101.1999.00111.x

Nice, C.C., Anthony, N., Gelembiuk, G., Raterman, D., Ffrench-Constant, R., 2005. The history and geography of diversification within the butterfly genus *Lycaeides* in North America. Mol. Ecol. 14 (6), 1741–1754. Doi: 10.1111/j.1365-294X.2005.02527.x

Poelstra, J.W., Vijay, N., Bossu, C.M., Lantz, H., Ryll, B., Muller, I., Baglione, V., Unneberg, P., Wikelski, M., Grabherr, M.G., Wolf, J.B.W., 2014. The genomic landscape underlying phenotypic integrity in the face of gene flow in crows. Science, 344 (6190), 1410–1414. Doi : 10.1126/science.1253226

Pritchard, J.K., Stephens, M., Donnelly, P., 2000. Inference of population structure using multilocus genotype data. Genetics. 155, 945-959

Rhymer, J.M., Simberloff, D., 1996. Extinction by hybridization and introgression. Annu. Rev. Ecol. Syst. 27 (1), 83–109. Doi: 10.1146/annurev.ecolsys.27.1.83

Rieseberg, L.H., 2003. Major ecological transitions in wild sunflowers facilitated by hybridization. Science, 301 (5637), 1211–1216. Doi: 10.1126/science.1086949

Seehausen, O., 2004. Hybridization and adaptive radiation. Trends Ecol.Evol. 19 (4), 198–207. Doi: 10.1016/j.tree.2004.01.003

Seehausen, O., 2006. Conservation: Losing Biodiversity by Reverse Speciation. Curr. Biol. 16 (9), R334–R337. Doi: 10.1016/j.cub.2006.03.080

Shafer, A.B.A., Cullingham, C. I., Côté, S.D., Coltman, D.W., 2010. Of glaciers and refugia: a decade of study sheds new light on the phylogeography of northwestern North America. Mol. Ecol. 19 (21), 4589–4621. Doi: 10.1111/j.1365-294X.2010.04828.x

Shimodaira, H., Hasegawa, M., 1999. Multiple comparisons of log-likelihoods with applications to phylogenetic inference. Mol. Biol. Evol.16 (8), 1114–1116. Doi: 10.1093/oxfordjournals.molbev.a026201

Smith, B.T., Harvey, M.G., Faircloth, B.C., Glenn, T.C., Brumfield, R.T., 2014. Target capture and massively parallel sequencing of ultraconserved elements for comparative studies at shallow evolutionary time scales. Syst. Biol. 63 (1), 83–95. Doi: 10.1093/sysbio/syt061

Starrett, J., Derkarabetian, S., Hedin, M., Bryson, R.W., McCormack, J.E., Faircloth, B. C. (2017). High phylogenetic utility of an ultraconserved element probe set designed for Arachnida. Mol. Ecol. Resour., 17 (4), 812–823. Doi: 10.1111/1755-0998.12621

Strimmer, K., Rambaut, A., 2001. Inferring confidence sets of possibly misspecified gene trees. Proc. R. Soc. Lond. 269, 137-142.

Stryjewski, K.F., Sorenson, M.D., 2017. Mosaic genome evolution in a recent and rapid avian radiation. Nat. Ecol. Evol. 1(12), 1912–1922. Doi: 10.1038/s41559-017-0364-7

Taylor, E.B., Boughman, J.W., Groenenboom, M., Sniatynski, M., Schluter, D., Gow, J.L., 2005. Speciation in reverse: morphological and genetic evidence of the collapse of a three-spined stickleback (Gasterosteus aculeatus) species pair: collapse of a stickleback species pair. Mol. Ecol. 15 (2), 343–355. Doi: 10.1111/j.1365-294X.2005.02794.x

Taylor, L.A., Powell, E.C., McGraw, K.J., 2017. Frequent misdirected courtship in a natural community of colorful *Habronattus* jumping spiders. PloS One. 12, 1-19

Toews, D.P.L., Brelsford, A., Grossen, C., Milá, B., Irwin, D.E., 2016. Genomic variation across the Yellow-rumped Warbler species complex. Auk. 133 (4), 698–717. Doi: 10.1642/AUK-16-61.1

Turelli, M. and Barton, N., 2004. Polygenic variation maintained by balancing selection: pleiotropy, sex-dependent allelic effects and Gx E interactions. Genetics. 166 (2), 1053–1079. Doi: 10.1534/genetics.166.2.1053

Wen, D., Yu, Y., Hahn, M.W., Nakhleh, L., 2016. Reticulate evolutionary history and extensive introgression in mosquito species revealed by phylogenetic network analysis. Mol. Ecol. 25 (11), 2361–2372. Doi: 10.1111/mec.13544

West-Eberhard, M.J., 1983. Sexual selection, social competition, and speciation. Q. Rev. Biol. 58 (2), 155–183. Doi: 10.1086/413215

Willis, S.C., Farias, I.P., Ortí, G., 2013. Multi-locus species tree for the Amazonian peacock basses (Cichlidae: Cichla): Emergent phylogenetic signal despite limited nuclear variation. Mol. Phylogenet. Evol. 69 (3), 479–490. Doi: 10.1016/j.ympev.2013.07.031

Zhang, J., Cong, Q., Shen, J., Opler, P.A., Grishin, N.V., 2019. Genomics of a complete butterfly continent. bioRxiv. Doi: 10.1101/829887

Zhou, X. and Stephens, M., 2012. Genome-wide efficient mixed-model analysis for association studies. Nat. Genet. 44, 821-824

Zurek, D.B., Cronin, T.W., Taylor, L.A., Byrne, K., Sullivan, M.L.G., Morehouse, N.I., 2015. Spectral filtering enables trichromatic vision in colorful jumping spiders. Curr. Biol. 25 (10), R403–R404. Doi: 10.1016/j.cub.2015.03.033

Tables

Table 1.1. Description of morphological characters and character states used to score morphological traits

.

ID	Description	States
A	Crest above AER: long erect hairs above the AER form a row or crest along posterior margin of the AER. Erect "eyebrows."	0 = absent; 1 = present
B	Centrally located white setae above AME	States: 0 = absent; 1 = spot; 2 = stripe
C	Iridescent scales – pattern: variable within species, may have iridescent patches, or completely iridescent clypeus.	0 = absence of iridescent scales; 1 = full rectangular; 2 = flat center, flared at ends; 3 = 'm' shaped 4 = four broken segments; 5 = low, four connected segments; 6 = low single, long segment on bottom of clypeus
D	Clypeal covering emarginate: clypeus covered with two scale types and/or colors forming a well-marked white transverse band	0 = absent/no white band; 1 = spans entire length of AER; 2 = present only under AMEs; 3 = present only under ALEs; 4 = spans entire length of AER, but thicker towards the ALEs expanding down to the side of the iridescence
E	Color of non-iridescent setae on clypeus, NOT including white transverse band if present.	0 = all of clypeus covered in iridescence; 1 = brown; 2 = black; 3 = black and white; 4 = black and tan; 5 = black, white, and red
F	Clypeal covering divided in center	States: 0 = absent/not divided; 1 = divided
G	Clypeus with vertical bands that extends above AER: clypeal integument marked with dark vertical bands that may between AME and ALE to oral margin, with pale vertical band between these.	0 = no banding pattern; 1 = two dark bands above AMEs (SCC) only; 2 = two dark bands extending from above AMEs to oral margin; 3 = two dark bands extending from above AMEs to just below AMEs, 4 = two dark vertical bands extending from above AMEs to oral margin bisected with red bands
H	Color of hair pencils/hairs covering chelicerae	States: 0 = blue; 1 = red; 2 = pale/white; 3 = yellow/gold; 4 = no hair pencils; 5 = dull red; 6 = tan/light brown; 7 = gold with black spot in middle
I	Presence of hair pencils covering chelicerae	States: 0 = absent; 1 = present; 2 = present, but very thin; 3 = present, but halfway cover the chelicerae
J	Leg I femur: Ventral fringe of elongate scales	States: 0 = absent; 1 = present
K	Leg I femur: Color of ventral side	0 = brown/dark; 1 = white/pale; 2 = yellow; 3 = orange + white; 4 = red; 5 = speckled tan and black; 6 = rusty red
L	Leg I femur: pattern	States: 0 = longitudinally striped; 1 = speckled; 2 = plain; 3 = cross between speckled and striped
M	Leg I tibia: Ventral fringe of elongate scales	States: 0 = absent; 1 = present
N	Leg I tibia: Color of ventral side	States: 0 = brown/dark; 1 = white/pale; 2 = yellow; 3 = orange; 4 = red, 5 = speckled tan and black; 6 = rusty red

O	Leg I tibia: pattern	States: 0 = longitudinally striped; 1 = speckled; 2 = plain, 3 = cross between speckled and striped
P	Leg I tarsus: expanded tarsus	States: 0 = absent; 1 = present
Q	Leg II femur: Ventral fringe of elongate scales	States: 0 = absent; 1 = present
R	Leg II femur: Color of ventral side	States: 0 = brown; 1 = white/pale; 2 = yellow; 3 = orange; 4 = red, 5 = speckled tan and black; 6 = rusty red
S	Leg II femur: pattern	States: 0 = longitudinally striped; 1 = speckled; 2 = plain; 3 = cross between speckled and striped
T	Leg III and IV pattern	States: 0 = longitudinally striped; 1 = speckled; 2 = plain
U	Color of hairs covering tarsal bulb	States: 0 = uniform, yellow/gold; 1 = uniform, white/pale; 2 = uniform, red; 3 = nonuniform, red/white; 4 = nonuniform, speckled tan and black; 5 = nonuniform, mostly black/some red/minimal white; 6 = nonuniform, black and pale/white; 7 = nonuniform brown and white; 8 = nonuniform brown and yellow; 9 = dip dyed red
V	Palpal patella color	0 = uniform, yellow/gold; 1 = uniform, white/pale; 2 = uniform, red; 3 = nonuniform, red with distinct white stripe; 4 = nonuniform, speckled tan and black, 5 = nonuniform, white/pale and orange
W	Presence of long, extended hairs covering tarsal bulb	0 = absent; 1 = present

Table 1.2. Results of constrained tree analyses for all datasets. deltaL = log likelihood difference from the maximal log likelihood in the set. bp-Rell = bootstrap proportion using RELL method (Kishino et al.1990). p-KH = p-value of one-sided Kishino-Hasegawa test (1989). p-SH = p-value of Shimodaira-Hasegawa test (2000). p-WKH = p-value of weighted KH test. p-WSH = p-value of weighted SH test. c-ELW = Expected Likelihood Weight (Strimmer and Rambaut 2002). Plus signs denote the 95% confidence sets. Minus signs denote significant exclusion.

Dataset / Trees	Log Likelihood	deltaL	bp-RELL	p-KH	p-SH	p-WKH	p-WSH	c-ELW
UCE Trees								
Unconstrained	-151937.5826	0	1 +	1 +	1+	1+	1+	1 +
Constraint 1	-152197.5883	260.01	0 -	0 -	0 -	0 -	0 -	$1.96 * 10^{-52}$ -
Constraint 2	-152317.9014	380.32	0 -	0 -	0 -	0 -	0 -	$3.31 * 10^{-86}$ -
ddRAD Minsamp 4								
Unconstrained	-11190202.17	0	1 +	1+	1+	1+	1+	1+
Constraint 1	-11200698.81	10497	0 -	0 -	0 -	0 -	0 -	0 -
Constraint 2	-11204447.28	14245	0 -	0 -	0 -	0 -	0 -	0 -
ddRAD Minsamp 10								
Unconstrained	-2765208.566	0	1 +	1+	1+	1+	1+	1+
Constraint 1	-2773211.958	8003.4	0 -	0 -	0 -	0 -	0 -	0 -
Constraint 2	-2776162.114	10954	0 -	0 -	0 -	0 -	0 -	0 -
ddRAD Minsamp 24								
Unconstrained	-884284.9398	0	1 +	1+	1+	1+	1+	1+
Constraint 1	-888737.6852	4452.7	0 -	0 -	0 -	0 -	0 -	0 -
Constraint 2	-890640.9283	6356	0 -	0 -	0 -	0 -	0 -	0 -
ddRAD Minsamp 48								
Unconstrained	-261217.5743	0	1 +	1+	1+	1+	1+	1+
Constraint 1	-263179.6385	1962.1	0 -	0 -	0 -	0 -	0 -	0 -
Constraint 2	-264235.2606	3017.7	0 -	0 -	0 -	0 -	0 -	0 -

Figures

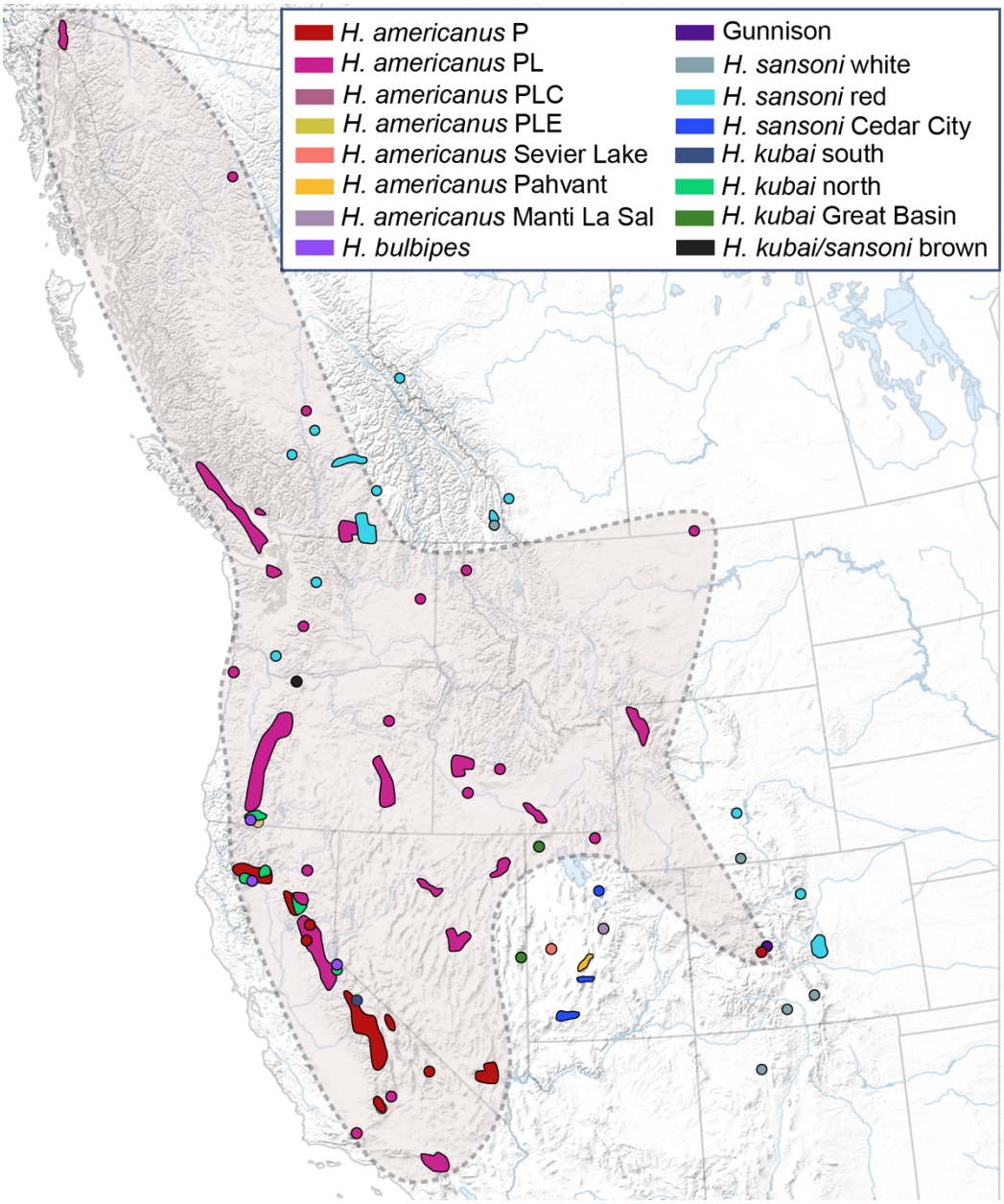

Figure 1.1. Approximate distribution of *americanus* subgroup species and morphs. Colors on map correspond to colors of boxes in legend. Opaque polygon with dashed lines indicate distribution of all *H. americanus* P, PL, and PLC morphs. Occurrences on map come from collection efforts from the Hedin lab and from public observations on iNaturalist.

Figure 1.2. Digital images of *americanus* subgroup morphs (*except for the *amer* PC morph). *amer* P = *H. americanus* P form, *amer* PL = *H. americanus* PL form, *amer* PLE = *H. americanus* PLE form, *amer* PLC = *H. americanus* PLC form, *amer* PC = *H. americanus* PC form, Pahvant = *H. americanus* Pahvant form, Manti La Sal = *H. americanus* Manti La Sal morph, Sevier Lake = *H. americanus* Sevier Lake morph, Gunnison = newly described morph collected near Gunnison, CO, *kub* south = *H. kubai* southern form, *kub* north = *H. kubai* northern form, *kub* Great Basin = *H. kubai* Great Basin morph, *bulb* = *H. bulbipes*, BSK = newly described brown form of *H. sansoni/ H. kubai* morph, *sans* white = *H. sansoni* white morph, *sans* red = *H. sansoni* red morph, SCC = *H. sansoni* Cedar City morph collected near Cedar City, UT. *sans* red photograph credit to Thomas Barbin, *amer* PLE, Gunnison, *kub* south, *kub* north, *bulb*, BSK, and *sans* white to Brendan Boyer, all other photos by M Hedin. Images not to scale.

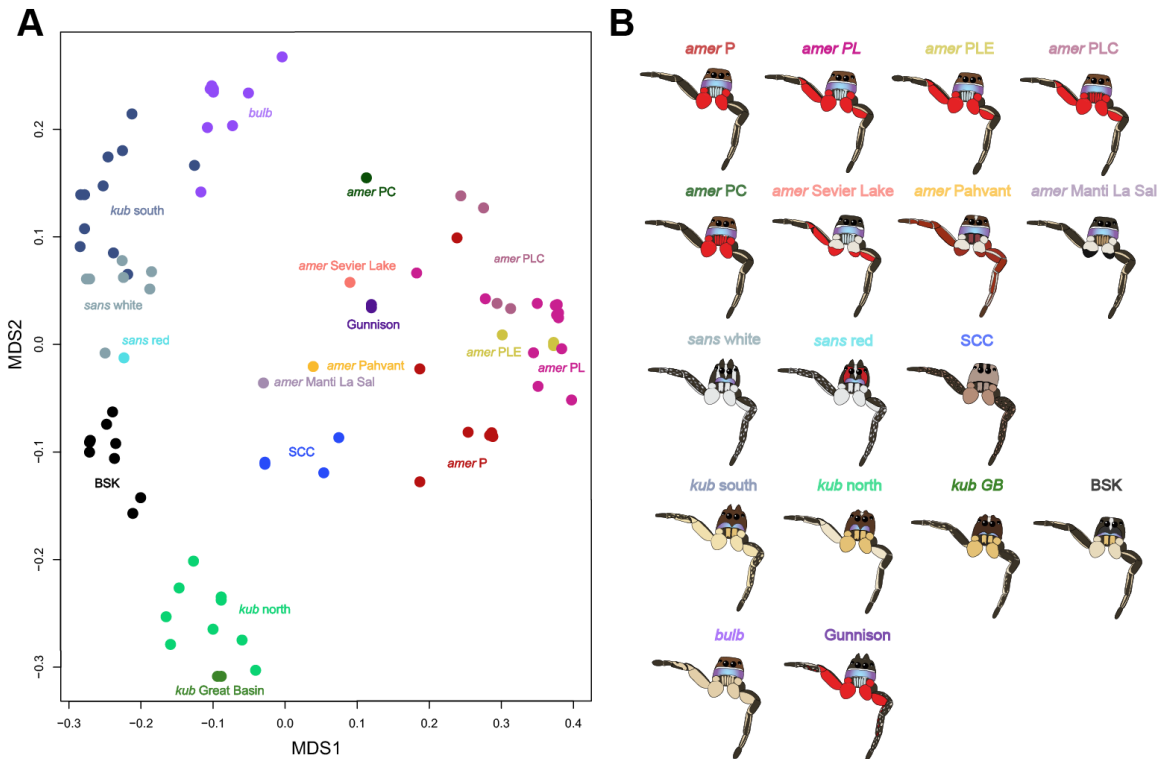

Figure 1.3. Results of NMDS analysis of morphological data (A) and cartoons of 17 species/morph identities (B). Colors of points correspond to colors of morph labels.

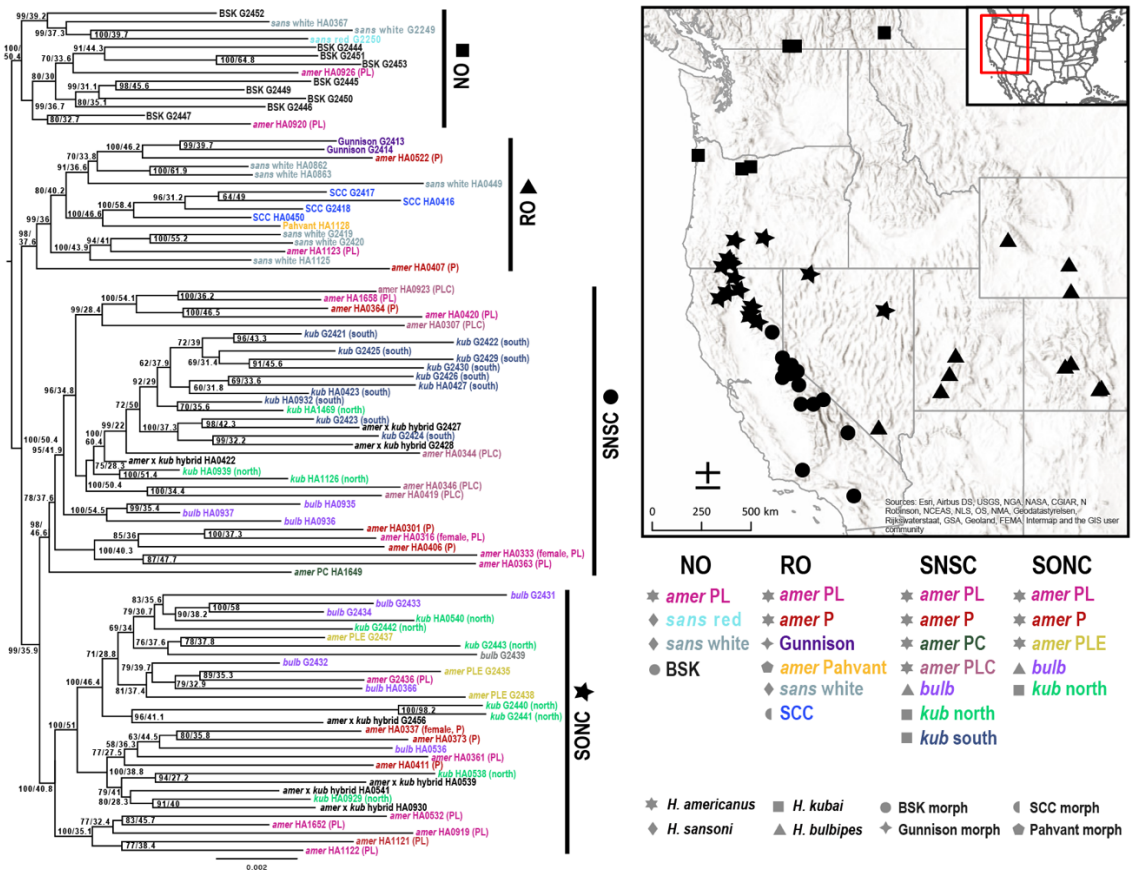

Figure 1.4. Concatenated, unconstrained rooted ddRADseq minsamp 4 phylogeny with map denoting collection location of specimens in each lineage. Symbols on map correspond to symbols on lineage labels. Lower right denotes all forms present in each lineage, along with symbols in gray to denote described species each morph belongs to. Node labels show bootstrap support / sCF (in percentage of sites supporting split). Tip labels colored by morph/ species identity as in Figure 2. SNSC = Sierra Nevada + Southern California clade, SONC = southern Oregon + northern California clade, RO = Rocky Mountain clade, NO = northern clade.

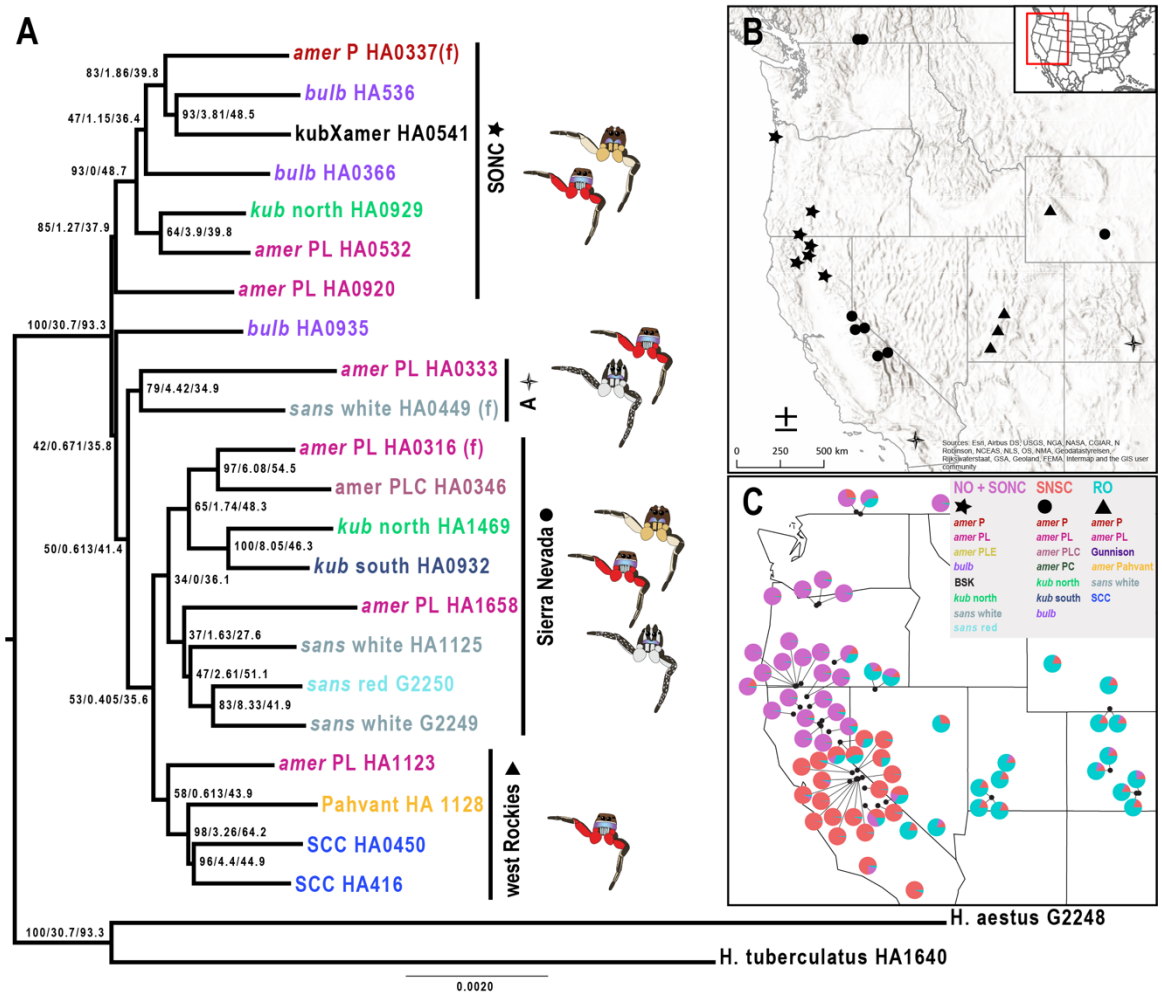

Figure 1.5. (A) Concatenated, unconstrained rooted UCE phylogeny. Tip labels colored by morph/ species identity as in Figure 2. Node labels show bootstrap support / gCF (in percentage of loci supporting split) / sCF (in percentage of sites supporting split). Cartoon *amer* PL, *kub* north, and *sans* white morphs shown to the right of all clades where each morph is present. (B) map denoting location where individuals in each lineage were collected, symbols on map reflect symbols on lineage labels. (C) Mapped admixture proportions estimated by STRUCTURE and shown as pie charts for the trimmed ddRADseq dataset. Upper right corner notes distinct species/morphs represented in each of the three clusters, ddRAD lineage names are color coordinated to denote which cluster they reflect most and UCE lineage symbols are listed beneath ddRAD lineage names to aid in comparison between the three analyses

CHAPTER 2

Variation of courtship displays in a group of jumping spiders exhibiting frequent introgression (*Habronattus americanus* subgroup; F. Salticidae)

Abstract

Introgression ultimately depends on mating interactions between individuals. As such, describing courtship characters and variation within and between them may be necessary to understand the evolutionary history of groups where sexual selection is important. I aimed to understand how repeated hybridization between *Habronattus americanus* subgroup members has affected variation in courtship displays and variation in male ornamentation of these diverging lineages. Various effects of introgression on genomes and morphology of the *americanus* subgroup have been investigated (see Chapter 1), yet courtship descriptions are lacking for the group. I first described courtship displays for many members of the group, including 15 morphs across four species. Displays are stereotyped consisting of mostly the same elements in the same order, where most of the variation occurs in the number of element repetitions and the time to complete certain display behaviors. I used statistical methods to visualize the diversity in courtship displays and evaluate the variation within and between species. I identified two distinguishable groups of courtship displays that follows a geographical pattern: a southeastern and a western+northern courtship group. Two characters of the courtship

displays were significant predictors of which geographic group a male's courtship display would fit under: number of fling repetitions and the time spent performing the introductory motif. I also discuss evidence of discordance between courtship display data and morphological/genomic data. Overall, I discovered a pattern of discordance between courtship display variation and courtship ornamentation variation potentially due to changes in female preferences and introgression during the evolution of the *americanus* subgroup.

I. INTRODUCTION

Hybridization is a widespread phenomenon that can have various evolutionary consequences. Many studies have assessed the genomic consequences to hybridization and the effects of gene flow across species barriers. Bennett et al. (2021) discuss several ways that hybrid zones have promoted active evolutionary change – providing new genetic diversity, reinforcing reproductive isolation and accelerating speciation, or providing conduits for gene flow between populations. Ultimately, introgression depends on mating interactions among individuals (Rosenthal 2013). In systems that experience pre-zygotic sexual selection, males may court females by showing off sexually attractive traits, including morphology, movements, and sounds. Hybridization between lineages with different sexual ornamentation has been documented to lead to unique courtship trait combinations or yield novel traits in hybrids (e.g., wing patterns in *Heliconius*, Jiggins et al. 2008, plumage and vocalization in manakins, Billo 2011). Studies investigating the effects of hybridization on courtship displays are relatively common in bird/vertebrate systems (Lorenz, 1958; Clark et al. 2012; Hiadlovská et al. 2012; McCallum and Pieplow 2022; Myers et al. 2022) but are less common in arthropods (but see Stratton and Uetz 1986; Gottsberger and Mayer 2007).

Habronattus jumping spiders engage in multimodal courtship displays. These spiders have particularly keen vision (Zurek et al. 2015) that is used during courtship displays in which the male displays a series of color, static ornaments, and movements to the female (Peckham and Peckham 1889, 1890; Griswold 1987; Maddison and Stratton

1988; Masta and Maddison 2002; Elias 2003; Elias et al. 2006; Rivera et al. 2021). In addition, *Habronattus* males use seismic signals during courtship displays which females perceive through the substrate (Elias et al. 2003, Elias et al. 2006). Previous studies have shown that components of *Habronattus* male displays might have been affected by hybridization (Masta and Maddison 2002, Elias 2003, Elias et al. 2006). Some individuals within the *H. pugillis* species complex have been shown to prefer males from different isolated populations that display different courtship characters, including movements and vibratory signals (Hebets and Maddison 2005). Males in the *H. pugillis* species complex show signs of past introgression between isolated populations leading to patterns of shared courtship ornamentation traits between geographically proximate populations, but not between more geographically distant populations (Maddison and McMahon 2000). Leduc-Robert and Maddison (2018) describe male courtship traits belonging to two different species complexes (*americanus* group and *clypeatus* group) that were likely affected by introgression based on evidence from phylogenetic analyses. Additionally, *Habronattus* is riddled with genomic evidence of introgression and hybridization (Masta 2000; Maddison and Hedin 2003; Hedin and Lowder 2009; Blackburn and Maddison 2014; Leduc-Robert and Maddison 2018; Hedin et al. 2020). In particular, the *americanus* subgroup – composed of 5 nominal species and many morphs – shows extreme levels of genomic homogenization with morphological divergence, primarily of male colors and static ornaments (Blackburn and Maddison 2014; Leduc-Robert and Maddison 2018; Hedin et al. 2020; Bougie et al. 2021).

The high degree of genomic similarity and morphological divergence makes the *americanus* subgroup an intriguing system for exploring potential impacts of introgression on courtship behavior and vice versa. There are currently five described species in the *americanus* subgroup: *H. americanus*, *H. kubai*, *H. bulbipes*, *H. sansoni*, and *H. waughi*. All species occur in mountainous regions of western North America, except for *H. waughi*, which is native to the far northeastern United States and southeastern Canada (Griswold 1987). In addition to the five described species, studies have documented extensive geographic variation within species, and unique morph types that do not seem to correspond to the aforementioned species (Blackburn and Maddison 2014; Bougie et al. 2021). Here, my data includes an additional *H. kubai* morph and three new *H. americanus* morphs (**Figure 2.1**). I decided to discuss these populations as morphs of species rather than potential incipient species based on facial character similarity and consistency with previously published studies, with one exception (Gunnison).

Identifying how repeated hybridization between *americanus* subgroup members has influenced variation in courtship displays and variation in male ornamentation of diverging lineages can provide insights into the speciation history of the group. Comparative studies of courtship traits with phylogenetic data can lead to inferences of why sexually important traits have evolved (e.g., wing pattern in *Heliconius*, *Heliconius* genome consortium 2012, Martin et al. 2013, swords in *Xiphophorus*, Cui et al. 2013, Schumer et al. 2016,), which in turn aids our understanding of the diversification histories of rapidly diverging groups. Fluctuations in female preference for courtship traits may

promote introgression events, potentially changing the course of speciation in groups with strong sexual selection (Fisher et al. 2009, Cui et al. 2013). As such, describing courtship characters and behaviors, and variation within and between species, may be necessary to understand the evolutionary history of groups where sexual selection is important.

There has yet to be a published description of the courtship displays of *americanus* subgroup males. Quantifying aspects of courtship routines in the group may shed light on how courtship displays are affected by hybridization and whether genes coding for behaviors reflect evolutionary patterns of the morphological genes coding for the colorful sexual ornamentation in the group. To this end, I use recorded videos of *americanus* subgroup males courting a female model to (1) describe the courtship displays of different *americanus* subgroup species and morphs, (2) characterize variation of courtship displays within and between different *americanus* subgroup species and morphs and (3) interpret results in the context of the genomic and morphological data already collected for the group (see Chapter 1). A key question I am interested in answering is: "how does courtship display variation compare to morphological variation of male ornamentation?"

II. MATERIALS AND METHODS

(1) Sample collection

Twenty-nine male individuals (11 *Habronattus americanus*, 2 *H. sansoni*, 4 *H. sansoni* Cedar City, 3 *H. kubai,* and 3 Gunnison morphs) were previously collected and had recordings of courtship dances in non-4k video. To supplement already available videos, I collected individuals from additional populations of the *americanus* subgroup in summer 2020 and summer 2021. In total, the final sample included courtship videos from species and unique morphs as follows (**Figure 2.2a**, **Appendix 2.1)**: *H. americanus* (n = 42; 7 P, 16 PL, and 7 PLC, 4 Pahvant, 3 eastern Pahvant, 4 Manti La Sal, and 1 Sevier Lake), *H. sansoni* white morph (n = 1), *H. sansoni* red (n = 2), *H. sansoni* Cedar City (SCC) morph (n = 10), *H. bulbipes* (n = 3), *H. kubai* (n = 16; 1 northern morph, 8 southern morphs, and 7 Great Basin *H. kubai*), Gunnison morph (n = 3). Live spiders were brought back to the lab and housed on a 12:12 hour light:dark cycle and fed weekly on a diet of pinhead crickets and *Drosophila melanogaster*.

(2) Recording procedures

Courtship was recorded for each individual using a custom-built arena using stretched nylon over a circular embroidery hoop (27 cm in diameter). Nylon fabric passes relevant frequencies in vibratory displays with little distortion and background noise, making it a reliable substrate for courtship recordings (Elias and Mason 2014). I did not score specific sound characters in this study, but the presence of vibrational sounds was

correlated with some courtship elements. As such, the use of nylon fabrics in the arena set up was useful for courtship descriptions. A female model was used to prompt courtship behavior from males. The model was prepared by affixing dead females to an insect pin with dental/bees wax on their ventral cephalothorax. To allow for rotation of the model, simulating a female response to the male display, the pin was attached to a belt-pulley system (Girard et al. 2011).

I analyzed previously videotaped courtship behaviors of newly collected males (2020-2021) in 30 frames/second using a Sony Lumix JAI CV-S3200 CCD camera with 4k video. Vibratory songs for newly collected males were recorded using a portable digital vibrometer (Polytec PDV-100). Males collected prior to 2020 were videotaped with a Navitar Zoom 7000 lens, JAI CV-S3200 CCD camera in 30 frams/second and songs were recorded using a Polytec PSV-400 vibrometer scan head with an OFV 5000 controller. Courtship of newly collected males was recorded under a standardized temperature of 40ºC using reptile heating lamps because temperature can impact courtship displays (Brandt et al. 2018, 2020). When the male would attempt copulation with the model, he was brushed away using a small paintbrush and recording would continue if he resumed courting after being brushed away.

(3) Courtship description

I recorded qualitative descriptions of male courtship dances by watching the videotaped displays and noting performance and repetition of signal notes. Courtship in the *americanus* subgroup is stereotyped, with most variation occurring in the number of

repeated elements, the types of elements, and the time spent performing each element. I build on naming conventions described in Rivera et al. (2021) and in detail by Elias et al. (2012). Display notations should be read as algebraic equations. I define complete courtship routines as display compositions, which are composed of stereotyped motifs. Each motif consists of a series of signal element notes that may be repeated. I define signal element notes by unique visual motions sometimes combined with substrate-borne vibrations. Repetition numbers of signal elements are denoted by superscripts in the display composition. An integral number (x) describes the typical repetition number, while a single asterisk (*) denotes a variable repetition number between 1-6 repetitions, a double asterisk (**) denotes a more variable repetition number between 5-15 repetitions and triple asterisk (***) denotes a variable repetition number typically between 20-50. If there is a pause (silence of more than 500 ms) in between signal elements or signal element repetitions, a comma (,) is placed between the signal elements where the break occurs. Subscripts of signal elements denote a variation of that element, but still along the same element theme.

(4) Courtship variation analyses

Variation within species

To visualize differences in courtship between different morphs of *H. kubai*, *H. americanus,* and *H. sansoni*, I quantified the amount of time each male spent performing three different display motifs and the number of repetitions of each signal element note and conducted principal components analyses (PCA) using these eight variables. PCAs

were conducted in R v4.0.3 using the prcomp() function. I explored courtship variation within *H. americanus* populations by performing a PCA using all individuals from PL, PLC, P, Pahvant, eastern Pahvant, Sevier Lake, and Manti La Sal morphs. Similarly, I explored courtship variation within *H. kubai* populations by performing a PCA using all individuals from *H. kubai* north, *H. kubai* south, and *H. kubai* Great Basin morphs. The *H. sansoni* PCA included *H. sansoni* white, *H. sansoni* red, and *H. sansoni* Cedar City morphs.

To test for differences in courtship display variables between morphs of *H. americanus*, I performed a non-parametric multivariate analysis of variance (PERMANOVA) using the eight courtship variables described above on all *H. americanus* morphs except for the Sevier Lake morph (n=1). I first calculated the Euclidean distance between variables in R v4.0.3 using 'dist()' function and checked for multivariate homogeneity of group variances by using the 'betadisper()' and 'permutest()' functions from the Vegan v2.4.2 R package. The PERMANOVA test was run using the 'adonis()' function from the same Vegan R package. To test for differences in courtship display variables between morphs of *H. kubai*, I performed a PERMANOVA in R v4.0.3 using the same functions as described above. The *H. kubai* PERMANOVA was calculated using the *H. kubai* Great Basin and *H. kubai* south morphs, excluding *H. kubai* north (n=1). Identical R functions were used to run a PERMANOVA test for *H. sansoni* using the *H. sansoni* Cedar City and *H. sansoni* red morphs, excluding *H. sansoni* white (n=1).

Variation between species and morphs

To visualize variation in courtship display variables across the entire *americanus* subgroup, I performed a PCA using all individuals from all populations using the same method as described for within species variation (see above). Since results from the *H. americanus* PCA and the PCA of the entire subgroup suggested a pattern consistent with two geographic groups of courtship displays (see results; a southeast group and a western+northern group), I ran two additional PCAs using the same R functions as above to visualize variation in courtship display within each geographic group.

To test for differences in courtship display variables between all species and morphs, I performed a PERMANOVA using the same eight courtship variables and R functions as described above. I did not include the *H. americanus* Sevier Lake, *H. kubai* north or *H. sansoni* white morphs because there was only one sample available for these populations.

Courtship variation across geography

I used logistic regression methods in R v4.0.3 to test if courtship display variables can predict if an individual was collected in the southeast geographic region or in the western+northern region. I coded data as 0 (southeast) and 1 (western+northern). I determined the courtship display covariates to be tested by considering results from the above PCAs, in which certain courtship display characters appeared to be responsible for the most differences across species and morphs (thump-bridge time, ThFl motif time, intro motif time, Fl and Th repetitions). I included two additional binary covariates not

included in the PCAs: the presence/absence of Th and Fl characters in a display. The Th presence/absence covariate was chosen because there are no idealized courtship displays that do not contain Th signal notes in morphs and species from the western+northern group, but four idealized courtship displays of morphs and species in the southeastern group do not contain Th notes (**Table 2.1**). The Fl presence/absence covariate was chosen because all southeast morphs and species contain Fl signal notes, but that is not true for morphs and species from the western+northern group (**Table 2.1**).

I formulated models to produce behaviorally and evolutionarily relevant and interpretable results. I created *a priori* models consisting of individual covariates and combinations of covariates. I excluded models where covariates were correlated (Pearson's correlation coefficient > 0.6; Manlick et al. 2017 and a Point-Biserial correlation coefficient > 0.3). Models were analyzed in R v4.03 using the 'glm()' function in the 'stacks' package. I evaluated support for each model using Akaike's information criterion scores corrected for small sample sizes (AICc, Burnham and Anderson 2002). The best supported model was considered to be the one with the lowest AICc score, but other models were considered if within two units of the top model (Burnham and Anderson 2002).

III. Results

(1) Courtship description

Courtship in the *H. americanus* subgroup is characterized by stereotyped signal element notes and motifs that include visual motions and substrate-borne vibrations. Stereotyped *americanus* subgroup display compositions consist of 4 – 6 elements and begin with the Introductory Motif followed by the Thump-Bridge Motif, and conclude with the Thump-Fling Motif, which occurs right before the pre-mount when the male prepares to mount the female. A generalized *americanu*s subgroup display composition and oscillogram (a visualization of the wave form and amplitude produced when the male produces vibratory signals) is shown in **Figure 2.3**, while descriptions of display elements are shown in **Figure 2.4** and **Table 2.2**). As the display composition progresses, the male moves closer to the female, eventually touching her. I describe stereotyped *americanus* subgroup courtship motifs below.

Introductory motif

Typical introductory motifs are composed of two or three signal element notes (**Figure 2.4**), including Sidles (Si), Still Sidles (Ss) and Settles (Se). Only the *H. americanus* PL morph with breaks and the *H. kubai* south morph regularly perform Ss notes in the introductory motif. The *H. americanus* PL morph, no-break individuals include an additional unique signal element to begin their display composition (**Table 2.1**).

Introductory Motif: Ss^{*} $Si^{**}Se$ or $Si^{**}Se$

The male begins with sidle signal elements, either Ss or Si movements as soon as he orients himself to the female model. The male is usually at a relatively long distance (~7-9cm) from the female during initial sidle movements. As soon as he orients himself to face her, the male raises his forelegs and palps laterally to expose the underside of the forelegs and face. In the case of the raised Sidle (Si_r), the forelegs are lifted higher above the head, while the parallel sidle (Si_p) keeps the forelegs raised, but parallel with the surface (**Figure 2.4**). The male then approaches the female in an arching zig-zag pattern while quickly alternating the palps up and down and keeping the forelegs raised. In the still sidle (Ss_r and Ss_p), the male engages in the same palp movements with forelegs raised as in Si_r and Si_p and may lean side to side but remains in the same place. When the male is within approximately 2 cm of the female, he settles (Se) into a position facing the female with his forelegs still raised and palps positioned laterally to show his face. The Se note acts as a transition from a moving sidle display to the remaining display elements. The introductory motif of *H. americanus* PL no break individuals begins instead with a unique signal element (PL) where the male shoots his forelegs up rapidly and backs away from the female while quickly alternating his palps up and down until he transitions into the Si_p pose and continues his display as all other *americanus* subgroup members.

Thump-bridge motif

The thump-bridge motif serves as a connection between the introductory motif and the thump-fling motif. The thump bridge is composed of two signal elements:

"chicken-wing" (Cw, defined below) and initial thump (Th_i) (**Figure 2.4**). However, *H. bulbipes* does not perform the Cw signal note.

Thump-bridge motif: $Cw^{*}Th_i$, Th_i

While in the Se pose, the male begins the thump-bridge motif by performing the Cw signal element. The male remains oriented toward the female with raised forelegs parallel to the ground and a slight bend in the patella joint. He then raises and lowers his forelegs in a "chicken-wing" fashion, keeping forelegs slightly bent and out in front of him. After the Cw note is performed, the male performs an initial thump (Th_i) signal element note, stereotyped by motions and substrate-borne vibrations. The male brings his palps up and close together to cover the face and then arches his forelegs downward and flicks them upward rapidly, straightening the forelegs so that they are oriented vertically. While the forelegs are flicked upward, the male bends and releases his abdomen to create a loud broad-band vibration using a stridulatory file on the back of the cephalothorax (Elias et al. 2003). Th_i differs from the Th signal element in that during the Th_i note, the male jumps to within 1cm of the female; in the regular Th note, the male stays in his position typically close to the female.

Thump-fling motif

The thump-fling motif begins with either a thump (Th) element or a fling (Fl) element and is the last courtship motif before the male attempts to mount the female. The thump-fling motif is the most variable element in *americanus* subgroup courtship displays. Some subgroup members perform both Th and Fl notes and others only perform

one of the two signal elements. There is a wide range in variability for the Fl signal note, some *americanus* members repeat the Fl signal over 40 times, while others (if they perform it at all) repeat the Fl note few times.

Thump-fling motif: $Th^{*}Fl^{*}$, Th^{*}, $Th^{*}Fl^{**}$, Fl^{**}

The thump-fling motif begins with the male within 1 cm of the female with his forelegs raised and palps raised up and close together to cover his face. He either performs a Th signal note and/or Fl notes. The Th signal element note includes stereotyped motions and substrate-borne vibrations and is similar to the Th_i element, the only difference is that the male does not jump forward when performing the Th note. The Fl element also includes stereotyped motions and substrate-borne vibrations similar to the Th note (**Figure 2.4**). In the same position as above, with his forelegs and palps raised, he arches his forelegs down over the female and flicks them upward, straightening the forelegs again so they are oriented vertically. Just before raising his forelegs back up, he flings the tarsi on his forelegs up and down while they are oriented down and straight out in front of him in the direction of the female. Often, this occurs while the forelegs are directly over the female. While the forelegs are flicked upward, the male bends and releases his abdomen to create a loud broad-band vibration using a stridulatory file on the back of the cephalothorax (Elias et. al 2003), similar to the Th note. The male repeats the Th or Fl notes until he attempts to mount the female for copulation by moving toward the female and reaching his forelegs around her and rises up to mount her.

(2) Diversity of courtship displays

Variation within species

The *H. americanus* PCA shows variation primarily between three morphs collected in the southeastern range of this species' distribution (Manti La Sal, Pahvant and eastern Pahvant), versus all other morphs (**Figure 2.5a).** Most of the variation between Manti La Sal morphs and western+northern specimens is attributed to the time to complete the time spent performing the intro motif. Other southeastern morphs appear to vary based on the number of Fl repeats and the time performing the ThFl motif (Pahvant) or a combination of those display characters and the time spent performing the intro motif (eastern Pahvant). Two *H. americanus* PL break individuals collected from WY spend more time performing the intro motif than other *H. americanus* PL break individuals. The *H. americanus* Sevier Lake specimen appears to vary from the western+northern courtship display group only slightly for most variables considered. The PERMANOVA of the *H. americanus* morphs support the results from the *H. americanus* PCA, indicating there is a significant difference in multivariate space of centroid location (F=9.0973, df=6, P=0.001, **Table 2.3**). This suggests that courtship traits do differ between *H americanus* morphs in multivariate space. The test for homogeneity of group variances failed to reject the null hypothesis of homogeneity, indicating that the significant PERMANOVA result was not affected by non-homogenous group variances (F=1.034, df=6, P=0.396).

The *H. kubai* PCA fails to identify any pattern of variation distinguishing morph type or geographic location (**Figure 2.5b**). Similarly, the PERMANOVA for *H. kubai*

morphs did not recover a significant relationship between *H. kubai* morphs and courtship traits (F=2.959, df=1, P=0.076, **Table 2.3**) and the test for homogeneity failed to reject the null (F=1.5529, df=1, P=0.218). These results support the lack of distinct groups found in the PCA of *H. kubai* morphs (**Figure 2.5b**).

The *H. sansoni* PCA suggests there may be a separate group of *H. sansoni* red morphs, but it is difficult to tell if this is a true signal or an effect of low sample size (**Figure 2.5c**). *H. sansoni* Cedar City morph occupies most of the space, indicating considerable variation within the courtship displays of this morph. The PERMANOVA for the *H. sansoni* morphs did not find a significant relationship between courtship display characters and morph (F=2.4896, df=1, P=0.142, **Table 2.3**).

Variation among species

The PCA of eight courtship display traits across all morphs and species of the *americanus* subgroup yielded some separation between morphs present in the southeastern range of their distribution (CO, eastern NV, and UT) and morphs present in the western+northern range (**Figure 2.6).** In particular, the Manti La Sal and eastern Pahvant morphs are most divergent from most western+northern and other southeastern morphs in the time spent performing the intro motif. Additionally, the *H. sansoni* Cedar City and *H. sansoni* white, and *H. sansoni* red morphs are most divergent from western+northern and other southeastern morphs in the time spent performing the thump-fling motif and the number of Fl repetitions. The PERMANOVA of all *americanus* subgroup morphs and species yielded a significant relationship between courtship display traits and morph or species identity (F=12.353, df=11, P=0.001). The test for

homogeneity of variances failed to reject the null hypothesis of homogeneity (F=1.0198, df=11, P=0.415).

The western+northern PCA showed some variation between some *H. kubai* Great Basin and some *H. kubai* south individuals in the number of Fl repeats and the time spent performing the ThFl motif. Additionally, two *H. americanus* PL break individuals and one *H. kubai* south individual appear to spend longer times performing the introductory motif compared to all other western+northern individuals. The *H. bulbipes* collected near Portola, CA appears to vary in most courtship display elements from the northern *H. bulbipes* specimens (**Figure 2.7a)**.

The southeastern PCA displays some variation between morphs (**Figure 2.7b**). The eastern Pahvant and Manti La Sal morphs vary from other morphs largely based on the time to perform the intro motif and the *H. sansoni* and *H. sansoni* Cedar City vary from many other morphs based on time to complete the thump-fling motif and the number of Fl repetitions, both of which are patterns supported by the PCA of all morphs and species.

Courtship variation across geography

The logistic regression identified one model explaining geographical region (**Table 2.4).** The top model was a multivariate model with the time spent performing the introductory motif and the number of Fl repetitions as the predicter covariates (**Table 2.4)**. No other model was within 2 AIC of the top model, leading me to remove all other models from consideration (Arnold 2010; **Table 2.4)**. The top model predicted that the time spent performing the introductory motif and the number of Fl repetitions was greater

for populations from the southeastern region, versus those from the western+northern region (**Figure 2.8**).

IV. DISCUSSION

(1) Display compositions

Displays of *americanus* subgroup members are stereotyped with males performing mostly identical signal element notes in the same progression. Some species or morphs perform different modifications of signal notes (e.g., Si_r vs Si_p), but the overall "theme" of the courtship movement remains the same. I recognize two major groups of displays within the *americanus* subgroup. Some morphs or species spend more time performing the introductory movements and their Thump-Fling Motif is shorter, with fewer repeats of Th and Fl signal elements. The other major group consists of species or morphs that spend a relatively longer time performing the Thump-Fling Motif, which is often accompanied by a large number of repeats of Th and Fl signal elements. It appears that the differentiation between display compositions is largely dependent on the amount of time allocated to certain motifs and the number of repetitions of signal elements that make up the motifs, as similarly observed for courtship of other *Habronattus* species (e.g., *clypeatus* group, Rivera et al. 2021, *coecatus* group, Elias et al. 2012).

Courtship of other *Habronattus* groups varies, but all seem to display by performing stereotyped movements in stereotyped orders. *Habronattus clypeatus* and *H. coecatus* species groups both include species with decorated ornamentation on the third

leg, an emphasized structure during courtship in both groups (Griswold 1987, Rivera et al. 2021, Elias et al. 2012) that is not observed in *americanus* subgroup males. Complexity of the *coecatus* group courtship displays rivals that of other *Habronattus* groups, including *americanus* subgroup members with some species having up to 18 ornaments, many appendage movements, and up to 20 distinct vibratory signals (Elias et al. 2012). Some *clypeatus* group species also perform distinct vibratory signals throughout courtship displays, but these species generally lack elaborate ornamentation on the third leg, a negative relationship that might suggest changes to female choice in buzzing vs non-buzzing species (Maddison and Maddison 2016, Rivera et al. 2021). Despite elaborate courtship described in *Habronattus*, signals of introgression and hybridization have been documented, including between *H. clypeatus* and *H. coecatus* group members (Maddison and Hedin 2003; Leduc-Robert and Maddison 2018; Bougie et al. 2021).

(2) Courtship variation

Variation within Species

I was unable to detect significant differences in courtship display variation among morphs of *H. kubai* (**Figure 2.5b**), but this result may partly be due to a lack of samples, particularly *H. kubai* north individuals. *H. kubai* south is clearly distinguishable from *H. kubai* north and *H. kubai* Great Basin morphs via courtship ornamentation (Bougie et al. 2021). An additional morph described as a brown form of *H. sansoni*/*H. kubai* (BSK, Bougie et al. 2021) would be interesting to include in analyses of courtship display

between *H. kubai* morphs. Unfortunately, I did not have access to video recordings of BSK courtship. My observations suggest a potential discordant pattern between courtship ornamentation and courtship display in morphs of *H. kubai*, but due to low sample sizes and unsampled populations, this remains uncertain. I was also unable to identify any patterns of courtship display variation within *H. sansoni,* which may be a consequence of a lack of samples, especially for non-*H. sansoni* Cedar City individuals. A more detailed investigation of courtship displays within *H. sansoni* is necessary to better understand the loss of courtship ornamentation in *H. sansoni* Cedar City, which may shed light on the different ways sexually selected traits behave when faced with hybridization.

Within species courtship display variation in *H. americanus* identified significant variation between morphs (**Table 2.3**, **Figure 2.5a**). The most obvious pattern implies differences in courtship displays between some *H. americanus* morphs in the southeastern range of the distribution and morphs in the western+northern range. The previous analysis on courtship ornamentation variation in the *americanus* subgroup showed larger within morph variation than between morph variation, making it difficult to identify clusters unique to each *H. americanus* morph (Bougie et al. 2021). It appears that there is less within morph variation than between morph variation regarding courtship displays of *H. americanus* males, a pattern inconsistent with the results of the courtship ornamentation analysis.

Variation across species

The PERMANOVA showed that morph and species identity significantly influenced the distribution of courtship display variable centroids, meaning that in

multivariate space, morphs and species can be distinguished by the courtship variables (**Table 2.3**). Visualization of courtship display variation supports the PERMANOVA conclusion and within-species analyses. Courtship display variation across all morphs and species of the *americanus* subgroup suggests a geographic pattern consistent with the pattern identified in the display variation within morphs of *H. americanus*. The PCA of all species and morphs identified four southeastern morphs clearly divergent from a cluster that contains all western+northern morphs and some additional southeastern morphs (**Figure 2.6**). Manti La Sal and eastern Pahvant morphs spend more time performing the intro-motif and the thump-bridge than any other morphs or species regardless of geography. The number of Fl repetitions and the time spent performing the ThFl-motif are largely responsible for the variation in *H. sansoni* Cedar City and *H. sansoni* white from other morphs, including southeastern morphs. Variation across courtship displays belonging to the southeastern group appears to better distinguish between some *americanus* subgroup morphs than the variation in displays belonging to the western+northern group (**Figures 2.6** and **2.9**).

The number of Fl repetitions and the time spent performing the introductory motif were both significant predicters of whether an individual was grouped into the southeastern courtship display category or the western+northern display category (**Table 2.4, Fig 2.7**). The more Fl signal element notes, longer intro motif and presence of Fl characters an individual performed increased the probability that he was collected from the southeastern distribution group as opposed to the western+northern group regardless of morph identity. The top model supports evidence from the variation analyses described

above that there seems to be a geographical pattern related to courtship display characters.

A geographic pattern in courtship displays could be explained by secondary contact between diverging populations in a shared geographic region (Davis 2001). Given the age of the *americanus* subgroup (~200,000 years old, Hedin et al. 2020), diverging populations were almost certainly subjected to climatic shifts during the Pleistocene epoch (2,580,000 – 11,700 years ago). Perhaps as glacial ice retreated, geographically adjacent populations expanded and came into contact enabling the sharing of genetic material and courtship display characteristics. This hypothesis is consistent with the null hypothesis of Bougie et al. (2021) that speciation of *americanus* subgroup members occurred along color lines (male morphologies) followed by introgression within geographic regions. However rather than courtship displays showing similar patterns as courtship morphology, displays seem more similar to genomic data, where introgression at geographic centers has had an impact (**Figure 2.2**).

(3) Display variation does not mirror courtship ornamentation variation

Previous phylogenomic studies of *americanus* subgroup members support geographically defined lineages rather than lineages defined by species or morph identity. The ddRAD phylogeny (**Figure 1.4**) and the STRUCTURE analysis (**figure 1.5C**) identify a southeastern lineage and southeastern cluster, respectively. The complex evolutionary history of the *americanus* subgroup may have also led to the geographic signal detected in courtship displays today. While the courtship display variation appears to be

concordant with genomic lineages, it seems to be discordant with the morphological diversity of male courtship ornamentation. In Chapter 1, I identified distinct morphological types across the *americanus* subgroup but found no evidence of a southeastern cluster of morphologically similar populations (see **Figure 1.3**).

Discordance between courtship display and sexual ornamentation of species and morphs is a pattern not often described in the literature, unless observed in hybrid zones (e.g., manakins in western Panama, Billo 2011, hummingbirds in the western US, Myers et al. 2022). However, preexisting biases before the divergence of a group could explain discordant patterns between sexually selected traits (Basolo 1995, Meyer et al. 2006, Cui et al. 2013). Before the *americanus* subgroup diverged, females may have preferred certain courtship display traits such that after divergence, *americanus* subgroup females were biased towards those same traits, leading divergent lineages to share similar courtship display characters. If courtship ornamentation was not biased in the same way display traits were, it is possible that there would be a different pattern of variation in courtship ornamentation across populations from the pattern for courtship display variation. Perhaps female preferences in *americanus* subgroup members in the southeastern range were biased towards a higher number of Fl signal element repetitions and/or introductory motif time and introgression between geographically proximate lineages led to many lineages sharing similar courtship display characters.

(4) Sensory drive leads to convergence in behavioral traits?

The null hypothesis of introgression at geographic centers could explain the patterns of variation in courtship displays between southeast and western+northern morphs, but other eco-evolutionary explanations are also possible. Pressures from the environment may also play a role in the sharing of some behavioral traits in populations from the southeast region. Sensory drive is a hypothesis that describes how habitat transmission, perceptual tuning, and signal matching might shape the evolution of signal properties (Endler 1992, Boughman 2002). Briefly, the sensory drive framework requires that a signaler gives off signals that have certain properties (reflectance, pitch), and these signals are given in particular places and/or times. To be successful, the signal needs to travel through the environment and be detected by the receiver while there are potentially additional stimuli in the background. As such, variation in the environmental conditions where signaling takes place may impact the evolution of signals, receiver systems, and behaviors (Fuller and Endler 2018).

Populations of the *americanus* subgroup in the southeast region share a higher likelihood of performing longer introductory motifs and more Fl repetitions during courtship displays than populations found elsewhere. According to the sensory drive hypothesis, rather than introgression alone (or at all) driving the variation of courtship behavioral traits across populations, there may have been some environmental influence in the southeast that *convergently* selected for the display behavioral traits common to southeastern populations (longer introductory motifs or more Fl repetitions). It is also possible that environmental factors in the southeast affect the receiver systems of

females. Unfortunately, I did not collect the environmental or female preference data required to test the sensory drive hypothesis here, but it is important to consider that there may be more than one factor driving the courtship variation patterns seen in the *americanus* subgroup.

V. CONCLUSION

Here I describe courtship displays of several *americanus* subgroup members, including morphs of currently described species and investigate variation of displays across different morphs and species. Displays are composed of stereotyped behaviors that vary mostly in repetition and length spent performing certain smaller elements of the display, as observed in other *Habronattus* species groups (Elias et al. 2012, Rivera et al. 2021). Variation in displays appears to reflect a geographic boundary defined by individuals collected from the southeastern range of their distribution and those collected elsewhere. Additionally, courtship display character variation does not mirror patterns of courtship ornamentation variation of the group. These results could be indicative of differences in pre-existing biases of female preferences for certain sexually selected traits and not others. More data is needed to understand how the patterns of variation between the courtship displays seen here have evolved and how that might relate to the variation of courtship ornamentation and genomic variation across the group. While I cannot identify for certain the modes in which these patterns arose, my results add insights into

how sexual selection, introgression, and potentially other factors might affect lineage diversification and trait evolution.

VI. REFERENCES

Arnold, T.W., 2010. Uninformative parameters and model selection using Akaike's information criterion. J. Wildl. Manage. 74(6), 1175–1178. doi:10.1111/j.1937-2817. 2010.tb01236.x.

Basolo, A.L., 1995. Phylogenetic evidence for the role of a pre-existing bias in sexual selection. Proc. R. Soc. Lond. B. 259, 307–311.

Bennett, K.F.P., Lim, H.C., Braun, M.J., 2021. Sexual selection and introgression in avian hybrid zones: spotlight on Manacus. Integr. Comp. Biol. 61, 1291–1309. https://doi.org/10.1093/icb/icab135

Billo, TJ., 2011. Sexual selection, vocal signals, and plumage introgression in an avian hybrid zone [dissertation]. Seattle (WA): University of Washington.

Blackburn, G.S., Maddison, W.P., 2015. Insights to the mating strategies of *Habronattus americanus* jumping spiders from natural behaviour and staged interactions in the wild. Behav. 152, 1169–1186. https://doi.org/10.1163/1568539X-00003273

Bodner, M.R., Maddison, W.P., 2012. The biogeography and age of salticid spider radiations (Araneae: Salticidae). Mol. Phylogenet. Evol. 65, 213–240. https://doi.org/10.1016/j.ympev.2012.06.005

Bougie, T.C., Brelsford, A., Hedin, M., 2021. Evolutionary impacts of introgressive hybridization in a rapidly evolving group of jumping spiders (F. Salticidae, *Habronattus americanus* group). Mol. Phylogenet. Evol. 161, 107165. https://doi.org/10.1016/j.ympev.2021.107165

Boughman, J.W. 2002. How sensory drive can promote speciation. Trends Ecol. Evol., 17, 571–577.

Brandt, E.E., Kelley, J.P., Elias, D.O., 2018. Temperature alters multimodal signaling and mating success in an ectotherm. Behav. Ecol. Sociobiol. 72, Article 191. https://doi.org/10.1007/s00265-018-2620-5

Brandt, E.E., Rosenthal, M.F., Elias, D.O., 2020. Complex interactions between temperature, sexual signals and mate choice in a desert-dwelling jumping spider. Animal Behaviour 170, 81–87. https://doi.org/10.1016/j.anbehav.2020.10.010

Burnham, K., Anderson, D. 2002. Model selection and multimodel inference: a practical information-theoretic approach. 2nd ed. Springer, New York.

Clark, C. J., Feo, T. J., Bryan, K. B., 2012. Courtship displays and sonations of a male broad-tailed black-chinned hummingbird hybrid. Condor: Ornithol. Appl. 114, 329e340.

Cui, R., Schumer, M., Kruesi, K., Walter, R., Andolfatto, P., Rosenthal, G.G., 2013. Phylogenomics reveals extensive reticulate evolution in Xiphophorus fishes. Evolution. 67, 2166–2179. https://doi.org/10.1111/evo.12099

Davis, M.B., Shaw, R.G., 2001. Range shifts and adaptive responses to quaternary climate change. Science. 292, 673–679. https://doi.org/10.1126/science.292.5517.673

Elias, D.O., Land, B.R., Mason, A.C., Hoy, R.R., 2006. Measuring and quantifying dynamic visual signals in jumping spiders. J. Comp. Physiol. A. 192, 785–797. https://doi.org/10.1007/s00359-006-0116-7

Elias, D.O., Maddison, W.P., Peckmezian, C., Girard, M.B., Mason, A.C., 2012. Orchestrating the score: complex multimodal courtship in the *Habronattus coecatus* group of *Habronattus* jumping spiders (Araneae: Salticidae): multimodal courtship in Habronattus. Biol. J. Linn. Soc. 105, 522–547. https://doi.org/10.1111/j.1095-8312.2011.01817.x

Elias, D.O., Mason, A.C., Maddison, W.P., Hoy, R.R., 2003. Seismic signals in a courting male jumping spider (Araneae: Salticidae). J. of Exper. Biol. 206, 4029–4039. https://doi.org/10.1242/jeb.00634

Elias, D.O., Mason, A.C., 2014. The role of wave and substrate heterogeneity in vibratory communication: practical issues in studying the effect of vibratory environments in communication. In *Studying vibrational communication*. Springer. doi: 10.1009/978-3-662-43607-3_12

Endler, J.A., 1992. Signals, signal conditions, and the direction of evolution. Amer. Nat., 139, S125–S153.

Fisher, H.S., Mascuch, S.J., Rosenthal, G.G., 2009. Multivariate male traits misalign with multivariate female preferences in the swordtail fish, *Xiphophorus birchmanni*. Anim. Behav. 78, 265-269.

Fuller, R.C., Endler, J.A., 2018. A perspective on sensory drive. Curr. Zool. 64, 465–470. https://doi.org/10.1093/cz/zoy052

Girard, M.B., Kasumovic, M.M., Elias, D.O., 2011. Multi-Modal Courtship in the Peacock Spider, *Maratus volans* (O.P.-Cambridge, 1874). PLoS One. 6, e25390. https://doi.org/10.1371/journal.pone.0025390

Gottsberger, B., Mayer, F., 2007. Behavioral sterility of hybrid males in acoustically communicating grasshoppers (Acrididae, Gomphocerinae). J. Comp. Physiol. A. 193, 703–714. https://doi.org/10.1007/s00359-007-0225-y

Griswold, C.E., 1987. A revision of the jumping spider genus *Habronattus* F.O.P. Cambridge (Araneae; Salticidae), with phenetic and cladistic analyses. Univ. California Pub. Ent. 107, 1-344.

Hebets, E.A., Maddison, W.P., 2005. Xenophilic mating preferences among populations of the jumping spider *Habronattus pugillis* Griswold. Behav. Ecol. 16, 981–988. https://doi.org/10.1093/beheco/ari079

Hedin, M., Foldi, S., Rajah-Boyer, B., 2020. Evolutionary divergences mirror Pleistocene paleodrainages in a rapidly-evolving complex of oasis-dwelling jumping spiders (Salticidae, *Habronattus tarsalis*). Mol. Phylogenet. Evol. 144, 106696. https://doi.org/10.1016/j.ympev.2019.106696

Hedin, M., Lowder, M.C., 2009. Phylogeography of the *Habronattus amicus* species complex (Araneae: Salticidae) of western North America, with evidence for localized asymmetrical mitochondrial introgression. Zootaxa. 2307, 39–60. https://doi.org/10.11646/zootaxa.2307.1.2

Hiadlovská, Z., Bímová, B.V., OndRej, M., Piálek, Macholán, M., 2012. Transgressive segregation in a behavioural trait? Explorative strategies in two house mouse subspecies and their hybrids. Biol. J. Linn. Soc. 108, 225e235.

Jiggins, C.D., Salazar, C., Linares, M., Mavarez, J., 2008. Hybrid trait speciation and *Heliconius* butterflies. Phil. Trans. R. Soc. B. 363, 3047–3054. https://doi.org/10.1098/rstb.2008.0065

Leduc-Robert, G., Maddison, W.P., 2018. Phylogeny with introgression in *Habronattus* jumping spiders (Araneae: Salticidae). BMC Evol. Biol. 18, 24. https://doi.org/10.1186/s12862-018-1137-x

Lorenz, K.Z., 1958. The evolution of behavior. Sci. Am. 199, 67e77.

Maddison W.P., Stratton G.E., 1988. Sound production and associated morphology in male jumping spiders of the *Habronattus agilis* species group (Araneae, Salticidae). J. Arachnol. 16:199–211.

Maddison, W., Hedin, M., 2003. Phylogeny of *Habronattus* jumping spiders (Araneae: Salticidae), with consideration of genital and courtship evolution: *Habronattus* spider phylogeny. Syst. Entom. 28, 1–22. https://doi.org/10.1046/j.1365-3113.2003.00195.x

Maddison, W., McMahon, M., 2000. Divergence and Reticulation among Montane Populations of a Jumping Spider (*Habronattus pugillis* Griswold). Syst. Biol. 49, 400–421.

Maddison, W.P., D.R., Maddison., 2016. Two new jumping spider species of the *Habronattus clypeatus* group (Araneae, Salticidae, Harmochirina). Zookeys 625:1–10. doi: 10.3897/zookeys.625.9891.

Manlick, P.J., Woodford, J.E., Zuckerberg, B., Pauli, J.N., 2017. Niche compression intensifies competition between reintroduced American martens (*Martes americana*) and fishers (*Pekania pennanti*). J. Mammal. 98(3), 690–702. doi:10.1093/ jmammal/gyx030.

Martin, S.H., Dasmahapatra, K.K., Nadeau, N.J., Salazar, C., Walters, J.R., Simpson, F., Blaxter, M., Manica, A., Mallet, J., Jiggins, C.D., 2013. Genome-wide evidence for speciation with gene flow in *Heliconius* butterflies. Genome Res. 23, 1817–1828. https://doi.org/10.1101/gr.159426.113

Masta, S.E., Maddison, W.P., 2002. Sexual selection driving diversification in jumping spiders. Proc. Natl. Acad. Sci. U.S.A. 99, 4442–4447. https://doi.org/10.1073/pnas.072493099

McCallum, D. A., & Pieplow, N. D., 2010. A reassessment of homologies in the vocal repertoires of phoebes. Western Birds, 41, 26e43.

Meyer, A., Salzburger, W., Schartl, M., 2006. Hybrid origin of a swordtail species (Teleostei: *Xiphophorus clemenciae*) driven by sexual selection: hybrid speciation via sexual selection. Mol. Ecol. 15, 721–730. https://doi.org/10.1111/j.1365-294X.2006.02810.x

Myers, B.M., Rankin, D.T., Burns, K.J., Brelsford, A., Clark, C.J., 2022. k-mer analysis shows hybrid hummingbirds perform variable, transgressive courtship sequences. Anim. Behav. 186, 67–84. https://doi.org/10.1016/j.anbehav.2022.01.018

Rivera, C., Hedin, M., Mason, A.C., Maddison, W.P., Elias, D.O., 2021. Complex courtship in the *Habronattus clypeatus* group (Araneae: Salticidae). J. Arachnol. 48. https://doi.org/10.1636/JoA-S-18-045

Rosenthal, G.G., 2013. Individual mating decisions and hybridization. J. Evol. Biol. 26, 252–255. https://doi.org/10.1111/jeb.12004

Peckham G., Peckham E., 1889. Observations on sexual selection in spiders of the family Attidae. Occas. Pap. Wis. Nat. Hist. Soc. 1, 3–60.

Peckham G, Peckham E, 1890. Additional observations on sexual selection in spiders of the family Attidae, with some remarks on Mr. Wallace's theory of sexual ornamentation. Occas. Pap. Wis. Nat. Hist. Soc. 1, 117–151.

Schumer, M., Cui, R., Powell, D.L., Rosenthal, G.G., Andolfatto, P., 2016. Ancient hybridization and genomic stabilization in a swordtail fish. Mol. Ecol. 25, 2661–2679. https://doi.org/10.1111/mec.13602

Stratton, G. E., Uetz, C. W., 1986. The inheritance of courtship behaviour and its role as a reproductive isolating mechanism in two species of Schizocosa wolf spiders. Evolution. 40, 129–141.

The Heliconius Genome Consortium, 2012. Butterfly genome reveals promiscuous exchange of mimicry adaptations among species. Nature 487, 94–98. https://doi.org/10.1038/nature11041

Zurek, D.B., Cronin, T.W., Taylor, L.A., Byrne, K., Sullivan, M.L.G., Morehouse, N.I., 2015. Spectral filtering enables trichromatic vision in colorful jumping spiders. Curr. Biol. 25, R403–R404. https://doi.org/10.1016/j.cub.2015.03.033

Tables

Table 2.1. Display compositions for each species and morph. See Table 2.3 for definitions of signal elements. An integral number (x) describes the typical repetition number, while a single asterisk (*) denotes a variable repetition number typically between 1-6 repetitions, a double asterisk (**) denotes a more variable repetition number typically between 5-15 repetitions and triple asterisk (***) denotes a variable repetition number typically between 20-50. Three main sets of parentheses denote singal element notes performed in each of the three motifs: first set is the introductory motif, second set is the Th bridge, and third set is the ThFl motif.

Species or Morph	Sample Size	Display Composition
H. americanus PL break	11	$((Si_r^{1,1})$**Se)(Cw*Th_i)(Th*Fl*)
H. americanus PL no break	6	(PLSi_p**Se)(Cw*Th_i)(Th*Fl*)
H. americanus P	6	(Si_p**Se)(Cw*Th_i)(Th**)
H. americanus PLC	7	(Si_p**Se)(Cw*Th_i)(Th**Fl*)
H. americanus Manti La Sal	4	($Si_r^{**,*}$Se)(Cw*, Th_i)(ThFl**)
H. americanus Pahvant	4	(Si_r*Se)(Cw*Th_i)(Fl***)
H. americanus eastern Pahvant	3	$((Ss_r^{1,1,1}(Si_r^{1,1})^{**}$Se)(Cw*$Th_i$)(Fl***)
H. americanus Sevier Lake	1	$(Ss_r(Si_r^{1,1})^{27}$Se)(Cw**Th_i)(ThFl**)
H. bulbipes	3	(Si_pSe)(Th_i)(Th*)
H. sansoni white	1	$(Si_r^{9}$ Se)$(Cw^{6}Th_i)(Fl^{41})$
H. sansoni red	3	$(Si_r^{2}$Se)(Cw**Th_i)(Fl***)
H. sansoni Cedar City	11	$(Si_r^{1,*,*}$Se)(Cw*Th_i)(Fl***)
H. kubai south	8	(Ss_pSi_pSe)(Cw*Th_i)(Th*Fl*)
H. kubai north	1	(Si_p**Se)(Cw*Th_i)(Th**)
H. kubai Great Basin	6	(Si_p**Se)(Cw*Th_i)(Th*Fl**)
Gunnison	3	$((Si_p^{1,1})$**Se)(Cw*Se)(Fl**)

Table 2.2. Ethogram for courtship behaviors in the *americanus* subgroup. Subscripts in the behavioral unit (also called signal element notes) abbreviations denote variations on a common theme for that particular element.

Behavioral Unit	Abbreviation	Description
PL no-break start	PL	When the male notices the female, he shoots his forelegs up rapidly and backs away while moving his palps up and down in an alternating pattern and waving his forelegs slowly up and down in no particular pattern.
Sidle	Si_r, Si_p	In all but some *H. americanus* PL individuals, the Sidle signal element begins the courtship routine. Si's typically begin when the male is at a relatively long distance away from the female. As soon as he orients himself to face her, the male raises his forelegs and palps laterally to expose the underside of the forelegs and face. In the case of the raised Sidle (Si_r), the forelegs are lifted higher above the head, while the parallel sidle (Si_p) keeps the forelegs raised, but parallel with the surface. The male then approaches the female in an arcing zig-zag pattern

		while quickly alternating the palps up and down and keeping the forelegs raised.
Still Sidle	Ss_r, Ss_p	The Still Sidle is composed of the same palp movements as the Sidle, but the male remains in the same place and may lean side to side. The raised Still Sidle (SSr) involves the forelegs lifted above the carapace while the parallel Still Sidle (SS_p) involves the forelegs raised, but parallel with the surface.
Settle	Se	The settle signal element marks the end of the Sidle movements, usually when he is within 2 cm from the female. The male positions himself to face the female with his forelegs still raised. The palps remain raised showing the face and occasionally still move alternatingly up and down. The Se element concludes the introductory motif.
Chicken Wing	Cw	The chicken wing signal element follows the Se and begins the thump bridge motif. The male remains oriented toward the female with raised forelegs parallel to the ground and a slight bend in the patella joint. He then raises and lowers his forelegs in a "chicken-wing" fashion, keeping forelegs slightly bent and out in front of him.
Thump	Th, Th_i	Th signal elements include stereotyped motions and substrate-borne vibrations. The male brings his palps up and close together to cover the face and then arches his forelegs downward and flicks them upward rapidly, straightening the forelegs so that they are oriented vertically. While the forelegs are flicked upward, the male bends and releases his abdomen to create a loud broad-band vibration using a stridulatory file on the back of the cephalothorax (Elias et al. 2003). Abdominal movements are delayed from foreleg movements and the delay varies (4-400ms). The initial thump (Th_i) signal note includes the male jumping closer to the female as he thumps so that he is within 1 cm directly in front of her.
Fling	Fl	The Fling element includes stereotyped motions and substrate-borne vibrations similar to the Th note. The male faces the female within 1 cm of her and covers his face with his palps. The male raises up on his legs and raises his forelegs so they are oriented vertically. Then he arches his forelegs down over the female and flicks them upward, straightening the forelegs again so they are oriented vertically. Just before raising his forelegs back up, he flings the tarsi on his forelegs up and down while they are oriented down and straight out in front of him in the direction of the female. Sometimes, this occurs while the forelegs are directly over the female. While the forelegs are flicked upward, the male bends and releases his abdomen to create a loud broad-band vibration using a stridulatory file on the back of the cephalothorax (Elias et. al 2003), similar to the Th note. The Fl note concludes the courtship display when performed.

Table 2.3. PERMANOVA results for analysis with all species and morphs, morphs within *H. americanus,* morphs within *H. kubai*, and morphs within *H. sansoni*. Df = degrees of freedom, Sum Sqs. = sum of squares, Mean Sqs. = mean squares, F = F statistic value, R = percentage of variance explained by groups. * denotes significance at alpha ≤ 0.05.

	Df	**Sum Sqs.**	**Mean Sqs.**	**F**	**R2**	**P value**
All individuals						
Species/morphs	11	68470	6224.5	12.353	0.6867	0.001*
Residuals	62	31240	503.9		0.3133	
H. americanus						
Morphs	6	41524	6920.7	16.584	0.7289	0.001*
Residuals	37	15441	417.3		0.2711	
H. kubai						
Morphs	1	1040.3	1040.35	2.959	0.1854	0.076
Residuals	14	4570.7	351.59		0.8146	
H. sansoni						
Morphs	1	9813	2443	2.490	0.1993	0.142
Residuals	11	12256	981.3		0.8007	

Table 2.4. Model selection results for geographic group membership of *americanus* subgroup courtship displays. AIC_c is Akaike's information criterion corrected for small sample sizes, ΔAICc is the change in AIC_c from the top model, LL is the log likelihood.

Model	**AIC_c**	**ΔAIC_c**	**Akaike weight**	**LL**
Intro motif time + Fl reps	79.3393	0	0.3960	-36.5053
Fl reps	80.2584	0.9191	0.2501	-38.0481
Intro motif time + Fl reps + Fl pres	81.56584	1.3074	0.2059	-36.50514
Fl presence + Fl reps	82.22626	1.9679	0.1480	-37.94875
Intro motif time + Th pres + Fl pres	102.2175	21.9591	$6.7497*10^{-6}$	-46.83098
Intro motif time + Th pres	102.3341	22.0757	$6.3675*10^{-6}$	-48.00269

Figures

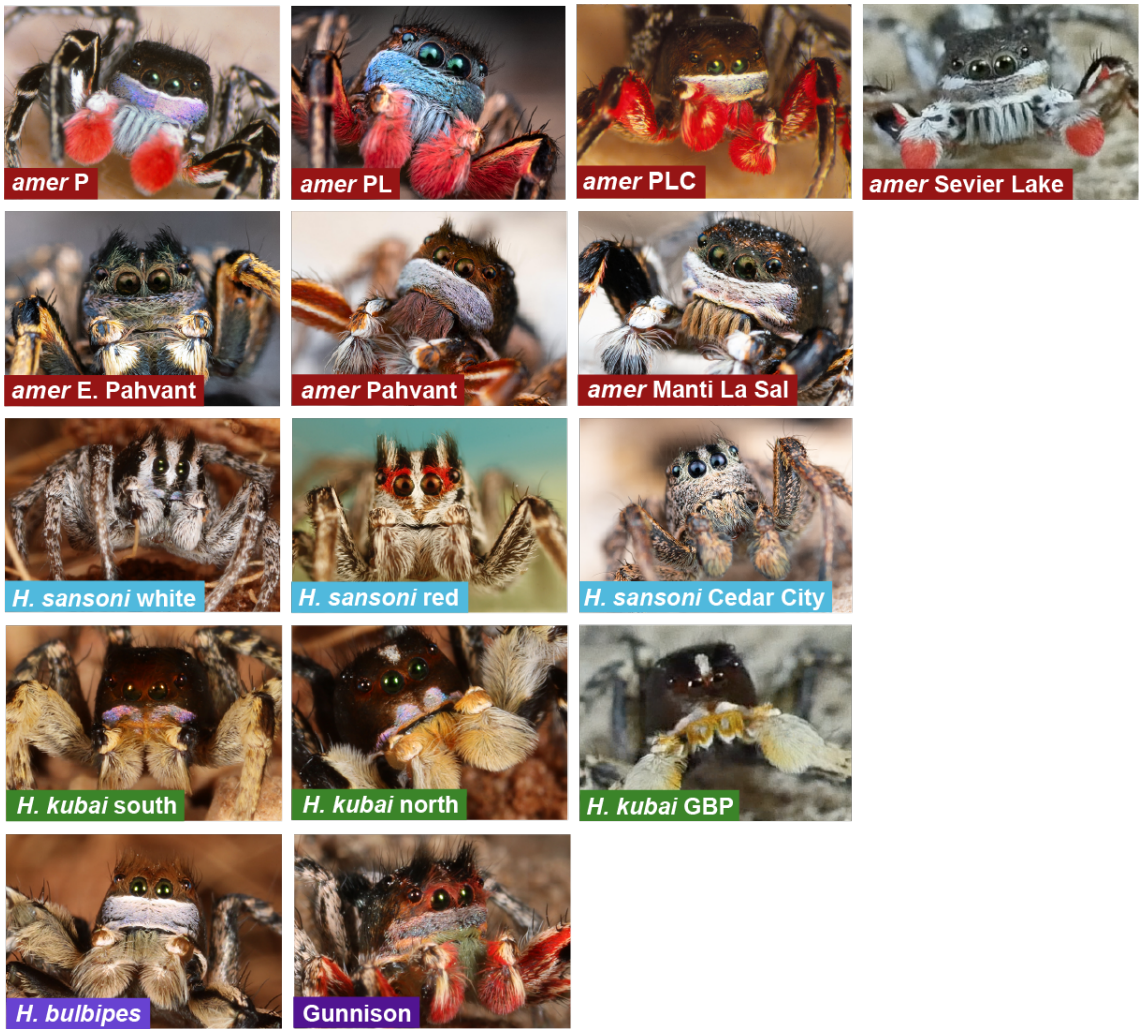

Figure 2.1 Digital images of representatives from all species and morphs included in behavioral analyses. Red boxes indicate morphs of *Habronattus americanus*, blue boxes indicate *H. sansoni* morphs, and green boxes indicate *H. kubai* morphs.

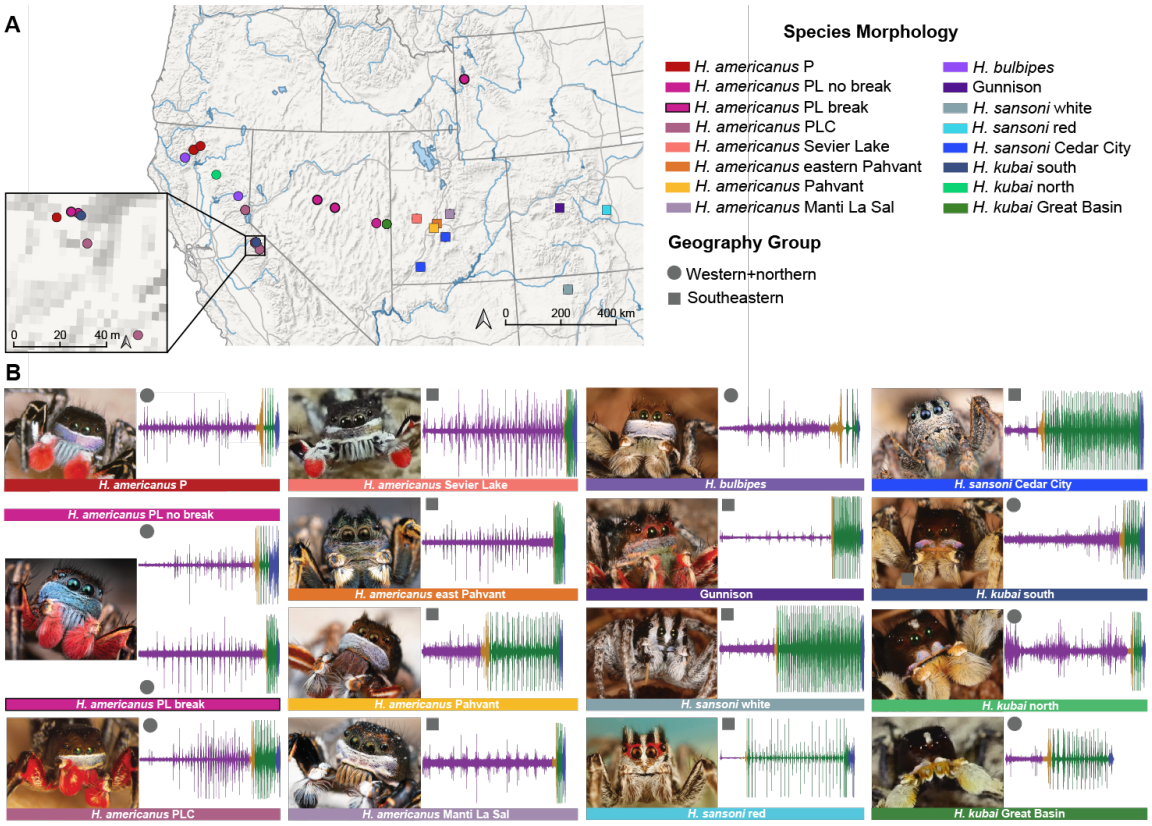

Figure 2.2. (A) Map of collection localities with (B) digital images of each species and morph with oscillograms (a visualization of the wave form and amplitude (y axis) versus time (x axis) produced when the male produces vibratory signals) of idealized courtship display for each morph. In the oscillograms), purple corresponds to seismic signals produced during the introductory motif, yellow corresponds to seismic signals produced during the Th bridge, and green corresponds to seismic signals performed during the ThFl motif. The blue portion at the end of each oscillogram corresponds to the time the male starts to mount the female. Colors of points on the map correspond to the colors of the labels on the images

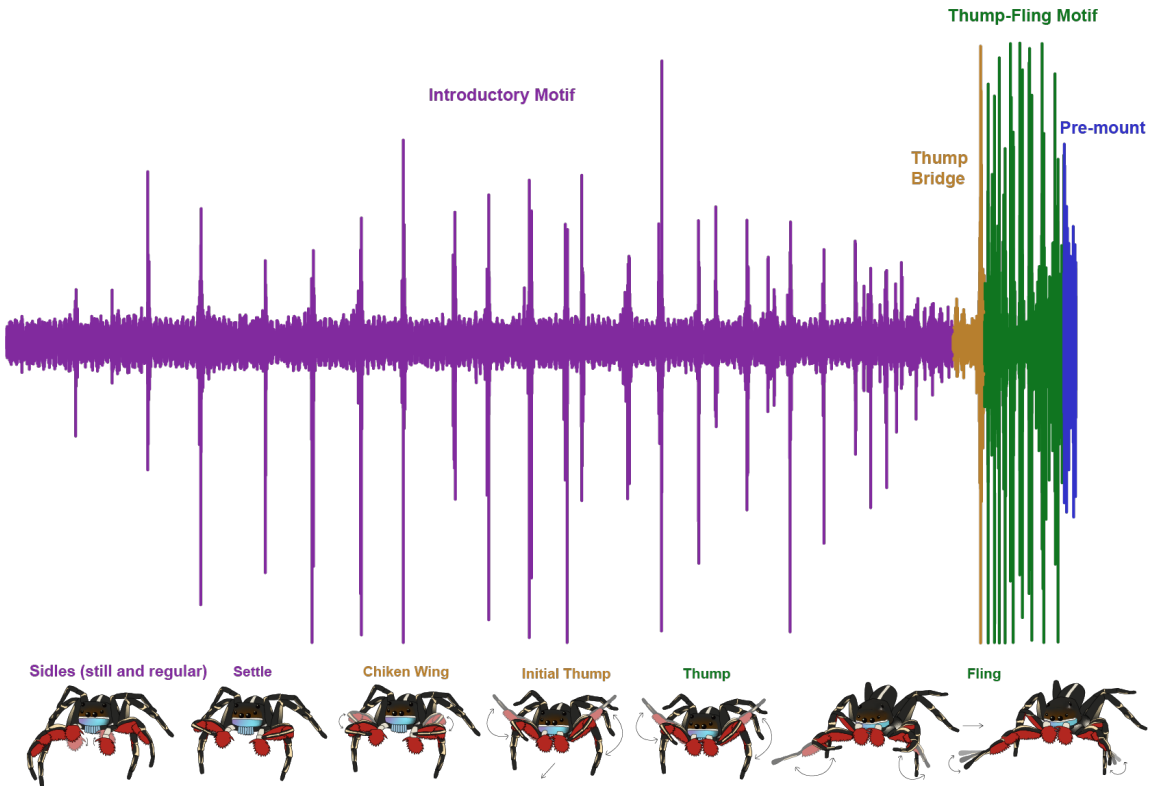

Figure 2.3. Generalized oscillogram of *americanus* subgroup courtship displays with cartoon drawings of signal element notes performed during each motif of the display. Purple denotes the proportion of time spent performing the introductory motif, yellow denotes the thump-bridge, and green denotes the thump-fling motif, which ends the courtship display. The pre-mount section in blue is when the male attempts to mount the female for copulation.

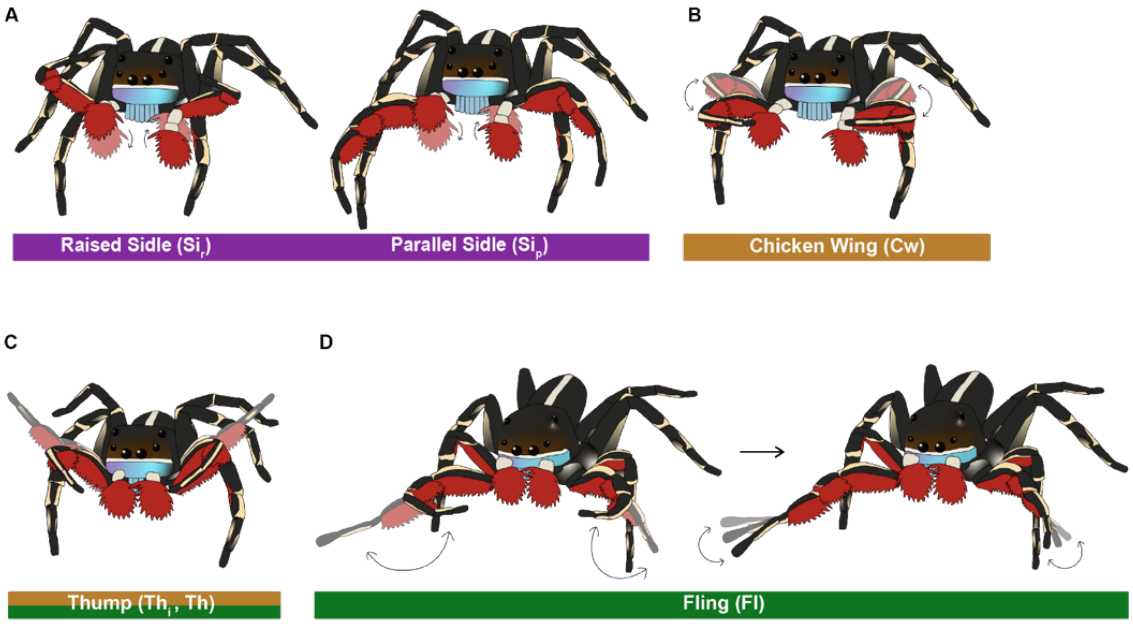

Figure 2.4. Motions of signal element notes performed by *americanus* subgroup members during courtship displays. The *H. americanus* PL morph is used as the model for cartoons depicting motions performed during courtship displays. (A) Raised and parallel sidle (Si_r and Si_p) signal note, (B) Chicken wing (Cw) signal note, (C) Thump (Th and Th_i) signal note, (D) Fling (Fl) signal note. Colored boxes correspond to courtship display motif during which each signal element is performed. Detailed descriptions of each signal element can be found in Table 2.3

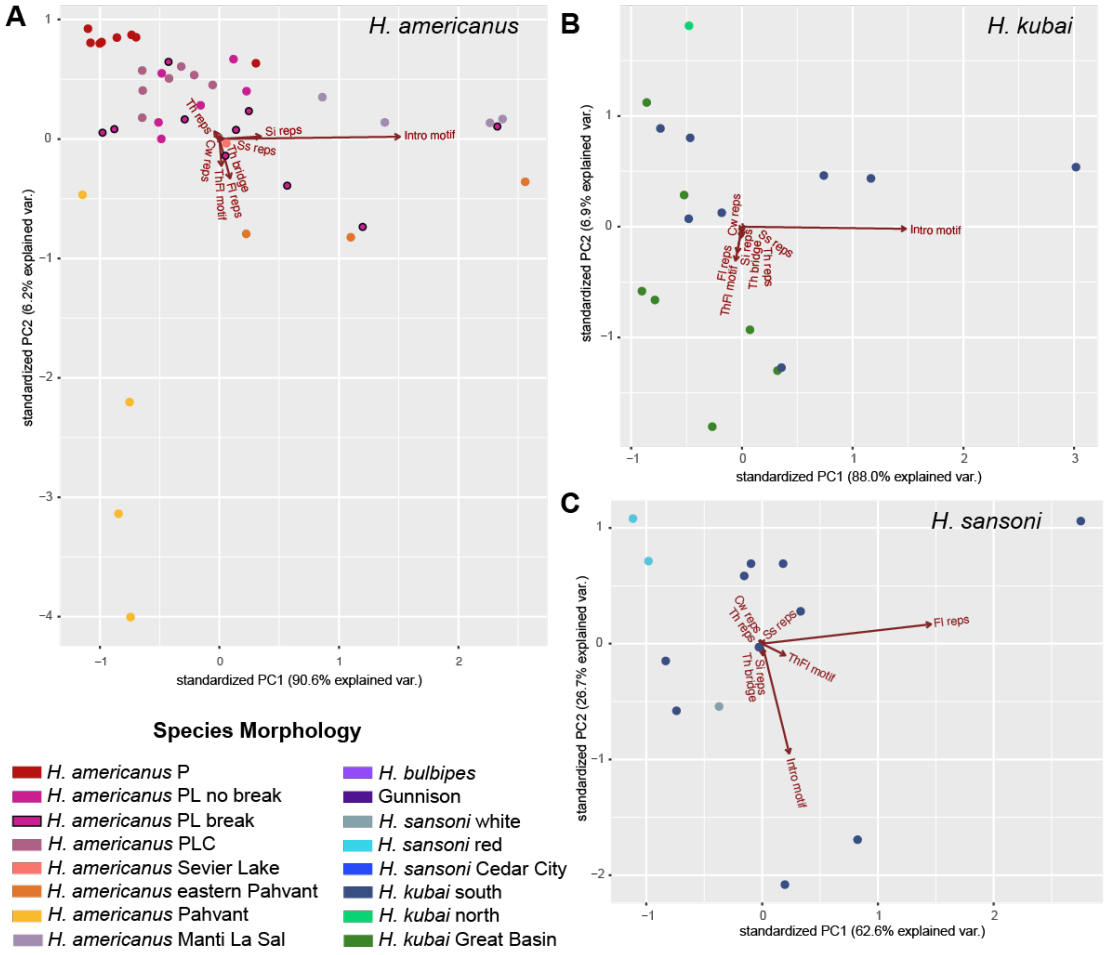

Figure 2.5. Principle Components Analysis (PCA) of eight courtship display characters. A. PCA of *H. americanus* morphs, B. PCA of *H. kubai* morphs, C. PCA of *H. sansoni* morphs. Colored points correspond to species morphology colors in the legend and each data point represents an individual.

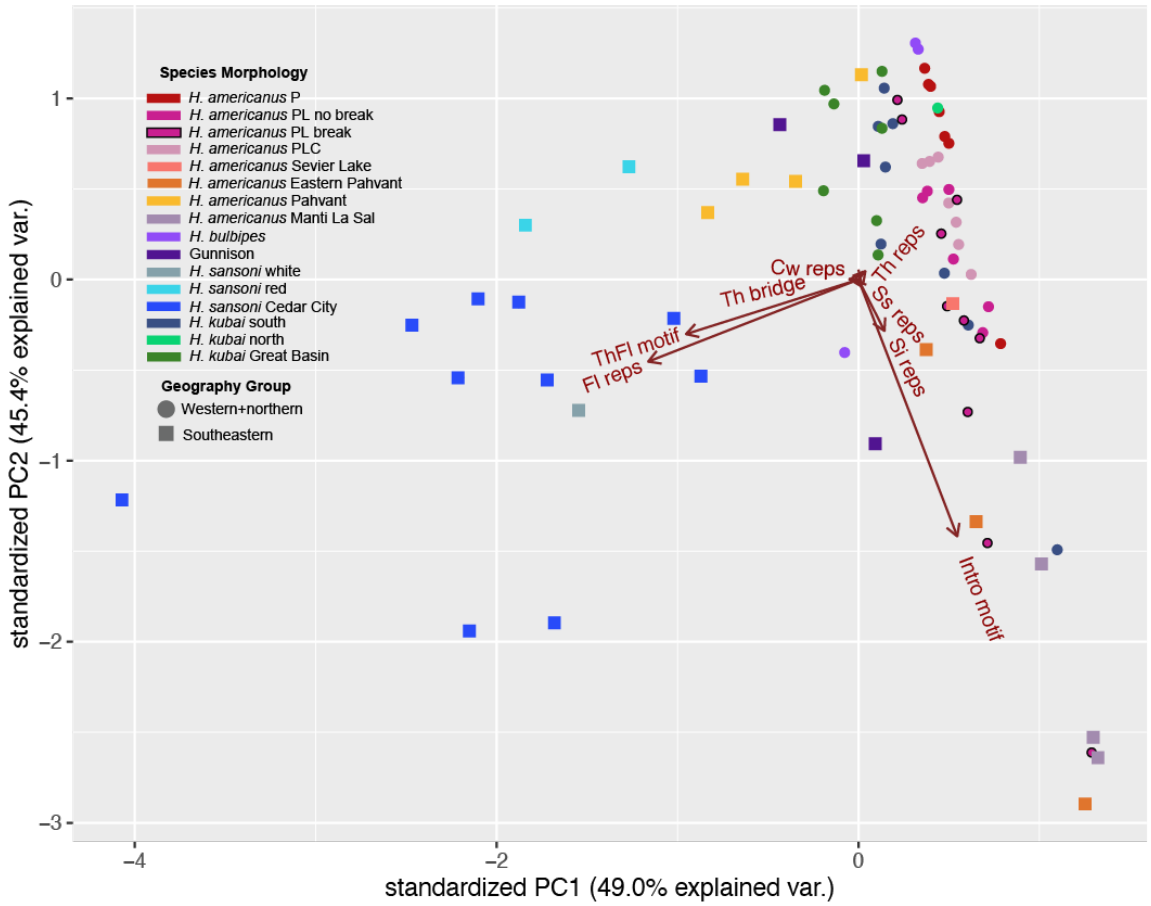

Figure 2.6. PCA of eight courtship display characters for all *americanus* subgroup species and morphs. Colors denote different described species or morphs. Symbols denote geographic region based on display element characters and each data point represents and individual.

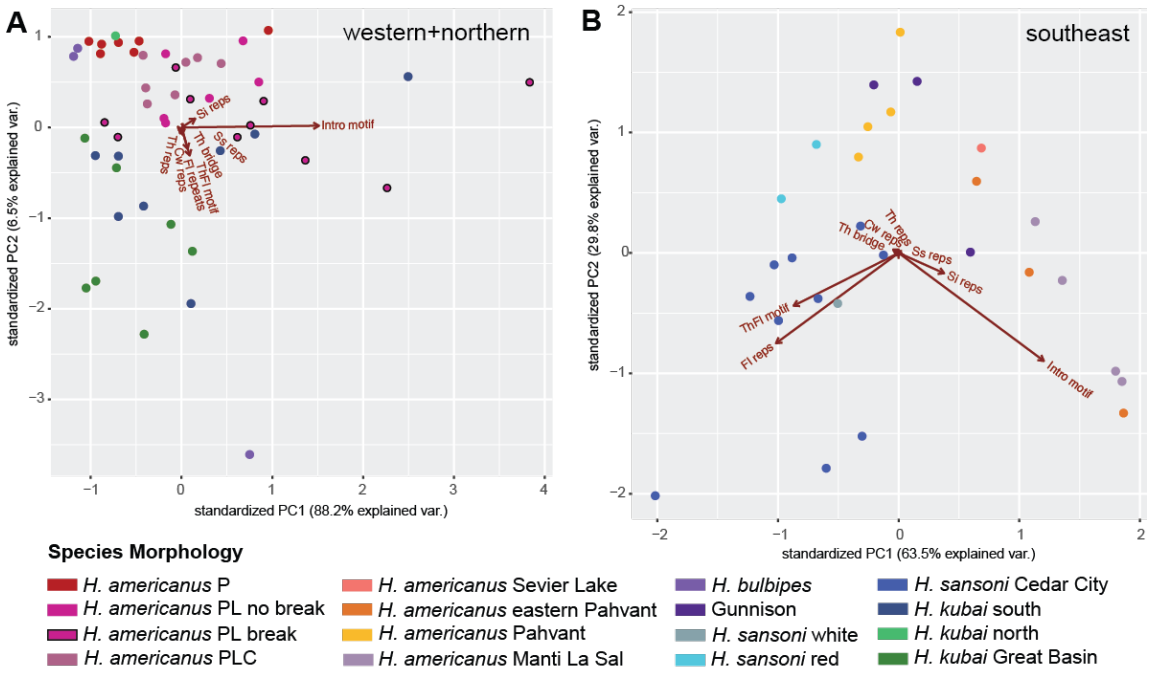

Figure 2.7. PCA of eight courtship display characters for morphs with courtship displays characteristic of the western+northern region (A) and those characteristic of the southeastern region (B). Colors of points correspond to colors of species morphology in the legend and each data point represents and individual.

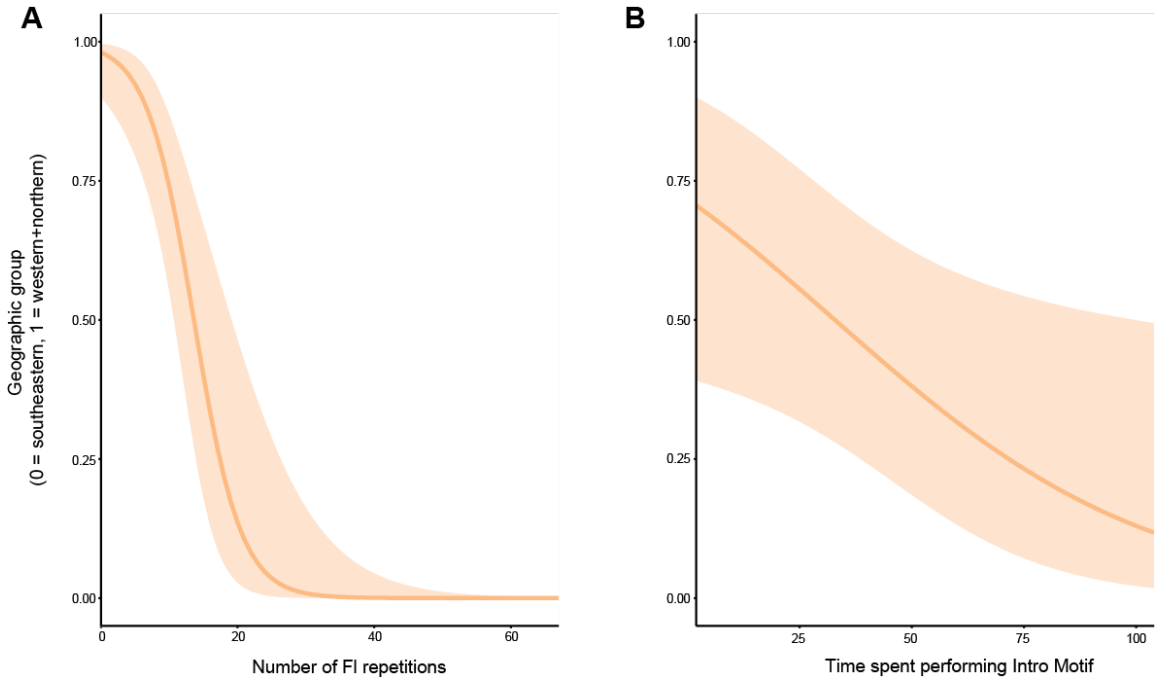

Figure 2.8. Probability of specimen belonging to the southeastern or western+northern courtship display group versus the number of Fl repetitions performed (A) and the time spent performing the introductory motif (B).

CHAPTER 3

Dynamics of hybridization in a complex hybrid zone between members of the *Habronattus americanus* subgroup (F. Salticidae)

Abstract

Contemporary hybrid zones may shed light on the process of speciation and whether and how species boundaries are maintained when rampant hybridization takes place. The *Habronattus americanus* subgroup consists of several closely related jumping spider species with substantial evidence of hybridization and introgression. I explored a hybrid zone involving *H. americanus* and *H. kubai* near Mt. Shasta, CA, where I characterized genetic variation using ddRADseq data. I also assessed the morphological diversity within the hybrid zone, including the fine-scale geographic distribution of hybrid and pure individuals. Our genetic results indicate a highly homogenized population with little genomic differentiation between morphs, including individuals with pure parental phenotypes. I identified 19 distinct, diagnosable hybrid morphs, highlighting the striking morphological diversity despite genomic homogenization. The hybrid zone is characterized by more hybrid individuals than parental-type individuals throughout the geographic space of the zone. The frequency of individuals with differently colored palps (both pure and hybrid-type) appears to differ across the elevational gradient of the hybrid zone. I also identify a novel trait not present in either parental species. My results contribute to an overall better understanding of how genetic

and morphological traits may behave in hybrid zones and enrich our understanding of the nature of species in the context of introgression.

I. INTRODUCTION

Hybrid zones offer unique opportunities to study introgression and the nature of isolating barriers between diverging lineages (Abbott et al. 2016; Gompert et al. 2017). Many studies have used hybrid zones to identify the genetic loci responsible for phenotypic traits corresponding to species identity (e.g., Brelsford et al. 2017; Funk and Taylor 2019; Yang et al. 2020). Additionally, introgression has been documented as a driver of speciation, in rapidly radiating taxa or otherwise, by introducing adaptive alleles (Jiggins et al. 2008; Meier et al. 2017; Valencia-Montoya et al. 2021). In cases involving rapidly radiating taxa, identifying loci correlated with certain phenotypes can provide information about mechanisms that fuel such radiations (Seehausen 2004), highlighting the usefulness of studying the evolutionary consequences of introgression in regard to rapid radiations.

Zhang et al. (2019) discusses rapidly radiating taxa as a community of closely related species that exchange genomic material, but essentially exist as a single lineage, evolving together. Taxa within such communities may include many nascent species – defined as recently-diverged lineages that have not developed complete reproductive isolation (Cutter and Gray 2016). Investigations of hybrid zones between current nascent species connected by repeated gene flow events throughout their evolution present opportunities to further understand how introgression may impact species divergence, particularly in “non-traditional” groups, where species show less “genetic closure” than for standard biological species.

A unique system to explore the dynamics of on-going hybridization is a group of jumping spiders in the genus *Habronattus*. *Habronattus* is a species rich (>100 described species) taxon that diverged relatively recently – possibly less than 5 million years ago (Bodner and Maddison 2012). *Habronattus* adult males have elaborate colored ornaments and courtship behavior and many of these traits are affected by hybridization (Masta and Maddison 2002, Elias 2003, Elias et al. 2006). Several *Habronattus* species groups also show genetic evidence of hybridization (Masta 2000; Maddison and Hedin 2003; Hedin and Lowder 2009; Blackburn and Maddison 2014; Leduc-Robert and Maddison 2018; Hedin et al. 2020). The *H. americanus* group is one such clade with documented evidence for hybridization (Blackburn and Maddison 2014; Leduc-Robert and Maddison 2018; Hedin et al. 2020).

The *H. americanus* group is comprised of 10 described species primarily distributed across western North America (Griswold 1987), including a clade of five closely related species, the *americanus* subgroup – *H. americanus, H. bulbipes, H. kubai, H. waughi,* and *H. sansoni*. Previous studies have documented hybridization and introgression within the *americanus* subgroup, both between phenotypically divergent populations of the same species (Blackburn and Maddison 2014) and between two or more different species (Leduc-Robert and Maddison 2018; Bougie et al. 2021). Members of this subgroup exhibit highly homogenized genomes, such that phylogenetic analyses recover geographically defined lineages with multiple described species as clades, rather than recovering individual described species as clades. It appears that throughout the evolution of the *americanus* subgroup, climatic fluctuations enabled diverging

populations to repeatedly come into contact and exchange genetic material, effectively homogenizing genomes, while selective forces maintained unique male traits as key species signals (see Chapter 1, Bougie et al. 2021). As such, the *americanus* subgroup seems to behave as a community of closely related nascent species evolving together. To maintain consistency with the literature and to avoid unnecessary confusion about the terminology as to what is and is not a species, I contend that the members within the *americanus* subgroup are species (although not as defined by a traditional biological species concept), and refer to them as such throughout this Chapter.

Several contact zones between two or more *americanus* subgroup members have been identified through morphological and preliminary genomic analyses. A hybrid zone near Mt. Shasta, CA includes *H. kubai* (north morph) and *H. americanus* (P morph) parental species, plus a variety of distinct morphological hybrid types (**Figure 3.1**; digital images, **Supplemental Figure 3.1**). The parental species are highly distinguishable morphologically. Briefly, *H. americanus* P has bright red palps, a high rectangular iridescent clypeus, a striped leg pattern, and blue hair bundles covering the chelicerae, while *H. kubai* north has gold palps, a low segmented pattern of iridescence on the clypeus, a banded leg pattern, and gold hair bundles covering the chelicerae. Despite the substantial morphological difference between the species, their courtship display behaviors are fairly similar (**e.g., Figure 2.2**).

The Mt. Shasta hybrid zone is located in an area that was impacted by glacial ice during the latest glacial maximum (LGM). Glacial ice covered much of the American west between about 21 and 16 thousand years ago (Reynolds et al. 2004). As glacial ice

retreated, range expansions enabled isolated, diverging populations to come into contact and hybridize if reproductive barriers were not yet established (Pielou 1991; Nice et al. 2005). It appears that the Mt. Shasta hybrid zone is one place where *H. americanus* and *H. kubai* presently (and historically) come into contact and engage in hybridization and introgression. The Mt. Shasta hybrid zone is located near Panther Meadows at an elevation of approximately 2286 meters. The last Pleistocene glaciation advance covered Mt. Shasta's south side down to around 1920 meters about 17-11 thousand years ago (Christiansen et al. 2017), covering the hybrid zone location in glacial ice, dating the hybrid zone as no older than 17-11 thousand years.

Given the extensive genomic homogenization of the *americanus* subgroup (Bougie et al. 2021), I first aimed to determine if genomes at this current contact zone remain homogenized. Because of the smaller geographic scale, I was able to recover more shared RAD loci across individuals in the zone, and look for potential genetic differences not detected in the broader study. Then I scored several morphological traits to assess the male morphological diversity and fine-scale geographical distribution of all forms present in the zone. I sought to identify whether components of the morphs (different male courtship traits) dissociate in any consistent pattern and whether male courtship traits segregate from the combinations present in the parental species when subjected to gene flow. By comparing patterns found in the genomic data with that of the morphological data I make inferences about possible divergence scenarios of the *americanus* subgroup.

II. METHODS

(1) Specimen Collection

The Mount Shasta hybrid zone is located near Panther Meadows in the Shasta-Trinity National Forest. The area of study is approximately 232,792 square meters at an elevation of approximately 2300 meters. Evidence of hybridization in this area was previously identified by the collection of male specimens with traits of both parental species, *H. kubai* and *H. americanus*. In July 2018, a team of three persons collected 89 specimens from across the zone – 78 adult males, 9 females, and two penultimate males (**Appendix 3.1**). This team surveyed the area at random and attempted to collect all adult males seen (hand-collected into glass vials); because females of the two different species cannot be morphologically separated, we collected a smaller number of adult females than encountered. Specimens were georeferenced at their specific site of collection using a Garmin Etrex 20x handheld GPS device.

(2) Morphological Data Collection and Analysis

Eleven discrete morphological characters were scored for all adult male specimens, for a total of 78 individuals (**Table 3.1**). Our sample includes individuals described as "standard" *H. americanus* and *H. kubai*, composed of specimens possessing character combinations that are typical for pure populations of these species (Bougie et al. 2021). The remaining specimens are described as *H. americanus* x *H. kubai* hybrids. I chose a subset of characters from Bougie et al. (2021), those that varied within the Mt.

Shasta hybrid population. Characters were scored by examining individuals in 100% ethanol under a dissecting microscope. A noticeable difference in color saturation is possible, especially for the red-palped forms. However, because color can fade while specimens are stored in ethanol, vibrancy was not scored. While the time between collection and scoring characters may have led to color loss, I found that most of the pigmentation was still noticeable and scoreable. To summarize morphological variation and identify morphological clusters, I performed a non-metric multidimensional scaling (NMDS) analysis using the metaMDS function with Bray-Curtis dissimilarity in the R package Vegan v2.5-6.

(3) Molecular Data Collection and Analysis

The molecular sample included 72 adult male samples, two penultimate males, and eight females collected in the hybrid zone, as well as four individuals collected from a nearby (~30 kilometers distant) pure *H. americanus* population (only *H. americanus* specimens found) and three individuals collected from a nearby (~31 kilometers distant) pure *H. kubai* population (**Figure 3.2**; **Appendix 3.1**). The pure *H. kubai* and *H. americanus* specimens were samples collected previously and are distant enough that it is unlikely they have contributed to the current dynamic near Panther Meadows. Two to three legs were used for DNA extraction, performed using the Qiagen DNeasy Blood & Tissue protocol (Qiagen, Valencia, CA). Quality and quantity of DNA was evaluated using gel electrophoresis and a Qubit Fluorometer, respectively.

I used double digest restriction-site associated DNA sequencing (ddRADseq) to collect genomic-scale data. I used the protocol described in Brelsford et al. (2016), using SbfI and MseI enzymes – a combination that increases sequencing depth while accounting for large *Habronattus* genome sizes (~5.586 Gb, Gregory and Shorthouse 2003). Sequencing was completed at Novogene using 150PE reads on an Illumina Hiseq 4000 platform.

Raw data were demultiplexed using STACKS v2.5.0 under default settings. After demultiplexing, the reads were processed using STACKS v2.5.0 with the –bound_high flag set to 0.05, --min-maf flag set to 0.05, and –min-samples-overall to 90 to require 90% of individuals across the dataset to process a locus. All other parameters were left as default.

I conducted a STRUCTURE 2.3.4 (Pritchard et al. 2000) analysis using 2182 unlinked SNPs from different RAD loci under the admixture model. STRUCTURE was run from K = 1 to K = 4, each replicated three times in R v4.0.3 using the package Rrunstruct and function 'structure_runs()'. To identify measures of genetic divergence between the different morph types, I estimated pairwise F_{ST} between palp color types using all ddRAD loci implemented in Arlequin v3.5.2.2 (Excoffier and Lischer 2010). I calculated F_{ST} using different palped colored individuals as "populations" and a separate analysis using the three different palped hybrid groups and the two standard morphs as "populations." Females, intermediate-palped individuals, and individuals sampled from the pure *H. kubai* and *H. americanus* populations were not included in measures of F_{ST}.

I performed a Mantel test using the R v 4.0.3 function 'mantel()' with 999 permutations in the Vegan v 2.5-7 package between the Haversine geographical distance

and Euclidean genetic distance to test for a correlation between genetic and geographic distance. The Euclidean genetic distance was calculated on a matrix of 6359 unlinked SNPs using the 'dist()' function in the R package stats. The Haversine distance uses the Haversine formula to determine the distance between two points on a sphere, making it an appropriate calculation for the distances between latitude/longitude points. The Haversine distance matrix was calculated using the R v 4.0.3 function 'distm()' in the geosphere package. To test for a correlation between genetic and morphological distance, I performed an additional Mantel test using the same R function as above between the Bray-Curtis dissimilarity matrix of scored morphology characters and the Euclidean genetic distance matrix of 6359 SNPs.

(4) Morphological Characterization of the Hybrid Zone

To identify if there are statistically more hybrids than standard type morphs, I performed a corrected one sided one-proportion z-test to compare the proportion of hybrids to a target proportion of 0.5 in R v4.0.3 using the function 'prop.test()'. The H_0 = the proportion of hybrids is not different from a 0.5 proportion and the H_A = the proportion of hybrids is significantly larger than 0.5, indicating there are more males with mixed characters than males with standard type characters of either species. To test if the number of differently colored palped individuals was skewed in any direction, I performed two X^2 goodness of fit tests. The first test included all male individuals with red, white, or yellow palps, while the second test only included hybrid morphs – no standard morphs were included. Both tests shared a null hypothesis that there are equal

numbers of red, yellow, and white-palped individuals across the hybrid zone. To further explore spatial characteristics of the zone, I mapped the spatial distribution of both standard morphs and each hybrid type. For ease of visualization, I categorized all hybrid morphs into three categories depending on palp color: red, white, or yellow hybrids.

Since the hybrid zone is oriented along an elevational gradient from the southern (2270 m) to the northern end (2424 m) of the zone, I tested for a relationship between palp color and mean elevation. I performed a one-way analysis of variance (ANOVA) using the function 'aov()' in R v4.0.3, with elevation as the dependent variable and palp color as the categorical independent variable with three categories: red, white, and yellow. I then performed a post hoc Tukey HSD test to identify if any comparison of means between specific pairs of palp color groups were statistically significant in R v4.0.3 using the 'TukeyHSD()' function.

To test for a possible relationship between palp color and habitat type, I recorded the number of red, yellow, and white-palped individuals in two (barren and shrub/scrub) of four recorded land cover types (barren, evergreen forest, developed, and shrub/scrub; **Supplemental Figure 3.2**) classified according to the National Land Cover Database (NLCD) 2019 Land Cover dataset (Wickham et al. 2021). I chose to use only the barren and shrub/scrub type because there are very few samples in both the evergreen forest and developed types such that confidence in the statistical analysis would be negatively impacted. Additionally, while the land cover shows individuals collected on a developed road, these individuals were not actually collected on the pavement, but nearby. Individuals collected on either evergreen forest or developed land were re-coded to

barren or shrub/scrub depending on which of the two land types was closest to them. Since the observations are binary (either barren or shrub/scrub) I performed a X^2 goodness of fit test with expected counts of red = 23.5, yellow = 9, and white = 5.5. The null hypothesis was that there is no relationship between palp color and habitat type.

To test for a correlation between morphology and geographical location, I performed a Mantel test using the Bray-Curtis dissimilarity matrix and the Haversine distance (as above) using the R v 4.0.3 function 'mantel()' with 999 permutations in the Vegan v 2.5-7 package.

III. RESULTS

(1) Genomic Analyses

ddRADseq data was recovered for 85 individuals. The STRUCTURE analysis was run using 2182 shared loci, a substantial increase from the 810 loci used in **Chapter 1**, increasing the chance of finding genetic differences between individuals. However, results still indicated a lack of genetic structure across different morph types within the hybrid zone and both pure populations (**Figure 3.3)**. The optimal K value was estimated as K = 2, using the Evanno method (Evanno et al. 2005), but was estimated as K = 3 using the Prob(K=k) method as described in Pritchard et al. 2000. Given the lack of confidence in estimating a best K, I show ancestry estimations for all values of K that I tested (1-4).

Estimation of F_{ST} values confirmed a lack of genetic difference between differently colored palps. F_{ST} values for comparisons between three colored palps, not including standard types as additional populations were all below 0.005 (**Table 3.2**). F_{ST} values for comparisons between the three hybrid palp colors and standard types ranged between 0.0215 and 0.0056 (**Appendix 3.3)**. The Mantel test to identify a correlation between genetic and morphological distance did not recover a significant result (r = 0.04217, $P = 0.1887$). There appears to be little to no relationship between our genetic data and the morphological features of male spiders within the hybrid zone.

(2) Morphological Analyses

The scored character matrix for morphological traits can be found in **Appendix 3.2**. I identified 19 diagnosable *H. americanus* x *H. kubai* hybrid morphs, defined (*a priori*) primarily by different combinations of palp color, chelicerae hair bundle color, leg I pattern, and iridescence pattern on the clypeus (**Figure 3.1**). The NMDS plot supports a pattern consistent with two morphologically distinct standard forms (*H. kubai* and *H. americanus* – of which includes five hybrid individuals grouped closely by standard *H. americanus* individuals) and a larger group composed of all hybrid types that encompasses a large area of the plot falling between the *H. kubai* and *H. americanus* clusters (**Figure 3.4**). The hybrid cluster appears to be extremely variable, demonstrated by the widespread area of the group on the plot. While there are different hybrid types categorized by palp color, there does not seem to be any evidence of separate clusters within hybrids. This pattern highlights the substantial morphological variation exhibited

by hybrids. There is some overlap between the hybrid group and the standard-type groups, suggesting that some hybrids may possess trait combinations that are more similar to either standard type rather than possessing an even mixture of both standard-type's traits. For example, an individual possessing mostly *H. americanus* traits, but with one trait belonging to the *H. kubai* standard type might be placed closer to the standard *H. americanus* cluster.

The proportion z-test revealed that there are more phenotypically-defined hybrid individuals than standard individuals hybrid zone, Z_1, $P = 7.402\ e^{-0.5}$ (**Appendix 3.4**). Our X^2 goodness of fit test showed that the number of individuals of each palp color in the hybrid zone are not at equal frequencies (**Appendix 3.5**; $X^2_2 = 28.7632$, $P < 0.00001$). As such, I may infer that the larger number of red-palped individuals is significantly different from both the number of white and yellow-palped individuals. When conducting the X^2 goodness of fit test only using hybrid-type specimens (no standard-type individuals), I also found that individuals of different palp color are present at significantly different frequencies throughout the zone ($X^2_2 = 20.468$, $P < 0.00001$; **Appendix 3.6**). These results should be considered with some caution as an assumption of the X^2 goodness of fit test is having a random sample. I believe our sampling was random across the hybrid zone, but it is certainly possible that spiders with brightly colored palps that stand out in the substrate are easier to spot (or catch) for collectors and/or we may not have surveyed the full extent of the hybrid zone and there may be an unsampled area of the zone with more yellow-palped individuals.

The ANOVA of elevation and palp color identified a significant difference between the mean elevations of each palp color ($F_2 = 5.143$, $P = 0.0081$; **Figure 3.5C**). The post-hoc Tukey HSD test recovered a significant relationship only between the white and red palped individuals ($P = 0.0149$; **Figure 3.5B and 3.5C**). Other pairwise comparisons were not significant, implying the main driver of the significance of our ANOVA is the elevation differences between red and white palped males.

The X^2 goodness of fit test to identify a relationship between palp color and two land cover types was significant ($X^2_2 = 12.4103$, $P < 0.002$; **Appendix 3.7**). These results and the ANOVA elevation results should be considered carefully because land cover type changes along the elevational gradient. As such altitude may conflate the tests of land cover differences or vice versa. The Mantel test to identify if there is a correlation between morphology and geographical location did not recover significant results ($r = -0.0496$, $P = 0.916$).

IV. DISCUSSION

(1) Lack of genetic structure

ddRADseq data show very little genetic structure between different morphs (**Table 3.2; Figure 3.3**), mirroring the dynamic between morphological and genetic diversity across many members of the *americanus* subgroup (Bougie et al. 2021). STRUCTURE analyses using hybrid zone individuals were run using many more loci than what was used for the STRUCTURE analyses of individuals across the entire *americanus*

subgroup in **Chapter 1** (2182 vs. 810), increasing the chances of finding differentiation across the genome, yet no additional structure was detected. While the Evanno method recovered an optimal K equal to 2 and the Prob(K=k) method recovered an optimal K value equal to 3, these results should be considered carefully. The Evanno method is incapable of recovering a best K of 1 (Evanno et al. 2005) – which seems to be the most likely scenario – and a K = 3 seems very unlikely within the hybrid zone considering the degree of genomic homogeneity in hybrid zone individuals themselves and across most *americanus* subgroup species (Bougie et al. 2021). F_{ST} between differently palp colored individuals further supports a lack of genetic structure. The degree of genomic similarity in the hybrid zone coupled with the extensive morphological diversity further highlights the evolutionary complexity of this group. Lack of genetic structure across morphs in the Mt. Shasta hybrid zone supports the hypothesis that a small number of genes are responsible for male morphologies of the group and our ddRADseq methods were simply unable to detect these loci, reflected by the lack of relationship between morphological and genomic distance. Additionally, the probability of missing diagnostic genomic regions is large given that our ddRADseq methods covered less than 0.0071% of the genome (see calculations in **Appendix 3.8**).

The Mt. Shasta hybrid zone does not seem to have any obvious genomic clinal pattern with pure forms on opposite sides and admixed individuals in between, but rather resembles a mixture of hybrids and standard types across the zone (**Figure 3.2**). Additionally, I can only identify "pure" types via morphology and I have no knowledge of whether truly pure populations exist on Mt. Shasta. A similar phenomenon of rampant

hybridization seems to be occurring at Bunny Flats (personal observation), a lower elevation location about 4 km downslope from Panther Meadows.

(2) Morphological diversity

Morphological analyses identified high diversity within the Mt. Shasta hybrid zone. Two standard type morphs exhibiting phenotypes belonging to *H. americanus* and *H. kubai* and 19 distinguishable hybrid morphs add to a striking 21 different male morphologies in a single hybrid zone (**Figure 3.1**). The proportion z-test revealed that there are significantly more hybrid individuals than pure-looking individuals within the zone, demonstrating how easily morphologies of described species can be unraveled via introgression (**Appendix 3.4**). Hybrids and/or introgressed individuals sharing traits from parental species is not uncommon in the literature (e.g., wing pattern in *Lycaeides*, Gompert et al. 2010; wing pattern in *Heliconius,* Jiggins et al. 2008, The *Heliconius* Genome Consortium 2012, Parado-Diaz et al. 2012, Brower 2012 plumage coloration in warblers, Brelsford et al. 2017). The Mt. Shasta hybrid zone adds yet another system demonstrating the high degree of morphological diversity that hybridization can create.

Hybrids sharing colored ornaments from both parental species adds further support to previous findings in *Habronattus* that suggest secondary sexual characteristics presented to females during courtship dances are greatly affected by hybridization (Masta and Maddison 2002; Maddison and McMahon 2000; Maddison and Hedin 2003). The number of distinct traits shared across species boundaries implies that these traits are likely encoded by genes in multiple independently segregating linkage groups, otherwise

there would be groups of certain traits that always appear together, which is not observed. Individuals descended from more than one generation of admixture may show novel trait combinations due to recombination and independent assortment. It is also possible that multiple genes coding for different sexually important traits are on the same linkage group, but occasionally recombine to generate less common trait combinations.

Clearly, male *H. americanus* x *H. kubai* hybrids share multiple traits from both species, but a new trait belonging to neither parental species also emerged: pure white palps (**Figure 3.1**). The appearance of a novel trait indicates a potential role introgression played throughout the evolution of this entire subgroup in creating unique traits in contact zones. Perhaps the number of unique courtship traits across the *americanus* subgroup emerged in a two-step process, (1) sexual selection driving the appearance of elaborate ornamentation followed by (2) gene flow transmitting ornamentation alleles between populations, potentially creating novel traits. Bower (2012) describes a similar hypothesis to explain high wing pattern diversity in *Heliconius* butterflies, but rather suggests that the initial evolution of wing patterns was driven by Müllerian mimicry instead of sexual selection. These white-palped hybrids present an opportunity to understand how hybridization could lead to new traits that in turn may spark incipient speciation events in systems experiencing high levels of sexual selection.

It appears that the sexual ornamentation in males of the *americanus* subgroup are the primary "species identifier" traits enabling spiders to maintain their specific identities. Thus, sharing of these traits highlights the fluidity of the species boundaries between *H. americanus* and *H. kubai,* which is likely a consequence of the divergence history

(discussed below). New phenotypes brought about by hybridization have been shown to spark speciation and rapid radiation events (e.g., Mavarez et al. 2006; Lamichhaney et al. 2018; Powell et al. 2021). It is possible that similar mechanisms that led to the new white-palp phenotype in the *H. americanus* x *H. kubai* hybrids also drove the appearance of new phenotypes in other *Habronattus* species complexes, such as *H. pugillis* populations in the Arizona sky islands (Maddison and McMahon 2000). Such mechanisms may have been a key player in fueling a rapid radiation of all *Habronattus* (Bodner and Maddison 2012; Leduc-Robert and Maddison 2018). I cannot identify whether the white-palp trait is adaptive or maladaptive with the data collected here. While it is expected that a favorable trait would spread beyond the hybrid zone boundaries, it is possible that that the zone was already too geographically isolated from other *americanus* subgroup populations to pass the white-palp trait to additional diverging lineages.

(3) Morphological patterns across space

The significant relationship between palp color and elevation (**Figure 3.5C**) suggests that there is an underlying pattern of a difference in mean elevations of red-palped males and white-palped males. Our land type X^2 goodness of fit test revealed a similar pattern that red, white, and yellow palped individuals are not at identical frequencies within the two different land types, of which the transition from one type to the other follows an elevational gradient (**Appendix 3.7**). White-palped individuals are more common at lower elevations and are mostly concentrated in the shrub/scrub habitat,

while red-palped individuals are present mostly concentrated in mid and high elevations and prefer bare habitat, although there are still several low-elevation red-palped males **(Figure 3.5, Supplemental Figure 3.2**). These results indicate there might be some selective advantage for white-palped individuals to remain in shrub/scrub habitat or lower elevations.

Other than the red-palped and white-palped elevational and land type pattern, there is no support for any other morphological patterns across space. This includes no clinal pattern or relationship between morphological distance and geographic distance.

(4) Snapshot in time of the divergence of the americanus subgroup

Previous research documented the extensive amount of genomic homogenization and striking morphological diversity of *americanus* subgroup members (Bougie et al. 2021; **Chapter 1**). Blackburn and Maddison (2014) similarly found low levels of genomic divergence among phenotypically distinct *H. americanus* populations in the southern Sierra Nevada. The Mt. Shasta hybrid zone offers a new perspective on the divergence of these isolated, phenotypically distinct populations. Perhaps as the climate fluctuated, these populations came back into contact with one another and exchanged genetic material, a pattern that may have occurred repeatedly until populations became isolated to their current habitats. Selection on male phenotypes would then have had to be strong enough to avoid homogenizing effects of gene flow, leading to isolated populations with distinct phenotypic divergence, but low genetic differentiation. The Mt. Shasta hybrid zone data aids our understanding of the divergence history of the

americanus subgroup at a fine geographic scale, which may act as a snapshot in time of the species interactions that occurred periodically throughout the divergence history of the group.

The Mt. Shasta hybrid zone can only be as old as about 11-17 thousand years due to the glacial cover of the area at the time (Christiansen et al. 2017). As glacial ice melted, populations of *H. kubai* and *H. americanus* came into contact without fully established reproductive barriers, leading to hybridization between the nascent species. I can assume this interaction has been occurring ever since the two species came in sympatry in this area. I can apply the current dynamics at the Mt. Shasta hybrid zone to events that may have occurred when other *americanus* subgroup populations came into contact following range expansions due to melting glacial ice (Bougie et al. 2021). Since the *americanus* subgroup is estimated at only 200,000 years old (Hedin et al. 2020), populations were almost certainly subject to changes in glacial ice cover during the Pleistocene (2,580,000 – 11,700 years ago).

The high morphological diversity of hybrids could indicate how evolving populations were fueled by morphological changes, ultimately leading to rapid divergences if certain traits became favored over others. The Mt. Shasta hybrid zones highlights how despite selection maintaining distinct male phenotypes across isolated populations of *americanus* subgroup members, when they come into contact, species-specific trait combinations become unraveled. Sexual selection is a strong force in *Habronattus* (Peckham and Peckham 1889; Peckham and Peckham 1890; Masta and Maddison 2002; Elias et al. 2003; Hebets and Maddison 2005; Elias et al. 2006; Elias et

al. 2012) and it is possible that females presented with novel trait combinations or novel traits altogether preferred these new traits over those more standard of their species. Unfortunately, I cannot know the mating preferences of *americanus* subgroup females without additional behavioral experiments. If this scenario occurred, I hypothesize that the diversity in male ornaments across the *americanus* subgroup and potentially many other *Habronattus* was driven by hybridization following secondary contact and then sexual selection (e.g., Maddison and McMahon 2000).

(5) *H. americanus* may promote introgression

The hybrid zone has more red-palped individuals than white or yellow-palped males (**Appendix 3.5**). Additionally, there are more red-palped hybrids that display mostly *H. kubai* traits (13) than yellow-palped hybrids that display mostly *H. americanus* traits (1) – a pattern that may indicate evidence for selection favoring red colored palps. Red coloration of male courtship traits seems to have repeatedly evolved across many *Habronattus* species complexes, including the *americanus* subgroup (Griswold 1987; Maddison and Hedin 2003; Blackburn and Maddison 2014, Bougie et al. 2021). Zurek et al. (2015) describes a spectral filter within *Habronattus* that enables trichromatic vision via the addition of receptors sensitive to red light. It appears the filter permitting trichromatic vision is a general feature of the genus and may have played an important role in courtship evolution of *Habronattus* (Zurek et al. 2015). Evidence suggests red coloration in at least one *Habronattus* species improves courtship success when courting occurs in certain lighting conditions (Taylor et al. 2013). It is possible that the abundance

of red-palped males in the Mt. Shasta hybrid zone may be partially due to a preference for red phenotypes. Behavioral experiments will be needed to gain a better understanding of the importance of the red palps and whether it is a preferred trait to females in the hybrid zone. However, if I accept that the red phenotype increases propensity for hybridization in some way, there are implications I can draw regarding the divergence of the *americanus* subgroup.

Standard *H. americanus* adult males exhibit vibrant, bright red palps presented to females during courtship. Populations of *H. americanus* can be found throughout mountainous western North America, including the Rockies, Canadian Rockies, Cascades, and Sierra Nevada mountains (**Figures 1.1** and **1.2;** Griswold 1987; Bougie et al. 2021). Other species within the *americanus* subgroup have more restricted ranges and appear to occupy fewer microhabitats (**Figures 1.1** and **1.2)**. *H. americanus* populations have been found in a range of habitats – near beaches in British Columbia, alpine sage brush in the Sierra Nevada, and saltgrass flats in central Nevada, among others. For these reasons, *H. americanus* seems to be more of a generalist, enabling populations to establish in many environments, including those where other *americanus* subgroup members reside. If throughout the divergence of the subgroup, *H. americanus* populations came in secondary contact with *H. kubai* populations (and populations of other species), perhaps hybridization was driven by a female preference of both species for the red-palp trait of *H. americanus* males. Most identified hybrid zones between *americanus* subgroup members involve *H. americanus*.

If the red palps of *H. americanus* males have indeed increased propensity for hybridization throughout the divergence of the subgroup, researchers may eventually be able to use loci corresponding to color or courtship trait to trace the evolutionary history. However, genomics research is required to identify these loci, and behavioral studies are needed to know whether red phenotypes are truly favored in the *americanus* subgroup.

V. CONCLUSIONS

Individuals within the Mt. Shasta hybrid zone are coupled through a history of repeated introgression that is still occurring today in an active hybrid zone. In Chapter 1, I suggested that the *americanus* subgroup may be best described as a complex unit of closely related taxa evolving together, at least within geographic regions of contact. The current dynamics at the Mt. Shasta hybrid zone highlight the evolutionary consequences when nascent species are brought into sympatry. Repeated hybridization and introgression continue to homogenize genomes, while maintaining important species-specific male courtship traits and even creating novel traits.

The Mt. Shasta hybrid zone appears to be a microcosm for processes that have been occurring periodically throughout the divergence of the *americanus* subgroup. As such, we are presented with a unique study site that can be further investigated to understand the consequences that frequent hybridization has had on the system. Behavioral experiments similar to Taylor et al. (2013) and Elias et al. (2006) could be conducted to identify preference functions of females across the zone and whether or not

the red phenotype is favored. Whole genome sequencing has the potential to identify the small, differentiated areas of the genome that likely correspond to some sexually selected traits (e.g., Toews et al. 2017). Coupling behavioral data with new genomic data could help paint a picture of how introgression has shaped the trajectory of evolution in groups of nascent species experiencing strong sexual selection. Moreover, similar high-elevation hybrid zones are repeated in other places of the Sierra Nevada and Cascade mountains, providing some level of replication to study these evolutionary dynamics.

VI. REFERENCES

Abbott, R., Albach, D., Ansell, S., Arntzen, J.W., Baird, S.J.E., Bierne, N., Boughman, J., Brelsford, A., Buerkle, C.A., Buggs, R., Butlin, R.K., Dieckmann, U., Eroukhmanoff, F., Grill, A., Cahan, S.H., Hermansen, J.S., Hewitt, G., Hudson, A.G., Jiggins, C., Jones, J., Keller, B., Marczewski, T., Mallet, J., Martinez-Rodriguez, P., Möst, M., Mullen, S., Nichols, R., Nolte, A.W., Parisod, C., Pfennig, K., Rice, A.M., Ritchie, M.G., Seifert, B., Smadja, C.M., Stelkens, R., Szymura, J.M., Väinölä, R., Wolf, J.B.W., Zinner, D., 2013. Hybridization and speciation. J. Evol. Biol. 26, 229–246. https://doi.org/10.1111/j.1420-9101.2012.02599.x

Abbott, R.J., Barton, N.H., Good, J.M., 2016. Genomics of hybridization and its evolutionary consequences. Mol. Ecol. 25, 2325–2332. https://doi.org/10.1111/mec.13685

Blackburn, G.S., Maddison, W.P., 2014. Stark sexual display divergence among jumping spider populations in the face of gene flow. Mol. Ecol. 23, 5208–5223. https://doi.org/10.1111/mec.12942

Bodner, M.R., Maddison, W.P., 2012. The biogeography and age of salticid spider radiations (Araneae: Salticidae). Mol. Phylogenet. Evol. 65, 213–240. https://doi.org/10.1016/j.ympev.2012.06.005

Bougie, T.C., Brelsford, A., Hedin, M., 2021. Evolutionary impacts of introgressive hybridization in a rapidly evolving group of jumping spiders (F. Salticidae, Habronattus americanus group). Mol. Phylogenet. Evol. 161, 107165. https://doi.org/10.1016/j.ympev.2021.107165

Brelsford, A., Dufresnes, C., Perrin, N. 2016. High-density sex-specific linkage maps of a European tree frog (*Hyla arborea*) identify the sex chromosome without information on offspring sex. Heredity. 116, 177-181 (2016). https://doi.org/10.1038/hdy.2015.83

Brelsford, A., Toews, D.P.L., Irwin, D.E., 2017. Admixture mapping in a hybrid zone reveals loci associated with avian feather coloration. Proc. R. Soc. B. 284, 20171106. https://doi.org/10.1098/rspb.2017.1106

Brower, A.V.Z., 2013. Introgression of wing pattern alleles and speciation via homoploid hybridization in *Heliconius* butterflies: a review of evidence from the genome. Proc. R. Soc. B. 280, 20122302. https://doi.org/10.1098/rspb.2012.2302

Christiansen, R.L., Calvert, A.T., and Grove T.L., 2017, Geologic field-trip guide to Mount Shasta volcano, northern California: U.S. Geological Survey Scientific Investigations Report 2017-5022-K3, 1-33. https://doi.org/10.3133/sir20175022K3

Cutter, A.D., Gray, J.C., 2016. Ephemeral ecological speciation and the latitudinal biodiversity gradient: perspecive. Evolution 70, 2171–2185. https://doi.org/10.1111/evo.13030

DeChaine, E.G., Wendling, B.M., Forester, B.R., 2014. Integrating environmental, molecular, and morphological data to unravel an ice-age radiation of arctic-alpine *Campanula* in western North America. Ecol. Evol. 4, 3940–3959. https://doi.org/10.1002/ece3.1168

Elias, D.O., Land, B.R., Mason, A.C., Hoy, R.R., 2006. Measuring and quantifying dynamic visual signals in jumping spiders. J. Comp. Physiol. 192, 785–797. https://doi.org/10.1007/s00359-006-0116-7

Elias, D.O., Mason, A.C., Maddison, W.P., Hoy, R.R., 2003. Seismic signals in a courting male jumping spider (Araneae:Salticidae). J. Exp. Biol. 206, 4029–4039. https://doi.org/10.1242/jeb.00634

Elias, D.O., Maddison, W.P., Peckmezian, C., Girard, M.B., Mason, A.C., 2012. Orchestrating the score: complex multimodal courtship in the *Habronattus coecatus* group of *Habronattus* jumping spiders (Araneae: Salticidae): multimodal courtship in *Habronattus*. Biol. J. Linn. Soc. 105 (3), 522–547. doi: 10.1111/j.1095-8312.2011.01817.x

Evanno, G., Regnaut, S., Goudet, J., 2005. Detecting the number of clusters of individuals using the software structure: a simulation study. Mol. Ecol. 14, 2611–2620. https://doi.org/10.1111/j.1365-294X.2005.02553.x

Excoffier, L. and H.E. L. Lischer (2010) Arlequin suite version 3.5: A new series of programs to perform population genetics analyses under Linux and Windows. Mol. Ecol. Res. 10: 564-567.

Funk, E.R., Taylor, S.A., 2019. High-throughput sequencing is revealing genetic associations with avian plumage color. The Auk 136, ukz048. https://doi.org/10.1093/auk/ukz048

Gompert, Z., Lucas, L.K., Fordyce, J.A., Forister, M.L., Nice, C.C., 2010. Secondary contact between Lycaeides idas and L. melissa in the Rocky Mountains: extensive admixture and a patchy hybrid zone: A patchy butterfly hybrid zone. Mol. Ecol. 19, 3171–3192. https://doi.org/10.1111/j.1365-294X.2010.04727.x

Gompert, Z., Mandeville, E.G., Buerkle, C.A., 2017. Analysis of Population Genomic Data from Hybrid Zones. Annu. Rev. Ecol. Evol. Syst. 48, 207–229. https://doi.org/10.1146/annurev-ecolsys-110316-022652

Gregory, T.R., 2003. Genome Sizes of Spiders. J. Hered. 94, 285–290. https://doi.org/10.1093/jhered/esg070

Griswold, C.E., 1987. A revision of the jumping spider genus Habronattus F.O.P. Cambridge (Araneae; Salticidae), with phenetic and cladistic analyses. Univ. California Pub. Ent. 107, 1-344.

Hebets, E.A., Maddison, W.P., 2005. Xenophilic mating preferences among populations of the jumping spider *Habronattus pugillis* Griswold. Behav. Ecol. 16, 981–988. https://doi.org/10.1093/beheco/ari079

Hedin, M., Foldi, S., Rajah-Boyer, B., 2020. Evolutionary divergences mirror Pleistocene paleodrainages in a rapidly-evolving complex of oasis-dwelling jumping spiders (Salticidae, *Habronattus tarsalis*). Mol. Phylogenet. Evol. 144, 106696. https://doi.org/10.1016/j.ympev.2019.106696

Hedin, M., Lowder, M.C., 2009. Phylogeography of the Habronattus amicus species complex (Araneae: Salticidae) of western North America, with evidence for localized asymmetrical mitochondrial introgression. Zootaxa 2307, 39–60. https://doi.org/10.11646/zootaxa.2307.1.2

Jiggins, C.D., Salazar, C., Linares, M., Mavarez, J., 2008. Hybrid trait speciation and *Heliconius* butterflies. Phil. Trans. R. Soc. B 363, 3047–3054. https://doi.org/10.1098/rstb.2008.0065

Lamichhaney, S., Han, F., Webster, M.T., Andersson, L., Grant, B.R., Grant, P.R., 2018. Rapid hybrid speciation in Darwin's finches. Science 359, 224–228. https://doi.org/10.1126/science.aao4593

Leduc-Robert, G., Maddison, W.P., 2018. Phylogeny with introgression in *Habronattus* jumping spiders (Araneae: Salticidae). BMC Evol. Biol. 18, 24. https://doi.org/10.1186/s12862-018-1137-x

Maddison, W., Hedin, M., 2003. Phylogeny of Habronattus jumping spiders (Araneae: Salticidae), with consideration of genital and courtship evolution: Habronattus spider phylogeny. Syst. Entomol. 28, 1–22. https://doi.org/10.1046/j.1365-3113.2003.00195.x

Maddison, W., McMahon, M., 2000. Divergence and Reticulation among Montane Populations of a Jumping Spider *(Habronattus pugillis* Griswold). Syst. Biol. 49, 400–421.

Mallet, J., Besansky, N., Hahn, M.W., 2016. How reticulated are species? BioEssays 38, 140–149. https://doi.org/10.1002/bies.201500149

Martin, S.H., Jiggins, C.D., 2017. Interpreting the genomic landscape of introgression. Curr. Opin. Genet. Dev. 47, 69–74. https://doi.org/10.1016/j.gde.2017.08.007

Masta, S.E., 2000. Phylogeography of the Jumping Spider *Habronattus pugillis* (Araneae: Salticidae): Recent Vicariance of Sky Island Populations? Evolution 54, 1699–1711.

Masta, S.E., Maddison, W.P., 2002. Sexual selection driving diversification in jumping spiders. PNAS 99, 4442–4447. https://doi.org/10.1073/pnas.072493099

Mavárez, J., Salazar, C.A., Bermingham, E., Salcedo, C., Jiggins, C.D., Linares, M., 2006. Speciation by hybridization in Heliconius butterflies. Nature 441, 868–871. https://doi.org/10.1038/nature04738

McKenzie, J.L., Bucking, C., Moreira, A., Schulte, P.M., 2017. Intrinsic reproductive isolating mechanisms in the maintenance of a hybrid zone between ecologically divergent subspecies. J. Evol. Biol. 30, 848–864. https://doi.org/10.1111/jeb.13055

Meier, J.I., Marques, D.A., Mwaiko, S., Wagner, C.E., Excoffier, L., Seehausen, O., 2017. Ancient hybridization fuels rapid cichlid fish adaptive radiations. Nat. Commun. 8, 14363. https://doi.org/10.1038/ncomms14363

Nice, C.C., Anthony, N., Gelembiuk, G., Raterman, D., Ffrench-Constant, R., 2005. The history and geography of diversification within the butterfly genus Lycaeides in North America. Mol. Ecol. 14, 1741–1754. https://doi.org/10.1111/j.1365-294X.2005.02527.x

Pardo-Diaz, C., Salazar, C., Baxter, S.W., Merot, C., Figueiredo-Ready, W., Joron, M., McMillan, W.O., Jiggins, C.D., 2012. Adaptive Introgression across Species Boundaries in Heliconius Butterflies. PLoS Genet 8, e1002752. https://doi.org/10.1371/journal.pgen.1002752

Peckham, G.W., Peckham, E.G., 1889. Observations on sexual selection in spiders of the family Attidae. Nat. History Soc. Wisconsin 1, 3–60.

Peckham, G.W., Peckham, E.G., 1890. Additional observations of sexual selection in spiders of the family Attidae: with some remarks on Mr. Wallace's theory of sexual ornamentation. Nat. History Soc. Wisconsin 1 (3), 117–151.

Pickup, M., Brandvain, Y., Fraïsse, C., Yakimowski, S., Barton, N.H., Dixit, T., Lexer, C., Cereghetti, E., Field, D.L., 2019. Mating system variation in hybrid zones: facilitation, barriers and asymmetries to gene flow. New Phytol. 224, 1035–1047. https://doi.org/10.1111/nph.16180

Pielou, E. C.. 1991. After the Ice Age: The Return of Life to Glaciated North America. University of Chicago Press. https://doi.org/10.7208/9780226668093

Powell, D.L., Payne, C., Banerjee, S.M., Keegan, M., Bashkirova, E., Cui, R., Andolfatto, P., Rosenthal, G.G., Schumer, M., 2021. The Genetic Architecture of Variation in the Sexually Selected Sword Ornament and Its Evolution in Hybrid Populations. Curr. Biol. 31, 923-935.e11. https://doi.org/10.1016/j.cub.2020.12.049

Pritchard, J.K., Stephens, M., Donnelly, P., 2000. Inference of Population Structure Using Multilocus Genotype Data. Genetics 155, 945–959. https://doi.org/10.1093/genetics/155.2.945

Ravinet, M., Faria, R., Butlin, R.K., Galindo, J., Bierne, N., Rafajlović, M., Noor, M.A.F., Mehlig, B., Westram, A.M., 2017. Interpreting the genomic landscape of speciation: a road map for finding barriers to gene flow. J. Evol. Biol. 30, 1450–1477. https://doi.org/10.1111/jeb.13047

Reynolds, R.L., Rosenbaum, J.G., Rapp, J., Kerwin, M.W., Platt Bradbury, J., Colman, S., Adam, D., 2004. Record of late Pleistocene glaciation and deglaciation in the southern Cascade Range. I. Petrological evidence from lacustrine sediment in upper Klamath Lake, southern Oregon. J. Paleolimnol. 31, 217–233. https://doi.org/10.1023/B:JOPL.0000019230.42575.03

Seehausen, O., 2004. Hybridization and adaptive radiation. Trends Ecol. Evol. 19, 198–207. https://doi.org/10.1016/j.tree.2004.01.003

Taylor, L.A. and McGraw, K.J. (2013) Male ornamental coloration improves courtship success in a jumping spider, but only in the sun. *Behav. Ecol.* 24 (4), 955-967, https://doi.org/10.1093/beheco/art011

Taylor, L.A., Powell, E.C., McGraw, K.J., 2017. Frequent misdirected courtship in a natural community of colorful Habronattus jumping spiders. PLoS ONE 12, e0173156. https://doi.org/10.1371/journal.pone.0173156

Toews, D.P.L., Taylor, S.A., Vallender, R., Brelsford, A., Butcher, B.G., Messer, P.W., Lovette, I.J. 2016. Plumage genes and little else distinguish the genomes of hybridizing warblers. Curr. Biol. 26 (17), 2313-2318. https://doi.org/10.1016/j.cub.2016.06.034

The Heliconius Genome Consortium, 2012. Butterfly genome reveals promiscuous exchange of mimicry adaptations among species. Nature 487, 94–98. https://doi.org/10.1038/nature11041

Valencia-Montoya, W.A., Elfekih, S., North, H.L., Meier, J.I., Warren, I.A., Tay, W.T., Gordon, K.H.J., Specht, A., Paula-Moraes, S.V., Rane, R., Walsh, T.K., Jiggins, C.D., 2020. Adaptive introgression across semipermeable species boundaries between local Helicoverpa zea and invasive Helicoverpa armigera moths. Mol. Biol. Evol. 37, 2568–2583. https://doi.org/10.1093/molbev/msaa108

Wickham, J., Stehman, S.V., Sorenson, D.G., Gass, L., and Dewitz, J.A., 2021, Thematic accuracy assessment of the NLCD 2016 land cover for the conterminous United States: Remote Sens. Environ. 257, 112357. https://doi.org/10.1016/j.rse.2021.112357

Yang, W., Feiner, N., Laakkonen, H., Sacchi, R., Zuffi, M.A.L., Scali, S., While, G.M., Uller, T., 2020. Spatial variation in gene flow across a hybrid zone reveals causes of reproductive isolation and asymmetric introgression in wall lizards. Evolution 74, 1289–1300. https://doi.org/10.1111/evo.14001

Zurek, D.B., Cronin, T.W., Taylor, L.A., Byrne, K., Sullivan, M.L.G., Morehouse, N.I., 2015. Spectral filtering enables trichromatic vision in colorful jumping spiders. Curr. Biol. 25 (10), R403–R404. https://doi.org/10.1016/j.cub.2015.03.033

Tables

Table 3.1. List of scored morphological characters and character states.

ID	Description	States
A	Iridescent scales on clypeus– pattern: variable within species, may have iridescent patches, or completely iridescent clypeus.	0 = absence of iridescent scales; 1 = full rectangular; 2 = 'm' shaped; 3 = 'm' shaped in middle, extends low to sides; 4 = four low semi-circle broken segments; 5 = two irregular iridescent patches separated at the center; 6 = very low iridescent rectangle; 7 = two broken semi-circle segments; 8 = four connected semi-circle segments; 9 = iridescent rectangle halfway up the clypeus and expanding at ends
B	Clypeal covering emarginate: clypeus covered with two scale types and/or colors forming a well-marked white transverse band	0 = absent/no white band; 1 = spans entire length of AER; 2 = present only under AMEs
C	Color of non-iridescent setae on clypeus, NOT including white transverse band if present.	0 = all of clypeus covered in iridescence; 1 = brown; 2 = black
D	Clypeal covering divided in center	States: 0 = absent/not divided; 1 = divided
E	Color of hair pencils/hairs covering chelicerae	States: 0 = blue; 1 = pale/white; 2 = yellow/gold;
F	Leg I femur: Color of ventral side	0 = brown/dark; 1 = white/pale; 2 = speckled tan and black; 3 = white stripe/patch, rest brown;
G	Leg I femur: pattern	States: 0 = longitudinally striped; 1 = banded at the patella joint, no stripe
H	Leg I tibia: Color of ventral side	States: 0 = brown/dark; 1 = pale; 2 = speckled pale and black; 3 = white patch, rest brown/dark
I	Leg I tibia: pattern	States: 0 = longitudinally striped; 1 = speckled; 2 = plain; 3 = banded at joints, no stripe; 4 = cross between speckled and striped
J	Palpal patella color	States: 0 = uniform, yellow/gold; 1 = uniform, white/pale; 2 = uniform, red; 3 = nonuniform, mostly white/pale, some red
K	Color of hairs covering tarsal bulb	0 = uniform, yellow/gold; 1 = uniform, white/pale; 2 = uniform, red; 3 = nonuniform, pale white with some pale red hairs.

Table 3.2. Pairwise F_{ST} estimated using all ddRADseq loci. *P*-values in parentheses.

	Red	White	Yellow
Red	0		
White	0.0090 (0.2703+-0.0359)	0	
yellow	0.0061 (0.4595+-0.0497)	0.0099 (0.5676+-0.0237)	0

Figures

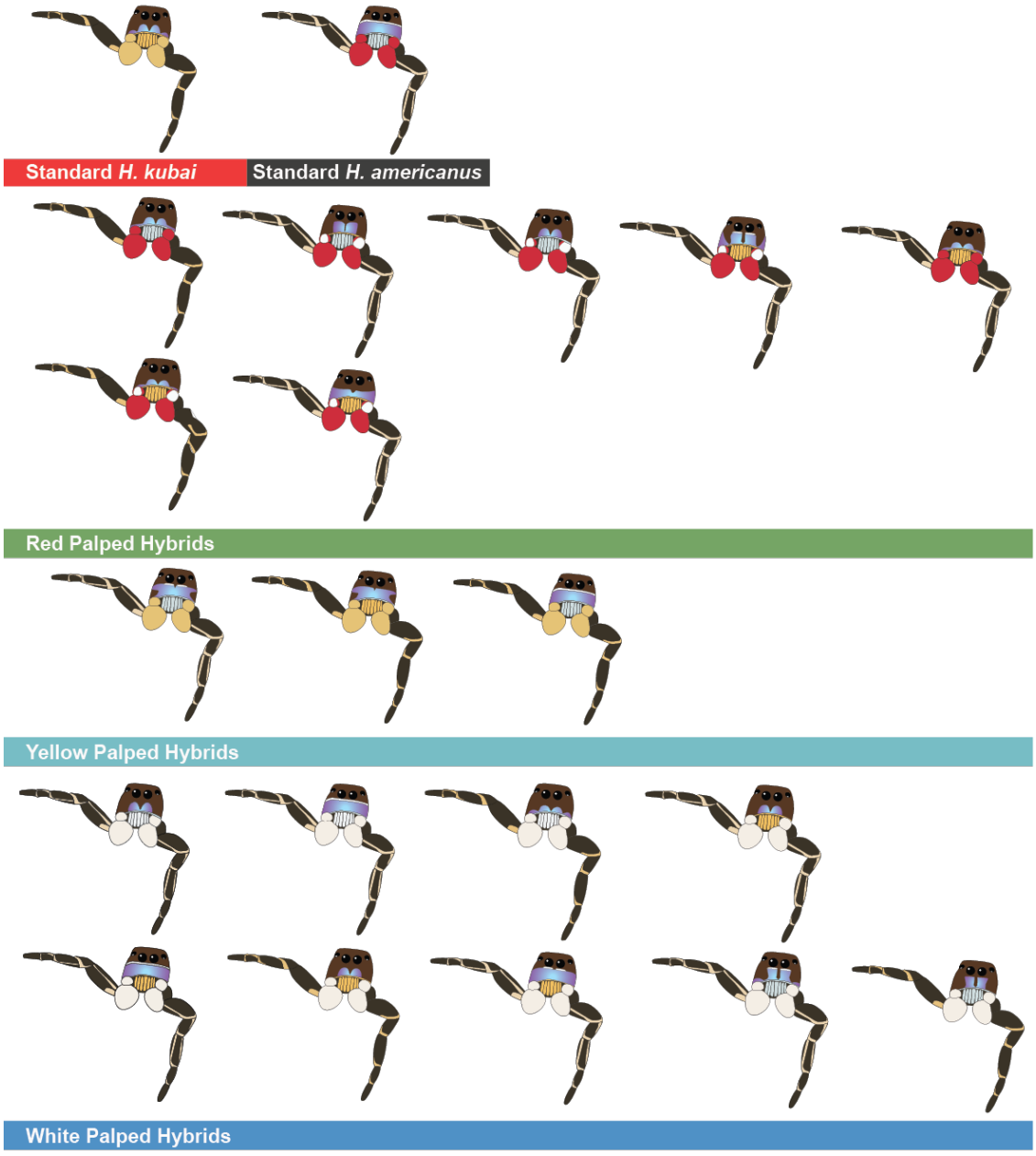

Figure 3.1. Cartoon illustrations of all morphological types collected in the Mt. Shasta hybrid zone.

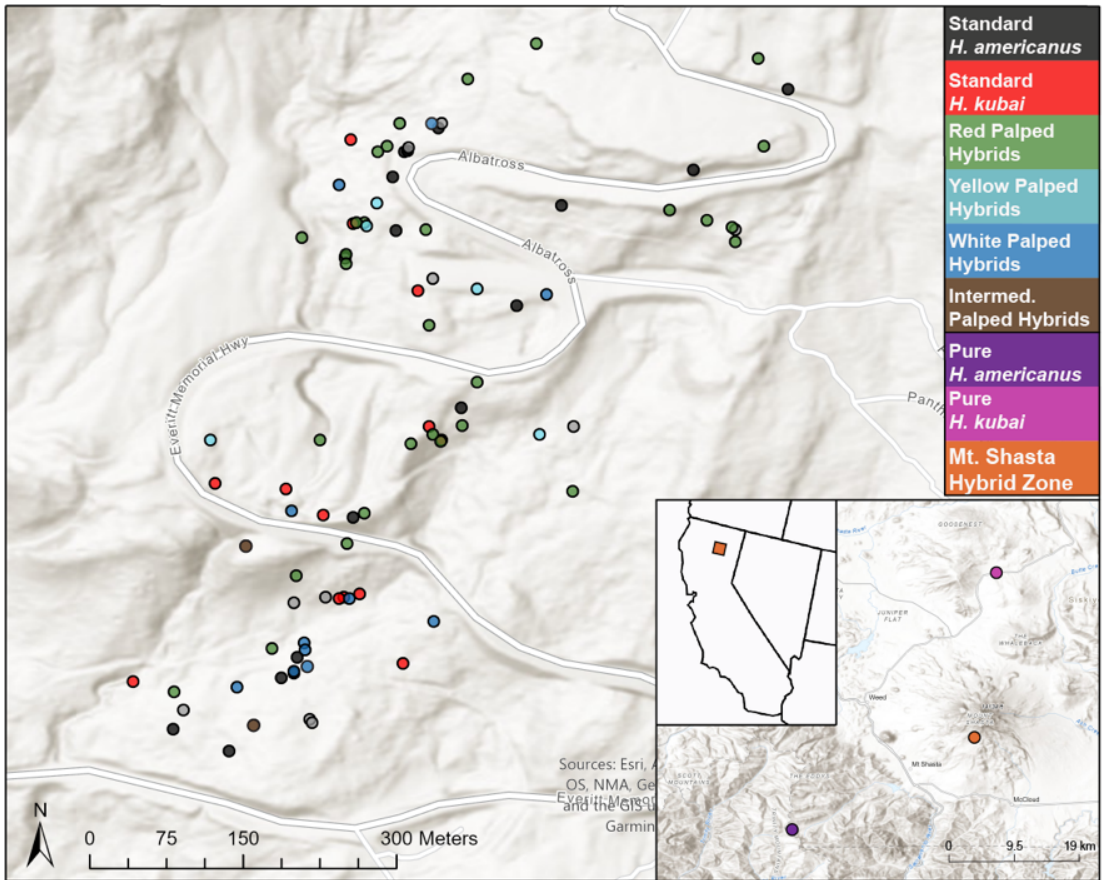

Figure 3.2. Map of Mt. Shasta hybrid zone collection. Black circles = standard *H. americanus* forms; red, green, light blue, and dark blue = standard *H. kubai,* red-palped hybrids, yellow-palped hybrids, and white-palped hybrids, respectively. Zoomed out map image shows where the two "pure" *H. americanus* (purple) and "pure" *H. kubai* (pink) populations are located with respect to the location of the Mt. Shasta hybrid zone (orange).

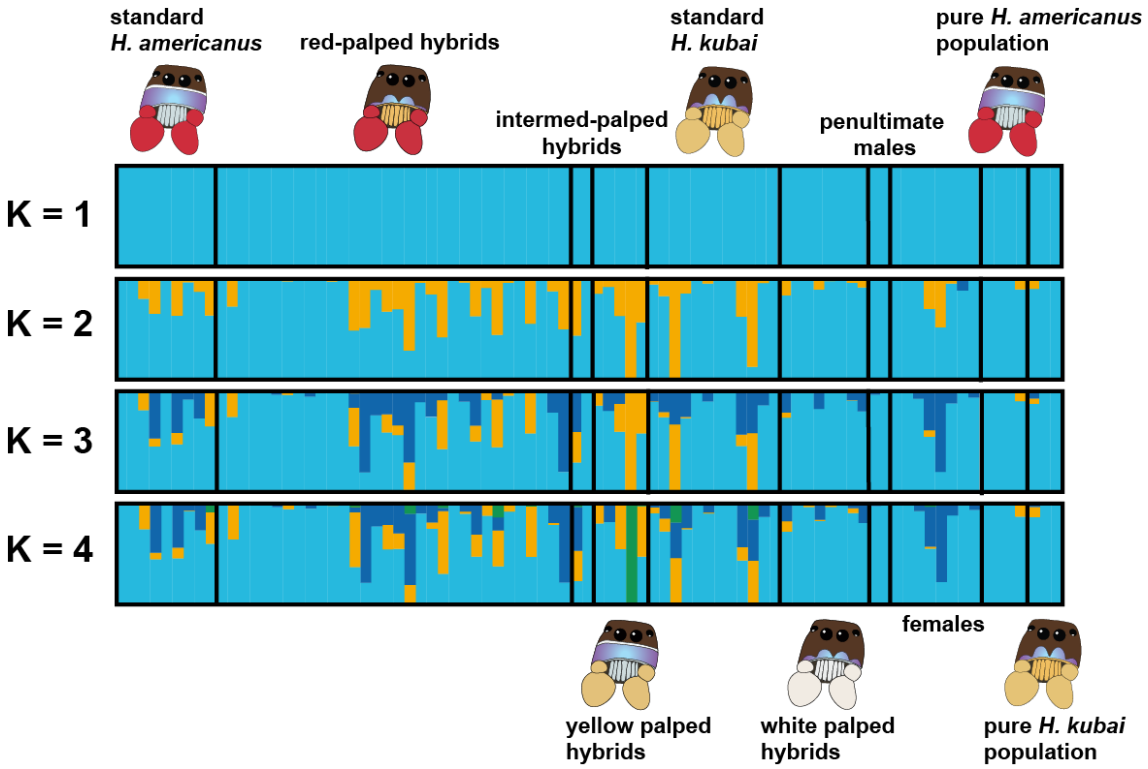

Figure 3.3. Bar charts showing admixture proportions estimated by STRUCTURE for values of K = 1-4 divided by pure populations of *H. americanus* and *H. kubai* and morph types, including standard forms and colored palp hybrid forms. Individuals in each group are organized left to right by increasing elevation. Females and penultimate males do not have a morph type assigned because they do not display colored courtship traits used to divide the chart.

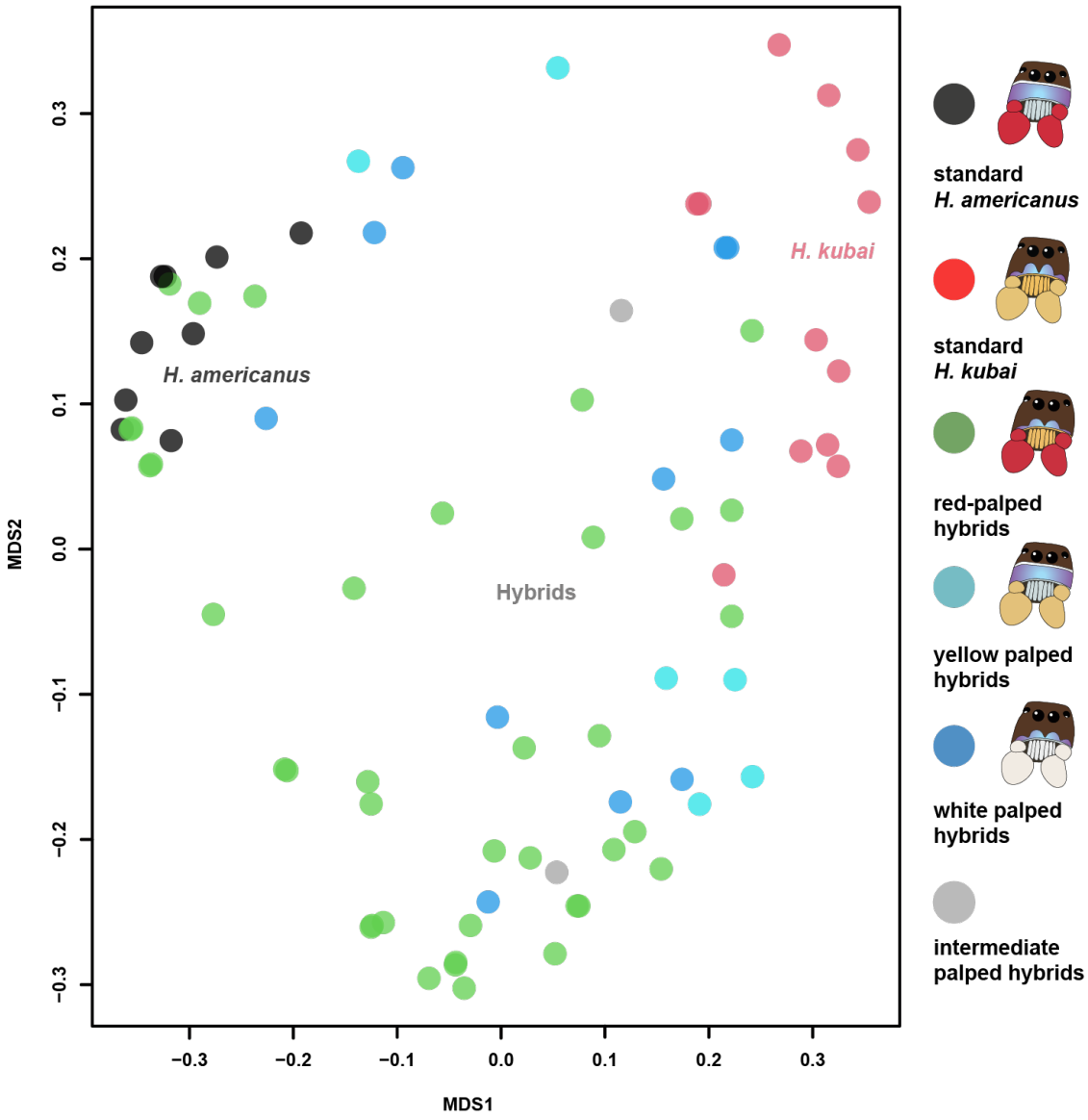

Figure 3.4. Results of NMDS analysis of morphological data matrix. Colored points correspond to either standard forms or colored palp hybrid forms.

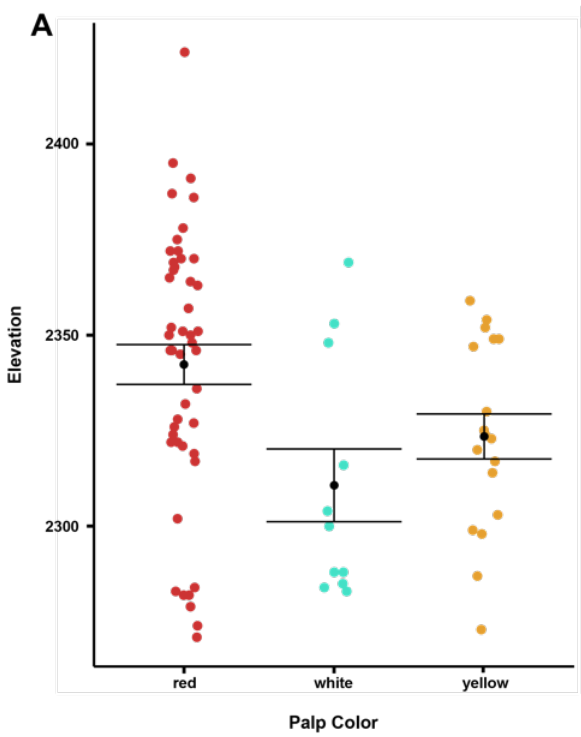

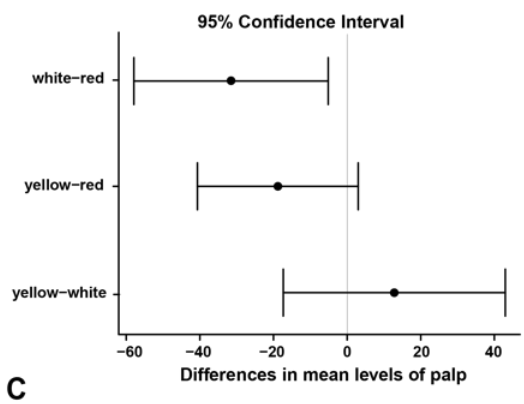

C

ANOVA

	df	Sum sq.	Mean sq.	F statistic	
Between groups	2	11157	5578	5.13	
Residuals	73	79183	1085		p-value 0.00814

TUKEY post-hoc test

	Difference	Lower	Upper	p-value
White-Red	-31.5919	-58.9833	-5.2004	0.0149
Yellow-Red	-18.8192	-40.06598	3.0215	0.1051
Yellow-White	12.7727	-17.3824	42.9278	0.5709

Figure 3.5. (A) Scatter plot of sample elevations, grouped by palp color, (B) Graph of Tukey post-hoc test. If line crosses zero, results are not statistically significant, (C) results for the ANOVA and Tukey pos-hoc tests.

CONCLUSIONS OF THE DISSERTATION

Introgression has the potential to alter the course of evolution. My dissertation explored how consequences of repeated gene flow between diverging lineages may affect genetic, morphological, and behavioral traits, creating multiple avenues for changes to evolutionary trajectories if the exchange of genetic material did not occur. Understanding the prolific effects of hybridization can give us more insight into the nature of speciation and species boundaries. In my dissertation, I used an integrative approach to evaluate the impacts introgression may have on a complex group of organisms experiencing strong sexual selection. Introgression coupled with biogeographical processes and rapid lineage divergence in *americanus* subgroup members appear to have led to discordant patterns between several data types. The multiple data types and results of each analysis included in my dissertation research highlight the degree to which introgression can influence species relationships.

In Chapter 1, I discovered extremely homogenized genomes but substantial morphological diversity of sexually selected male ornamentation across members of the *americanus* subgroup, a reflection of introgression between diverging lineages and selective pressures on sexual ornamentation. In Chapter 2, I explored the diversity of courtship ornamentation across the *americanus* subgroup and found evidence for a geographical split between courtship displays of the southeast and those of elsewhere, in part potentially due to gene flow between geographically proximate populations. Finally, in Chapter 3 I examined genetic and morphological diversity within and around a hybrid

zone in Mt. Shasta, CA. I discovered that while genomes remain extremely homogenized, the morphological diversity remains high and courtship ornamentation traits are easily introgressed across species boundaries. Overall, my integrative dissertation research offers a unique perspective on the nature of speciation that diverging lineages may sometimes be closely intertwined by introgression throughout their evolution such that the group is evolving as a unit of closely related, but distinct lineages. While investigating evolutionary relationships of complex species groups – such as the *americanus* subgroup – can sometimes feel like being caught in a messy spider web of introgression, research devoted to understanding these topics has great potential to shed light on the evolutionary pathways that created the great diversity of life we see today.

VI. APPENDIX

Appendix 1.1. Detailed collection information for specimens, including type of data available for each. ddRADseq data available for all specimens except for *H. americanus* Manti La Sal, *H. americanus* Sevier Lake, and *H. kubai* Great Basin specimens. Lat = Latitude, Long = Longitude, hybrid = *H. kubai/americanus* hybrid, KxA = *H. kubai/americanus* hybrid, UCEs = UCE data collected for specimen, 'Y' denotes yes, UCE data was collected for that specimen, 'N' denotes no, UCE data was not collected for that specimen.

ID	UCEs	Morph Analysis	Scientific Name	Morph	Sex	Lat	Long
G2249	Y	Y	*H. sansoni*	sans_white	M	49.0932	-119.5207
G2250	Y	Y	*H. sansoni*	sans_red	M	49.1111	-119.6669
G2413	N	Y	*H. americanus*	Gunnison	M	38.6762	-106.8500
G2414	N	Y	*H. americanus*	Gunnison	M	38.6762	-106.8500
G2417	N	Y	*H. sansoni Cedar City*	SCC	M	37.5674	-112.8498
G2418	N	Y	*H. sansoni Cedar City*	SCC	M	37.5674	-112.8498
G2419	N	Y	*H. sansoni*	sans_white	M	41.1602	-106.8936
G2420	N	Y	*H. sansoni*	sans_white	M	41.1602	-106.8936
G2421	N	Y	*H. kubai*	kub south	M	38.3133	-119.6017
G2422	N	Y	*H. kubai*	kub south	M	38.3134	-119.6018
G2423	N	Y	*H. kubai*	kub south	M	38.3134	-119.6018
G2424	N	Y	*H. kubai*	kub south	M	38.3137	-119.6020
G2425	N	Y	*H. kubai*	kub south	M	38.3133	-119.6019
G2426	N	Y	*H. kubai*	kub south	M	38.3133	-119.6019
G2427	N	N	Hybrid	KxA	M	38.0795	-119.6017
G2428	N	N	Hybrid	KxA	M	38.3137	-119.6017
G2429	N	Y	*H. kubai*	kub south	M	38.3133	-119.6017
G2430	N	Y	*H. kubai*	kub south	M	38.3134	-119.6017
G2431	N	Y	*H. bulbipes*	bulb	M	42.0777	-122.7147
G2432	N	Y	*H. bulbipes*	bulb	M	42.0777	-122.7146
G2433	N	Y	*H. bulbipes*	bulb	M	42.0787	-122.7466
G2434	N	Y	*H. bulbipes*	bulb	M	42.0779	-122.7145
G2435	N	Y	*H. americanus*	PLE	M	42.0797	-122.7097
G2436	N	Y	*H. americanus*	PL	M	42.0799	-122.7102
G2437	N	Y	*H. americanus*	PLE	M	42.0799	-122.7097
G2438	N	Y	*H. americanus*	PLE	M	42.0799	-122.7096
G2439	N	Y	*H. bulbipes*	bulb	M	42.0787	-122.7466
G2440	N	Y	*H. kubai*	kub north	M	42.075	-122.7474
G2441	N	Y	*H. kubai*	kub north	M	42.07497	-122.7474
G2442	N	N	*H. kubai*	kub north	M	42.07492	-122.7472
G2443	N	Y	*H. kubai*	kub north	M	42.07543	-122.7473
G2444	N	Y	*H. sansoni/kubai* brown	BSK	M	45.3941	-121.5703
G2445	N	Y	*H. sansoni/kubai* brown	BSK	M	45.3936	-121.5705

G2446	N	Y	*H. sansoni/kubai* brown	BSK	M	45.3934	-121.5705
G2447	N	Y	*H. sansoni/kubai* brown	BSK	M	45.3941	-121.5708
G2449	N	Y	*H. sansoni/kubai* brown	BSK	M	45.3941	-121.5708
G2450	N	Y	*H. sansoni/kubai* brown	BSK	M	45.3937	-121.5706
G2451	N	Y	*H. sansoni/kubai* brown	BSK	M	45.3938	-121.5708
G2452	N	Y	*H. sansoni/kubai* brown	BSK	M	45.3939	-121.5707
G2453	N	Y	*H. sansoni/kubai* brown	BSK	M	45.3941	-121.5709
G2456	N	N	Hybrid	KxA	M	42.0799	-122.7096
HA0301	N	Y	*H. americanus*	P	M	37.3850	-118.1823
HA0307	N	Y	*H. americanus*	PLC	M	38.8885	-120.0008
HA0316	Y	N	*H. americanus*	PL	F	37.3850	-118.1823
HA0333	Y	N	*H. americanus*	PL	F	33.8242	-116.7522
HA0337	Y	N	*H. americanus*	P	F	41.2119	-122.5090
HA0344	N	Y	*H. americanus*	PLC	M	38.3490	-119.3752
HA0346	Y	Y	*H. americanus*	PLC	M	37.2471	-118.5891
HA0361	N	Y	*H. americanus*	PL	M	40.1981	-121.0723
HA0363	N	Y	*H. americanus*	PL	M	34.8125	-119.1033
HA0364	N	Y	*H. americanus*	P	M	38.3245	-119.6934
HA0366	Y	Y	*H. bulbipes*	bulb	M	42.0757	-122.7145
HA0367	N	Y	*H. sansoni*	sans_white	M	49.4740	-115.4498
HA0373	N	Y	*H. americanus*	P	M	41.2409	-122.0252
HA0406	N	Y	*H. americanus*	P	M	36.2280	-117.0735
HA0407	N	Y	*H. americanus*	P	M	36.3571	-115.6370
HA0411	N	Y	*H. americanus*	P	M	40.6847	-121.4190
HA0416	Y	Y	*H. sansoni* Cedar City	SCC	M	37.5679	-112.8486
HA0419	N	Y	*H. americanus*	PLC	M	37.9408	-119.2432
HA0420	N	Y	*H. americanus*	PL	M	38.2210	-119.9990
HA0422	N	N	Hybrid	KxA	M	38.3301	-119.6363
HA0423	N	Y	*H. kubai*	kub south	M	38.3301	-119.6363
HA0427	N	Y	*H. kubai*	kub south	M	38.3056	-119.5926
HA0449	Y	N	*H. sansoni*	sans_white	F	37.7328	-105.4548
HA0450	Y	Y	*H. sansoni* Cedar City	SCC	M	38.2831	-112.4491
HA0522	N	Y	*H. americanus*	P	M	38.4729	-107.2105
HA0532	Y	Y	*H. americanus*	PL	M	42.9679	-122.1481
HA0536	Y	Y	*H. bulbipes*	bulb	M	40.9355	-122.8582
HA0538	N	Y	*H. kubai*	kub north	M	40.4600	-121.4705
HA0539	N	N	Hybrid	KxA	F	40.4600	-121.4705
HA0540	N	Y	*H. kubai*	kub north	M	2.16901	-122.4623
HA0541	Y	N	Hybrid	KxA	M	40.5562	-121.5345
HA0862	N	Y	*H. sansoni*	sans_white	M	37.7399	-105.5186
HA0863	N	Y	*H. sansoni*	sans_white	M	37.7399	-105.5186
HA0919	N	Y	*H. americanus*	PL	M	43.0355	-120.7935
HA0920	Y	Y	*H. americanus*	PL	M	45.7018	-123.9312
HA0923	N	Y	*H. americanus*	PLC	M	38.5435	-119.8116
HA0926	N	Y	*H. americanus*	PL	M	45.3326	-121.6740
HA0929	Y	Y	*H. kubai*	kub north	M	41.6429	-122.1674

HA0930	N	N	Hybrid	KxA	F	41.6429	-122.1674
HA0932	Y	Y	*H. kubai*	kub south	M	38.3251	-119.6433
HA0935	Y	N	*H. bulbipes*	bulb	M	39.8069	-120.4837
HA0936	N	Y	*H. bulbipes*	bulb	M	39.8069	-120.4837
HA0937	N	Y	*H. bulbipes*	bulb	M	39.8069	-120.4837
HA0939	N	Y	*H. kubai*	kub north	M	38.6716	-119.6287
HA1121	N	Y	*H. americanus*	PL	M	41.9095	-118.7353
HA1122	N	Y	*H. americanus*	PL	M	41.9095	-118.7353
HA1123	Y	Y	*H. americanus*	PL	M	42.9447	-109.7737
HA1125	Y	Y	*H. sansoni*	sans_white	M	42.1009	-106.9478
HA1126	N	Y	*H. kubai*	kub north	M	38.6716	-119.6287
HA1128	Y	Y	*H. americanus*	Pahvant	M	38.9590	-112.1122
HA1469	Y	Y	*H. kubai*	kub north	M	38.5425	-119.8853
HA1649	N	Y	*H. americanus*	PC	M	37.2392	-119.2257
HA1652	N	N	*H. americanus*	PL	F	40.5267	-115.3433
HA1658	Y	Y	*H. americanus*	PL	M	38.5425	-119.8853

Appendix 1.2. Scored morphological character matrix for each male. "-" denotes a missing character. Sevier = Sevier Lake morph, Manti LS = Manti La Sal morph.

			Character Code																					
Sample ID	**Scientific Name**	**Morph**	**A**	**B**	**C**	**D**	**E**	**F**	**G**	**H**	**I**	**J**	**K**	**L**	**M**	**N**	**O**	**P**	**Q**	**R**	**S**	**T**	**U**	**V**	**W**
HA0301	*H. americanus*	P	0	0	1	1	0	0	0	1	1	0	0	0	0	0	0	0	0	0	0	-	3	2	1
HA0364	*H. americanus*	P	0	0	1	1	0	0	0	0	1	0	0	0	0	1	0	0	-	-	-	-	5	2	1
HA0373	*H. americanus*	P	0	0	1	1	0	0	0	0	1	0	0	1	0	0	1	0	0	0	1	-	3	2	1
HA0406	*H. americanus*	P	0	0	1	1	0	0	0	0	1	0	0	0	0	1	0	0	0	0	0	-	3	2	1
HA0407	*H. americanus*	P	0	0	1	1	0	0	0	0	1	0	0	0	0	1	0	0	0	0	0	-	3	2	1
HA0411	*H. americanus*	P	0	0	1	1	0	0	0	0	1	0	0	0	0	1	0	0	0	0	0	-	3	2	1
HA0522	*H. americanus*	P	1	0	0	3	2	0	0	0	1	0	0	0	0	0	0	0	0	0	0	-	3	2	1
G2436	*H. americanus*	PL	0	0	1	1	0	0	0	0	1	1	4	0	0	0	0	0	0	0	0	0	3	2	1
HA0361	*H. americanus*	PL	0	0	1	1	0	0	0	0	1	1	4	0	0	1	0	0	1	4	0	-	3	2	1
HA0363	*H. americanus*	PL	0	0	1	0	0	0	0	0	1	1	4	0	0	1	0	0	-	-	-	-	3	2	1
HA0532	*H. americanus*	PL	0	0	1	1	0	0	0	0	1	1	4	0	0	1	0	0	1	4	0	0	3	2	1
HA0420	*H. americanus*	PL	0	0	1	1	0	0	0	0	1	0	0	0	0	1	0	0	0	0	0	-	6	2	1
HA0919	*H. americanus*	PL	0	0	1	1	0	0	0	0	1	1	4	0	0	1	0	0	1	4	0	0	3	2	1
HA0920	*H. americanus*	PL	0	0	1	1	0	0	0	0	1	1	4	0	0	0	0	0	1	4	0	0	3	2	1
HA0926	*H. americanus*	PL	0	0	1	4	0	0	0	0	1	1	4	0	0	0	0	0	1	4	0	0	6	2	1
HA1121	*H. americanus*	PL	0	0	1	1	0	0	0	0	1	1	4	0	0	1	0	0	1	4	0	0	3	2	1
HA1122	*H. americanus*	PL	0	0	1	1	0	0	0	0	1	1	4	0	0	1	0	0	1	4	0	-	3	2	1
HA1123	*H. americanus*	PL	0	0	1	1	0	0	0	0	1	1	4	0	0	1	0	0	0	0	0	0	3	2	1
HA1658	*H. americanus*	PL	0	0	1	1	0	0	0	0	1	-	-	-	-	-	-	-	-	-	-	-	1	2	1
HA0307	*H. americanus*	PLC	1	0	1	1	0	0	0	1	1	1	4	0	0	2	1	0	1	4	0	-	5	2	1
HA0344	*H. americanus*	PLC	1	0	1	1	0	0	0	1	1	1	4	0	0	1	0	0	1	4	0	-	5	2	1
HA0346	*H. americanus*	PLC	0	0	1	1	0	0	0	1	1	1	4	0	1	4	0	0	1	4	0	-	3	2	1
HA0419	*H. americanus*	PLC	0	0	1	1	0	0	0	1	1	1	4	0	1	4	0	0	-	-	-	-	3	3	1
HA0923	*H. americanus*	PLC	0	0	1	1	1	0	0	1	1	1	4	0	1	4	3	0	1	4	0	-	3	2	1
G2435	*H. americanus*	PLE	0	0	1	1	0	0	0	0	1	1	4	0	0	0	0	1	0	1	0	2	3	2	1
G2437	*H. americanus*	PLE	0	0	1	1	0	0	0	0	1	1	4	0	0	0	0	1	1	4	0	0	3	2	1
G2438	*H. americanus*	PLE	0	0	1	1	0	0	0	0	1	1	4	0	0	0	0	1	1	4	0	0	3	2	1
HA1649	*H. americanus*	PC	0	0	1	1	0	0	0	1	1	0	0	0	0	1	0	0	0	1	0	1	6	2	1
MH2087	*H. americanus*	Sevier	0	0	1	4	0	0	0	0	1	1	4	0	0	1	0	0	0	0	3	1	9	1	1
HA1128	*H. americanus*	Pahvant	0	2	1	1	1	0	0	5	1	0	6	0	0	6	0	0	0	6	0	1	9	1	1
MH21068_39	*H. americanus*	Manti LS	0	0	1	1	0	0	0	6	1	0	0	0	0	0	3	0	0	0	0	1	10	1	1

G2249	*H. sansoni*	sans white	1	2	3	0	3	0	3	2	0	1	1	3	0	1	3	0	0	0	3	-	6	1	1
G2419	*H. sansoni*	sans white	1	2	3	0	3	0	2	2	0	1	1	1	0	1	1	0	0	1	1	1	6	1	1
G2420	*H. sansoni*	sans white	1	2	3	0	3	0	2	2	0	1	1	1	0	1	1	0	0	1	1	1	6	1	1
HA0367	*H. sansoni*	sans white	1	2	2	0	3	0	3	2	1	0	1	1	0	1	1	0	0	1	1	-	6	1	1
HA0862	*H. sansoni*	sans white	1	2	2	0	3	0	3	2	1	1	1	1	0	1	3	0	0	1	1	1	6	1	1
HA1125	*H. sansoni*	sans white	1	2	0	0	3	0	2	2	1	0	1	1	0	1	1	0	0	1	1	1	6	1	1
HA0863	*H. sansoni*	sans white	1	2	2	0	3	0	3	2	0	1	1	0	0	1	0	0	1	1	1	1	6	1	1
G2250	*H. sansoni*	sans red	1	2	3	0	5	0	4	2	0	1	1	3	0	1	3	0	0	1	3	-	6	1	1
G2417	*H. sansoni* Cedar City	SCC	0	0	0	0	4	0	1	2	0	0	0	1	0	0	1	0	0	0	1	1	4	4	1
G2418	*H. sansoni* Cedar City	SCC	0	0	0	0	4	0	1	2	0	0	0	1	0	0	1	0	0	0	1	1	4	4	1
HA0416	*H. sansoni* Cedar City	SCC	0	0	0	0	4	0	1	4	0	0	5	1	0	5	1	0	0	5	1	1	4	4	0
HA0450	*H. sansoni* Cedar City	SCC	0	0	0	0	5	0	1	2	1	0	5	1	0	5	1	0	0	5	1	1	4	4	0
G2421	*H. kubai*	kub south	0	0	3	0	1	1	0	3	0	1	1	2	1	1	2	0	1	1	3	1	6	1	1
G2422	*H. kubai*	kub south	0	0	3	0	1	0	0	3	0	1	1	2	1	1	2	0	1	1	3	1	6	1	1
G2423	*H. kubai*	kub south	0	0	3	0	1	1	0	3	0	1	1	1	1	1	1	0	1	1	1	1	6	1	1
G2424	*H. kubai*	kub south	0	0	3	2	1	0	0	0	0	1	1	1	1	1	1	0	1	1	1	1	6	1	1
G2425	*H. kubai*	kub south	0	0	3	2	1	0	0	3	0	1	1	1	1	1	1	0	1	1	1	1	6	1	1
G2426	*H. kubai*	kub south	0	0	3	0	7	0	0	3	0	1	1	1	1	1	1	0	1	1	1	1	6	1	1
G2429	*H. kubai*	kub south	0	0	3	0	1	0	0	2	0	1	1	1	1	1	1	0	1	1	1	1	6	1	1

G2430	*H. kubai*	kub south	0	0	3	0	1	1	0	3	0	1	1	1	1	1	1	0	1	1	1	1	6	1	1
HA0423	*H. kubai*	kub south	1	0	3	0	4	1	0	2	2	1	1	3	1	1	3	0	-	-	-	-	6	1	1
HA0427	*H. kubai*	kub south	1	0	3	0	1	1	0	2	2	1	1	1	1	1	1	0	0	1	1	-	6	1	1
HA0932	*H. kubai*	kub south	1	0	3	2	1	1	0	2	1	1	1	1	0	1	1	0	1	1	1	1	6	1	1
G2440	*H. kubai*	kub north	0	1	5	0	1	1	0	3	1	1	1	0	1	1	0	1	0	0	0	0	0	1	1
G2441	*H. kubai*	kub north	0	1	5	0	1	1	0	3	1	1	1	0	1	1	0	1	0	0	0	0	0	1	1
G2443	*H. kubai*	kub north	0	1	5	0	1	1	0	3	0	1	1	0	1	1	0	1	0	0	0	0	0	1	1
HA0538	*H. kubai*	kub north	0	0	4	0	1	1	0	3	1	0	0	0	0	0	0	0	0	0	0	0	0	1	1
HA0540	*H. kubai*	kub north	0	0	5	0	1	1	0	3	1	1	1	0	0	1	0	1	0	0	0	0	0	0	1
HA0929	*H. kubai*	kub north	0	0	4	0	1	1	0	3	1	0	0	3	0	0	3	0	0	0	3	1	0	1	1
HA0939	*H. kubai*	kub north	1	2	4	0	1	1	0	3	1	1	0	2	0	1	0	0	0	0	2	2	0	0	1
HA1126	*H. kubai*	kub north	1	2	4	0	1	1	0	3	1	0	0	2	0	1	0	0	0	0	2	2	0	0	1
HA1469	*H. kubai*	kub north	1	0	3	0	1	1	0	3	0	1	2	1	1	2	1	0	-	-	-	-	0	0	1
G3590	*H. kubai*	*kubai* GB	1	2	6	0	1	1	0	7	3	0	0	1	0	5	1	0	0	0	1	1	0	0	1
G3591	*H. kubai*	*kubai* GB	1	2	6	0	1	1	0	7	3	0	0	1	0	5	1	0	0	0	1	1	0	0	1
G2431	*H. bulbipes*	bulb	0	0	1	1	0	0	0	2	1	1	1	3	0	1	1	1	1	1	1	1	7	1	1
G2432	*H. bulbipes*	bulb	0	0	1	1	0	0	0	2	1	1	1	3	0	1	1	1	1	1	1	1	7	1	1
G2433	*H. bulbipes*	bulb	0	0	1	1	0	0	0	2	1	1	1	3	0	1	1	1	1	1	1	1	7	1	1
G2434	*H. bulbipes*	bulb	0	0	1	1	0	0	0	2	1	1	1	3	0	1	1	1	1	1	1	1	7	1	1
G2439	*H. bulbipes*	bulb	0	0	1	1	0	0	2	2	1	1	1	3	0	1	1	1	1	1	1	1	7	1	1
HA0366	*H. bulbipes*	bulb	0	0	1	1	0	0	0	2	1	0	1	3	0	1	3	1	-	-	-	-	6	1	1
HA0536	*H. bulbipes*	bulb	0	0	1	1	0	0	0	2	1	1	1	0	0	1	0	1	-	-	1	1	6	1	1
HA0936	*H. bulbipes*	bulb	1	0	1	1	0	0	0	2	1	1	1	3	0	1	3	0	0	1	5	-	6	1	1
HA0937	*H. bulbipes*	bulb	1	0	1	1	0	0	0	1	1	1	1	3	0	1	3	0	-	-	-	1	6	1	1
G2413	*H. americanus*	Gunnison	1	2	1	1	0	0	0	0	1	1	4	3	1	4	3	0	1	4	3	1	3	3	1
G2414	*H. americanus*	Gunnison	1	2	1	1	0	0	0	0	1	1	4	3	1	4	3	0	1	4	3	1	3	3	1
G2444	*H. sansoni/ kubai* brown	BSK	1	2	6	0	1	0	0	3	0	0	0	3	0	1	3	0	0	0	2	2	8	1	1
G2445	*H. sansoni/ kubai* brown	BSK	1	2	6	0	1	0	0	3	0	0	1	3	0	0	3	0	0	1	3	3	8	1	1
G2446	*H. sansoni/ kubai* brown	BSK	1	2	6	0	1	0	0	3	0	0	1	3	0	0	3	0	0	1	3	3	8	1	1

G2447	*H. sansoni/ kubai* brown	BSK	0	2	6	0	1	0	0	3	0	0	0	0	0	0	0	0	0	0	3	3	8	1	1
G2449	*H. sansoni/ kubai* brown	BSK	0	2	6	0	1	0	0	3	2	0	1	0	0	1	0	0	0	1	3	3	8	1	1
G2450	*H. sansoni/ kubai* brown	BSK	1	2	6	0	1	0	0	3	2	0	1	0	0	1	0	0	0	0	3	3	8	1	1
G2451	*H. sansoni/ kubai* brown	BSK	0	2	6	0	1	0	0	3	0	0	1	0	0	1	0	0	0	1	3	3	8	1	1
G2452	*H. sansoni/ kubai* brown	BSK	0	2	6	0	1	0	0	3	2	0	0	0	0	0	0	0	0	0	3	3	8	1	1
G2453	*H. sansoni/ kubai* brown	BSK	0	2	6	0	1	0	0	3	0	0	1	0	0	1	0	0	0	0	3	3	8	1	1

Appendix 2.1. Data for each specimen used in this study. P = *H. americanus* P, PL = *H. americanus* PL, PLC = *H. americanus* PLC, Sevier Lake = *H. americanus* Sevier Lake, east Pahvant = *H. americanus* eastern Pahvant, Pahvant = *H. americanus* Pahvant, Manti La Sal = *H. americanus* Manti La Sal, s*ans* white = *H. sansoni* white, s*ans* red = *H. sansoni* red, SCC = *H. sansoni* Cedar City, *kubai* south = *H. kubai* south, *kubai* north = *H. kubai* north, *kubai* GB = *H. kubai* Great Basin, *bulbipes = H. bulbipes,* Gunnison = *H.* Gunnison morph.

Sample Name	Species	Morph	State	Lat	Long
MH2096_01	*H. americanus*	P	CA	41.2120	-122.5119
MH2096_2	*H. americanus*	P	CA	41.2120	-122.5119
MH2096_3	*H. americanus*	P	CA	41.2120	-122.5119
MH2096_4	*H. americanus*	P	CA	41.2120	-122.5119
MH2096_5	*H. americanus*	P	CA	41.2120	-122.5119
428 GB-B	*H. americanus*	P	CA	38.3250	-119.6950
MH2095_5	*H. americanus*	P	CA	41.3545	-122.2334
TCB2005_02	*H. americanus*	PL	CA	38.3351	-119.6424
TCB2005_03	*H. americanus*	PL	CA	38.3351	-119.6424
TCB2005_04	*H. americanus*	PL	CA	38.3351	-119.6424
TCB005-01	*H. americanus*	PL	CA	38.3351	-119.6424
MH2089_1 P	*H. americanus*	PL	NV	39.0248	-114.6455
MH2089_2	*H. americanus*	PL	NV	39.0248	-114.6455
GB-B_504	*H. americanus*	PL	CA	38.3370	-119.6600
americanus3.mov	*H. americanus*	PL	WY	43.6199	-110.6228
americanus735	*H. americanus*	PL	CA	38.3370	-119.6600
JH_2	*H. americanus*	PL	WY	43.6199	-110.6228
JH_MR18259	*H. americanus*	PL	WY	43.6190	-110.6228
JH_4	*H. americanus*	PL	WY	43.6199	-110.6228
JH_MR18262	*H. americanus*	PL	WY	43.6199	-110.6228
JH_MR18272	*H. americanus*	PL	WY	43.6199	-110.6228
MCH2073	*H. americanus*	PL	NV	39.7769	-117.1356
MH2090_3	*H. americanus*	PL	NV	39.5283	-116.3870
1073	*H. americanus*	PLC	CA	38.2770	-119.6170
TCB_007_5	*H. americanus*	PLC	CA	39.3682	-120.1570
TCB_2007_01	*H. americanus*	PLC	CA	39.3682	-120.1570
TCB_2007_04	*H. americanus*	PLC	CA	39.3682	-120.1570
TCB20_007_02	*H. americanus*	PLC	CA	39.3682	-120.1570
TCB2007-03	*H. americanus*	PLC	CA	39.3682	-120.1570
GB-A_541	*H. americanus*	PLC	CA	38.1040	-119.4830
MH2087	*H. americanus*	Sevier Lake	UT	39.1451	-112.9514
MH21067_068	*H. americanus*	east Pahvant	UT	38.9594	-112.1103
MH21067_055	*H. americanus*	east Pahvant	UT	38.9594	-112.1103
MH21067_56b	*H. americanus*	east Pahvant	UT	38.9594	-112.1103
MH2085_01	*H. americanus*	Pahvant	UT	38.8259	-112.2356
MH2085_2	*H. americanus*	Pahvant	UT	38.8259	-112.2356
MH2085_3	*H. americanus*	Pahvant	UT	38.8259	-112.2356
MH2085_4	*H. americanus*	Pahvant	UT	38.8259	-112.2356
MH21067_021	*H. americanus*	Mant La Sal	UT	39.2562	-111.5529
MH21068_39	*H. americanus*	Mant La Sal	UT	39.2562	-111.5529
MH21068_40	*H. americanus*	Mant La Sal	UT	39.2562	-111.5529

MH21068_01	*H. americanus*	Mant La Sal	UT	39.2562	-111.5529
MH1940_01	*H. sansoni*	s*ans* white	NM	36.2768	-106.9499
Hsansoni_02_PP_Redo	*H. sansoni*	*sans* red	CO	37.7331	-105.4549
Hsansoni_03_PP	*H. sansoni*	*sans* red	CO	37.7331	-105.4548
Hsansoni_01_Carson	*H. sansoni* Cedar City	SCC	UT	37.5678	-112.8489
Hsansoni_02_carson	*H. sansoni* Cedar City	SCC	UT	37.5678	-112.8489
Hsansoni_03_Carson	H. *sansoni* Cedar City	SCC	UT	37.5678	-112.8489
Hsansoni_04_carson	H. *sansoni* Cedar City	SCC	UT	37.5678	-112.8489
MH2084_02	*H. sansoni* Cedar City	SCC	UT	37.5678	-112.8489
MH2084_03	*H. sansoni* Cedar City	SCC	UT	37.5678	-112.8489
MH2084_06	*H. sansoni* Cedar City	SCC	UT	37.5678	-112.8489
MH2086_01	*H. sansoni* Cedar City	SCC	UT	38.514	-111.7832
MH2084_1	*H. sansoni* Cedar City	SCC	UT	37.5678	-112.8489
sansoni_MH2084_05	*H. sansoni* Cedar City	SCC	UT	37.5678	-112.8489
TCB2006_04	*H. kubai*	*kubai* south	CA	38.3305	-119.6351
TCB2006_05	*H. kubai*	*kubai s*outh	CA	38.3305	-119.6351
TCB2006_01	*H. kubai*	*kubai* south	CA	38.3305	-119.6351
TCB2006-02	*H. kubai*	*kubai* south	CA	38.3305	-119.6351
TCB2006_03	*H. kubai*	*kubai* south	CA	38.3305	-119.6351
Hsansoni#	*H. kubai*	*kubai* south	CA	38.3305	-119.6351
Hsansoni##	*H. kubai*	*kubai* south	CA	38.3305	-119.6351
Hsansoni###	*H. kubai*	*kubai* south	CA	38.3305	-119.6351
MH2093_01	*H. kubai*	*kubai* north	CA	40.4599	-121.4704
MH2077_1	*H. kubai*	*kubai* GB	NV	38.9894	-114.2125
MH2077_2b	*H. kubai*	*kubai* GB	NV	38.9894	-114.2125
MH2077_3	*H. kubai*	*kubai* GB	NV	38.9894	-114.2125
Hsansoni_03_GBP	*H. kubai*	*kubai* GB	NV	38.9894	-114.2125
Hsansoni_04_GBP	*H. kubai*	*kubai* GB	NV	38.9894	-114.2125
Hsansoni_02_GBP	*H. kubai*	*kubai* GB	NV	38.9894	-114.2125
Hsansoni_01_GP	*H. kubai*	*kubai* GB	NV	38.9894	-114.2125
MH2098_1_1	*H. bulbipes*	*bulbipes*	CA	40.9358	-122.8594
MH2098_1_2	*H. bulbipes*	*bulbipes*	CA	40.9358	-122.8594
TCB19_024c	*H. bulbipes*	*bulbipes*	CA	39.8069	-120.4837
Hamericanus_01_area10	Gunnison	Gunnison	CO	38.9397	-106.9808
Hamericanus_02_LML	Gunnison	Gunnison	CO	38.9397	-106.9808
Hamericanus_01_ALT	Gunnison	Gunnison	CO	38.9397	-106.9808

Appendix 3.1. Detailed collection information for specimens, including sequencing statistics for each individual.

									ddRADseq Stats	
Sample ID	**Morph**	**ddRAD**	**Scientific Name**	**palp color**	**Sex**	**Lat**	**Long**	**Elev. (m)**	**raw reads**	**Loci in Assembly**
G2765	x	x	*H. americanus/kubai* hybrid	red	M	41.3606	-122.2022	2375	1978684	16485
G2766	x	x	*H. americanus/kubai* hybrid	red	M	41.3602	-122.2006	2372	1929155	23638
G2767	-	x	penultimate male	n/a	M	41.3603	-122.2006	2373	3259637	29323
G2768	x	x	*H. americanus/kubai* hybrid	red	M	41.3605	-122.2012	2372	2435200	22073
G2769	x	x	*H. americanus/kubai* hybrid	red	M	41.3603	-122.2007	2370	2446932	19013
G2770	x	x	*H. americanus/kubai* hybrid	red	M	41.3604	-122.2009	2370	1552797	19522
G2771	x	x	*H. americanus*	standard red	M	41.3616	-122.2002	2424	1814763	16199
G2772	x	-	*H. americanus/kubai* hybrid	red	M	41.3618	-122.2004	2395	-	-
G2774	x	x	*H. americanus/kubai* hybrid	red	M	41.3601	-122.2041	2345	4653526	25757
G2775	x	x	*H. americanus/kubai* hybrid	yellow	M	41.3604	-122.2040	2349	4452801	23780
G2776	x	x	*H. americanus/kubai* hybrid	yellow	M	41.3604	-122.2039	2349	2659419	17867
G2777	x	x	*H. americanus/kubai* hybrid	yellow	M	41.3606	-122.2038	2354	3446280	23948
G2778	x	x	*H. americanus/kubai* hybrid	red	M	41.3603	-122.2034	2357	3845528	19737
G2779	x	x	*H. americanus/kubai* hybrid	red	M	41.3611	-122.2037	2368	3802930	25883
G2780	x	x	*H. americanus/kubai* hybrid	red	M	41.3604	-122.2039	2350	3952659	26516
G2781	x	x	*H. americanus/kubai* hybrid	white	M	41.3607	-122.2041	2353	6948839	42447
G2782	x	x	*H. kubai*	standard yellow	M	41.3571	-122.2039	2297	6138918	48645
G2784	x	x	*H. americanus/kubai* hybrid	white	M	41.3569	-122.2033	2300	7017665	39058
G2785	x	x	*H. kubai*	standard yellow	M	41.3565	-122.2036	2287	4533440	31827
G2786	x	x	*H. americanus*	standard red	M	41.3564	-122.2046	2284	4182378	24352
G2787	x	x	*H. kubai*	standard yellow	M	41.3564	-122.2059	2273	4726456	33120
G2788	x	x	*H. americanus/kubai* hybrid	red	M	41.3563	-122.2056	2279	3074328	20904
G2789	x	x	*H. americanus/kubai* hybrid	red	M	41.3576	-122.2040	2317	3634705	29189
G2790	x	x	*H. americanus/kubai* hybrid	yellow	M	41.3585	-122.2052	2323	5388110	27355
G2791	x	x	*H. americanus/kubai* hybrid	red	M	41.3584	-122.2035	2328	6229429	45479
G2792	x	x	*H. americanus/kubai* hybrid	red	M	41.3586	-122.2030	2327	5693479	44328
G2793	x	x	*H. americanus/kubai* hybrid	red	M	41.359	-122.2029	2336	4357099	33279
G2794	x	x	*H. kubai*	standard yellow	M	41.3571	-122.2041	2303	2436734	24694
G2795	x	x	*H. americanus*	standard red	M	41.3566	-122.2045	2283	4850921	35438
G2796	x	x	*H. americanus/kubai* hybrid	red	M	41.3585	-122.2043	2319	4737406	48806

G2797	x	x	*H. americanus*	standard red	M	41.3588	-122.2030	2332	4131760	36702
G2798	x	x	*H. americanus/kubai* hybrid	white	M	41.3567	-122.2044	2288	3365549	29365
G2799	x	x	*H. americanus/kubai* hybrid	intermediate	M	41.356	-122.2049	2280	4364172	27983
G2800	x	x	*H. americanus/kubai* hybrid	white	M	41.3563	-122.2050	2283	6300683	33645
G2801	x	x	*H. kubai*	standard yellow	M	41.3586	-122.2033	2330	3680620	20718
G2802	x	-	*H. americanus/kubai* hybrid	red	M	41.3585	-122.2033	2326	-	-
G2803	x	x	*H. americanus/kubai* hybrid	red	M	41.3585	-122.2032	2324	7747849	52436
G2804	x	x	*H. kubai*	standard yellow	M	41.3585	-122.2032	2324	3560075	32204
G2805	x	x	*H. americanus/kubai* hybrid	white	M	41.3566	-122.2044	2288	2232208	29173
G2806	x	x	*H. kubai*	standard yellow	M	41.3581	-122.2052	2314	6380198	53419
G2807	x	x	*H. kubai*	standard yellow	M	41.358	-122.2046	2320	3369263	39191
G2808	x	x	*H. americanus/kubai* hybrid	white	M	41.3579	-122.2045	2316	3134756	42335
G2809	x	x	*H. kubai*	standard yellow	M	41.3578	-122.2043	2317	4309073	54380
G2810	x	x	*H. americanus/kubai* hybrid	red	M	41.3578	-122.2040	2321	3647292	48841
G2811	x	-	*H. americanus/kubai* hybrid	red	M	41.3578	-122.2039	2322	-	-
G2812	x	x	*H. kubai*	standard yellow	M	41.3598	-122.2034	2347	4348319	38489
G2813	x	-	*H. americanus/kubai* hybrid	yellow	M	41.3598	-122.2029	2352	-	-
G2814	x	-	*H. americanus/kubai* hybrid	red	M	41.3597	-122.2026	2351	-	-
G2815	x	-	*H. americanus/kubai* hybrid	white	M	41.3598	-122.2023	2348	-	-
G2816	x	-	*H. americanus/kubai* hybrid	red	M	41.3609	-122.2010	2386	-	-
G2817	x	x	*H. americanus/kubai* hybrid	red	M	41.3611	-122.2004	2391	3196293	41668
G2818	x	-	*H. americanus/kubai* hybrid	white	M	41.3571	-122.2040	2304	-	-
G2819	x	-	*H. kubai*	standard yellow	M	41.3571	-122.2041	2286	-	-
G2820	-	x	penultimate male	n/a	M	41.356	-122.2044	2288	5802212	75814
G2822	x	x	*H. americanus*	standard red	M	41.3558	-122.2051	2272	4581759	44945
G2823	-	x	*H. americanus*	n/a	F	41.3561	-122.2055	2272	3842751	44760
G2824	x	x	*H. americanus/kubai* hybrid	red	M	41.356	-122.2056	2271	2998924	33448
G2825	x	x	*H. americanus/kubai* hybrid	intermediate	M	41.3575	-122.2049	2312	2460439	30779
G2826	x	x	*H. americanus/kubai* hybrid	red	M	41.3566	-122.2047	2282	3456713	32663
G2827	x	x	*H. americanus/kubai* hybrid	red	M	41.3565	-122.2045	2282	4548957	49448
G2828	x	x	*H. americanus/kubai* hybrid	white	M	41.3564	-122.2045	2285	4146369	47255
G2829	x	x	*H. americanus/kubai* hybrid	red	M	41.3573	-122.2045	2302	3980440	40658
G2830	x	x	*H. americanus/kubai* hybrid	white	M	41.3565	-122.2044	2344	5727826	69932
G2831	-	x	*H. americanus*	n/a	F	41.3571	-122.2042	2294	7086015	80840
G2832	-	x	*H. americanus*	n/a	F	41.3601	-122.2041	2344	5609939	46507
G2833	x	x	*H. americanus/kubai* hybrid	red	M	41.36	-122.2041	2346	4013053	43093
G2834	x	-	*H. americanus*	standard red	M	41.3601	-122.2041	2346	-	-

G2835	x	x	*H. kubai*	standard yellow	M	41.3611	-122.2040	2330	5841869	60475
G2836	-	x	*H. americanus*	n/a	F	41.3586	-122.2021	2330	2509958	32799
G2837	x	x	*H. americanus/kubai* hybrid	red	M	41.358	-122.2021	2322	4463066	30898
G2838	x	x	*H. americanus/kubai* hybrid	yellow	M	41.3585	-122.2024	2325	6442066	60962
G2839	x	x	*H. americanus/kubai* hybrid	red	M	41.3603	-122.2044	2352	4800756	49400
G2841	x	x	*H. americanus/kubai* hybrid	red	M	41.362	-122.2024	2387	4538620	39677
G2842	x	x	*H. americanus/kubai* hybrid	red	M	41.3616	-122.2030	2378	6622808	56926
G2843	x	x	*H. americanus/kubai* hybrid	red	M	41.3611	-122.2035	2365	6494806	59727
G2844	x	x	*H. americanus/kubai* hybrid	red	M	41.3604	-122.2040	2350	3216574	40035
G2845	x	x	*H. americanus/kubai* hybrid	red	M	41.3595	-122.2033	2346	3805504	58325
G2846	x	x	*H. americanus/kubai* hybrid	white	M	41.3613	-122.2033	2369	6867345	59479
G2847	x	x	*H. americanus*	standard red	M	41.3613	-122.2032	2367	4827570	49035
G2848	-	x	*H. americanus*	-	F	41.3613	-122.2032	2367	6963075	64738
G2849	x	x	*H. americanus*	standard red	M	41.3611	-122.2035	2364	4618966	50000
G2850	-	x	*H. americanus*	n/a	F	41.361	-122.2035	2366	6290890	63626
G2851	x	x	*H. americanus/kubai* hybrid	red	M	41.361	-122.2038	2352	4147912	39019
G2852	x	x	*H. americanus/kubai* hybrid	red	M	41.3613	-122.2036	2367	5455165	50979
G2853	-	x	*H. americanus*	n/a	F	41.36	-122.2033	2350	5750929	53357
G2855	x	x	*H. americanus/kubai* hybrid	red	M	41.3604	-122.2036	2351	2898704	27249
G2857	x	x	*H. americanus*	standard red	M	41.3608	-122.2036	2363	3861128	36020
G2859	-	x	*H. americanus*	-	F	41.357	-122.2045	2286	7079309	88235
HA0337	-	x	H. americanus	parental americanus	F	41.2119	-122.5090	1852	4911892	50199
HA0338	-	x	H. americanus	parental americanus	F	41.2119	-122.5090	1852	4959391	59119
HA0376	-	x	H. americanus	parental americanus	M	41.2119	-122.5090	1852	5423747	55389
HA0409	-	x	H. americanus	parental americanus	M	41.2119	-122.5090	1852	2611292	35451
HA0929	-	x	H. kubai	parental kubai	M	41.6429	-122.1674	1538	1318700	27662
HA0930	-	x	H. kubai	parental kubai	F	41.643	-122.1674	1538	4072459	82012
HA0931	-	x	H. kubai	parental kubai	F	41.643	-122.1674	1538	3487997	61461

Appendix 3.2. Scored morphology matrix for all male individuals.

Sample ID	A	B	C	D	E	F	G	H	I	J	K
G2765	1	0	0	0	0	3	0	0	0	3	2
G2766	2	2	0	1	0	3	0	3	0	3	2
G2768	3	0	1	1	0	0	1	2	0	1	2
G2769	4	0	1	1	2	0	1	3	0	1	2
G2770	2	0	1	1	1	3	0	2	0	2	2
G2771	1	1	0	0	0	3	0	3	0	3	2
G2772	8	0	1	1	1	3	1	3	0	1	2
G2774	5	2	1	1	0	3	0	2	0	3	2
G2775	6	0	1	1	1	3	1	3	0	0	0
G2776	5	0	1	1	2	3	0	3	0	1	0
G2777	1	1	0	0	0	3	1	0	0	1	0
G2778	5	0	1	1	0	0	1	0	0	1	2
G2779	3	0	1	1	0	0	0	0	0	1	2
G2780	6	0	1	0	2	0	1	0	3	1	2
G2781	1	1	0	0	1	3	0	3	0	1	1
G2782	4	0	1	1	2	3	1	0	0	0	0
G2784	1	2	0	0	2	3	0	0	0	0	1
G2785	7	0	1	1	2	0	1	0	0	0	0
G2786	1	1	0	0	0	3	0	0	0	1	2
G2787	7	0	1	1	2	0	1	0	2	0	0
G2788	5	2	1	1	2	3	0	0	0	1	2
G2789	5	0	1	1	0	3	0	0	0	1	2
G2790	5	0	1	1	2	3	1	3	0	1	0
G2791	5	2	1	1	0	3	0	3	0	3	2
G2792	2	0	1	1	0	0	1	3	0	3	2
G2793	7	0	1	1	0	3	0	3	0	1	2
G2794	2	0	1	1	2	3	1	0	3	0	0
G2795	1	1	0	0	0	3	0	1	0	1	2
G2796	2	0	1	1	2	3	0	3	0	3	2
G2797	1	1	0	0	0	0	0	3	0	1	2
G2798	5	0	1	1	0	3	1	0	0	1	1
G2799	2	0	1	1	2	0	0	0	0	1	3
G2800	1	1	0	0	2	3	0	0	0	1	1
G2801	8	0	1	1	2	3	1	0	0	0	0
G2802	9	0	1	0	0	3	0	3	0	1	2
G2803	4	0	1	1	0	3	0	3	0	1	2
G2804	4	0	1	1	2	0	1	0	3	0	0
G2805	5	0	1	1	0	3	0	0	0	1	1
G2806	7	0	1	1	2	3	1	0	3	0	0
G2807	7	0	1	1	2	0	1	3	0	0	0
G2808	2	0	1	1	2	0	1	0	0	1	1
G2809	2	0	1	1	2	0	1	0	0	0	0
G2810	1	2	0	0	0	3	0	0	0	3	2
G2811	5	2	1	1	0	3	0	0	0	1	2
G2812	2	0	1	1	2	3	1	0	3	0	0
G2813	1	0	0	0	2	3	1	0	0	0	0
G2814	1	0	0	0	0	3	0	0	0	1	2
G2815	4	0	1	0	1	0	1	3	0	1	1
G2816	1	0	0	0	0	3	0	3	0	3	2

G2817	7	0	1	1	0	3	0	3	0	3	2
G2818	2	0	1	1	2	3	0	3	0	1	1
G2819	7	0	1	1	2	3	1	0	0	0	0
G2822	1	1	0	0	0	3	0	0	0	3	2
G2824	1	0	0	0	0	3	0	3	0	3	2
G2825	7	0	1	1	0	3	0	3	0	1	3
G2826	2	0	1	1	0	3	0	2	0	3	2
G2827	1	0	1	1	0	3	0	2	0	0	2
G2828	8	0	1	0	1	0	1	2	0	1	1
G2829	9	0	1	0	2	3	0	3	0	1	2
G2830	2	0	1	1	2	0	1	0	0	1	1
G2833	4	0	1	0	2	0	1	2	0	1	2
G2834	1	1	0	0	0	3	0	1	0	3	2
G2835	4	0	1	1	2	3	1	2	3	1	0
G2837	5	0	1	1	0	3	0	0	0	1	2
G2838	5	2	1	1	2	3	0	2	0	0	0
G2839	8	0	1	1	2	3	1	2	0	3	2
G2841	5	0	1	1	0	3	0	2	0	3	2
G2842	5	2	1	1	0	3	0	2	0	1	2
G2843	1	2	0	0	0	3	0	3	0	3	2
G2844	5	2	1	1	0	3	0	2	0	3	2
G2845	2	0	1	1	0	3	0	2	0	3	2
G2846	5	2	1	1	0	3	0	3	0	1	1
G2847	1	1	0	0	0	3	0	2	0	3	2
G2849	1	1	0	0	0	3	0	0	0	3	2
G2851	5	0	1	1	0	3	1	0	0	3	2
G2852	5	2	1	1	0	3	0	2	0	1	2
G2855	1	2	0	0	0	3	0	3	0	3	2
G2857	1	1	0	0	0	3	0	3	0	1	2

Appendix 3.3. Pairwise F_{ST} estimated using all ddRADseq loci and implemented in Arlequin. Includes hybrid palp colors as different populations, along with standard type specimens as different populations. *P*-values recorded in parentheses.

	Standard Red	**Standard Yellow**	**Hybrid Red**	**Hybrid White**	**Hybrid Yellow**
Standard Red	0				
Standard Yellow	0.0081 (0.9460+-0.0246)	0			
Hybrid Red	0.0056 (0.9910+-0.0030)	0.0083 (0.6487+-0.0354)	0		
Hybrid White	0.0110 (0.7207+-0.0193)	0.0103 (0.8018+-0.0417)	0.0102 (0.2162+-0.0433)	0	
Hybrid Yellow	0.0187 (0.6216+-0.0417)	0.0192 (0.5766+-0.0454)	0.0163 (0.4865+-0.0278)	0.0215 (0.3333+-0.0360)	0

Appendix 3.4. One sided proportion z-test input data and results.

Data		Results		
Observed proportion of hybrids	0.7308	Z	df	p-value
Observed proportion of standard morphs	0.2692	15.705	1	$7.402e^{-5}$
Expected proportion of hybrids	0.5			

Appendix 3.5. X^2 goodness of fit test for palp color counts with two degrees of freedom. N_0 = no relationship between palp color and number of individuals in the zone.

	Red	Yellow	White
Observed Counts	5	18	13
Expected Counts	16	16	16
$\frac{(obs-exp)^2}{exp}$	12.2500	7.5625	0.5625
			Df = 2, critical value = 9.21
			X^2 = 20.0375, p ≤ 0.001

Appendix 3.6. X^2 goodness of fit test for palp color counts of only hybrid types with two degrees of freedom. N_0 = no relationship between palp color and location in the hybrid zone.

	Red	Yellow	White
Observed Counts	47	18	11
Expected Counts	25.3333	25.3333	25.3333
$\frac{(obs-exp)^2}{exp}$	18.5307	2.1228	8.1096
			Df = 2, critical value = 9.21
			X^2 = 28.7632, p < 0.00001

Appendix 3.7. X^2 goodness of fit test for land cover type with two degrees of freedom. N_0 = no relationship between palp color land cover type in the zone.

	Red	Yellow	White
Observed Counts	39	13	4
Expected Counts	23.5	9	5.5
$\frac{(obs-exp)^2}{exp}$	10.2234	1.7778	0.4091
			Df = 2, critical value = 9.21
			X^2 = 12.4103, p < 0.002

Appendix 3.8. Calculation of percent genome coverage by ddRADseq data.

ddRADseq sequencing coverage

Habronattus genome size: ~5.586 Gb
Mean length of loci: 182.28 bp
Number of loci: 2182

$$\frac{(\mathbf{182.28bp} \times \mathbf{2182})}{\mathbf{5,586,000,000bp}} \times \mathbf{100} = \mathbf{0.0071}\%$$

VII. SUPPLEMENTAL FILES

Supplemental File 1.1. Minsamp 10 unconstrained concatenated phylogeny with rooting placed as in Figure 3. Node labels show bootstrap support / sCF (in percentage of sites supporting split). Tip labels colored by morph/ species identity.

Supplemental Figure 1.2. Minsamp 24 unconstrained concatenated phylogeny with rooting placed as in Figure 3. Node labels show bootstrap support / sCF (in percentage of sites supporting split). Tip labels colored by morph/ species identity.

Supplemental Figure 1.3. Minsamp 48 unconstrained concatenated phylogeny with rooting placed as in Figure 3. Node labels show bootstrap support / sCF (in percentage of sites supporting split). Tip labels colored by morph/ species identity.

Supplemental Figure 1.4. Minsamp 4 constraint 1 concatenated phylogeny. Constraint tree required currently described species to form individual clades, without any constraints on internal nodes. Node labels show bootstrap support / sCF (in percentage of sites supporting split). Tip labels colored by morph/ species identity.

Supplemental Figure 1.5. Minsamp 4 constraint 2 concatenated phylogeny. Constraint 2 tree required currently described species to form individual clades, with the addition that morphological variants within each described species were also constrained as clades nested within the species clade. Node labels show bootstrap support / sCF (in percentage of sites supporting split). Tip labels colored by morph/ species identity.

Supplemental Figure 1.6. Minsamp 10 constraint 1 concatenated phylogeny. Constraint tree required currently described species to form individual clades, without any constraints on internal nodes. Node labels show bootstrap support / sCF (in percentage of sites supporting split). Tip labels colored by morph/ species identity.

Supplemental Figure 1.7. Minsamp 10 constraint 2 concatenated phylogeny. Constraint 2 tree required currently described species to form individual clades, with the addition that morphological variants within each described species were also constrained as clades nested within the species clade. Node labels show bootstrap support / sCF (in percentage of sites supporting split). Tip labels colored by morph/ species identity.

Supplemental Figure 1.8. Minsamp 24 constraint 1 concatenated phylogeny. Constraint tree required currently described species to form individual clades, without any constraints on internal nodes. Node labels show bootstrap support / sCF (in percentage of sites supporting split). Tip labels colored by morph/ species identity.

Supplemental Figure 1.9. Minsamp 24 constraint 2 concatenated phylogeny. Constraint 2 tree required currently described species to form individual clades, with the addition that morphological variants within each described species were also constrained as clades

nested within the species clade. Node labels show bootstrap support / sCF (in percentage of sites supporting split). Tip labels colored by morph/ species identity.

Supplemental Figure 1.10. Minsamp 48 constraint 1 concatenated phylogeny. Constraint tree required currently described species to form individual clades, without any constraints on internal nodes. Node labels show bootstrap support / sCF (in percentage of sites supporting split). Tip labels colored by morph/ species identity.

Supplemental Figure 1.11. Minsamp 48 constraint 2 concatenated phylogeny. Constraint 2 tree required currently described species to form individual clades, with the addition that morphological variants within each described species were also constrained as clades nested within the species clade. Node labels show bootstrap support / sCF (in percentage of sites supporting split). Tip labels colored by morph/ species identity.

Supplemental Figure 1.12. Minsamp 4 Tetrad species tree with rooting placed as in Figure 3. Node labels show bootstrap support. Tip labels colored by morph/ species identity.

Supplemental Figure 1.13. Minsamp 10 Tetrad species tree with rooting placed as in Figure 3. Node labels show bootstrap support. Tip labels colored by morph/ species identity.

Supplemental Figure 1.14 Minsamp 24 Tetrad species tree with rooting placed as in Figure 3. Node labels show bootstrap support. Tip labels colored by morph/ species identity.

Supplemental Figure 1.15. Minsamp 48 Tetrad species tree with rooting placed as in Figure 3. Node labels show bootstrap support. Tip labels colored by morph/ species identity.

Supplemental Figure 1.16. STRUCTURE bar plot using K = 4 under the non-admixture model.

Supplemental Figure 1.17. GEMMA results for all SNPs in the minsamp48 dataset. Red line denotes the significance cutoff at a p-value of 0.0000768.

Supplemental Figure 1.18. GEMMA results for unlinked SNPs in the minsamp48 dataset. Red line denotes the significance cutoff at a p-value of 0.00000421.

Supplemental Figure 1.19. UCE constraint 1 concatenated phylogeny. Constraint tree required currently described species to form individual clades, without any constraints on internal nodes. Tip labels colored by morph/ species identity.

Supplemental Figure 1.20. UCE constraint 2 concatenated phylogeny. Constraint 2 tree required currently described species to form individual clades, with the addition that morphological variants within each described species were also constrained as clades nested within the species clade. Tip labels colored by morph/ species identity.